Final Report Submitted to California Air Resources Board
for Contract A3-106-32

Snow Deposition, Melt, Runoff, and Chemistry in a Small Alpine Watershed, Emerald Lake Basin, Sequoia National Park

Final Report

Principal Investigator
JEFF DOZIER
Professor of Geography

Co-Principal Investigator
JOHN M. MELACK
Professor of Biological Sciences

Project Manager:
DANNY MARKS
Assistant Research Hydrologist

Contributing Scientists:
KELLY ELDER
RICK KATTELMANN
MARK WILLIAMS

Center for Remote Sensing and Environmental Optics

University of California
Santa Barbara, CA 93106
(805) 961-2309

Reporting Period: July 1, 1984 to March 31, 1987

Snow Deposition, Melt, Runoff, and Chemistry in a Small Alpine Watershed, Emerald Lake Basin, Sequoia National Park

Abstract

Investigation of the snow hydrology and chemistry of a small alpine watershed in the southern Sierra Nevada, California, was initiated in Fall 1984 as part of the California Air Resources Board's Integrated Watershed Study program to assess the current status and sensitivity of this alpine environment to damage from acid deposition. The objective of our study was to determine the role of snowmelt runoff in chemical processes in the watershed. The watershed was surveyed, control points were located, and an overflight was arranged so that a large scale topographic map and ortho-photo could be generated. A high resolution (5 m) digital elevation model (DEM) was generated, and software developed to do rapid calculation of terrain parameters. Four sites were instrumented and meteorological parameters continously monitored during the 1986 water year. These data were evaluated to determine the range of climatic variation in the watershed. The 1986 snow season was one of the largest on record, depositing 200% of the 50-year mean snowfall in the Emerald Lake region. Snowfall volume and chemistry were sampled on an event basis from snowboards, and at intervals from snow pits at several sites in the watershed. During spring, several detailed snow surveys were done to estimate the volume and distribution of snow in the watershed. Outflow stream stage has been monitored since mid-1983, and inflow stream stage since mid-1985. Stage-discharge rating functions were developed and discharge calculated for the outflow and the two major inflow streams. Energy transfer at the snow surface was calculated, and the relative magnitude of each transfer term evaluated. An energy balance snowmelt model was developed and tested. Calculated discharge volume from the outflow was nearly equal to the estimated maximum snow water equivalence in the watershed. Chemical loading to the watershed was calculated for the 1985 and 1986 water years. Snowfall during the 1986 snow season had uniformly low ionic concentrations, but the initial melt wave appeared to produce an acidic pulse that significantly lowered the ph and acid neutralizing capacity (ANC) of the basin surface waters. Spatial and temporal variations in the onset of melt over the watershed prolonged the time of elevated ionic concentrations, depressed pH and ANC. Energy transfer calculations showed net radiation as dominating the energy budget during melt, but indicated that sensible and latent heat exchange could be important in the colder months, January and February. Calculated sublimation and evaporation accounted for the loss of 20-25% of the snowfall which should also increase the ionic concentration of snowmelt. Calculated snowmelt, using monthly energy flux totals, corresponded closely with measured discharge. Preliminary testing of the snowmelt model indicates that it is an effective tool that could be coupled with calculations of meltwater ionic concentrations to better predict the duration and strength of acidic inputs during snowmelt.

TABLE OF CONTENTS

1. General Introduction 1
2. The Emerald Lake Watershed 2
    2.1. Topographic Data 2
    2.2. The Terrain Structure of the Emerald Lake Watershed 3
    2.3. References 3
3. Summary of Snowfall - 1986 Water Year 7
    3.1. Introduction 7
    3.2. Snowfall 7
    3.3. Emerald Lake Basin Event Summary 8
    3.4. Snow Pit Summary 9
    3.5. Summary 10
    3.6. References 10
4. Chemical Characteristics of the Seasonal Snowpack 15
    4.1. Introduction 15
    4.2. Background 15
    4.3. Methods 19
    4.4. Results 20
    4.5. Discussion 22
    4.6. References 26
5. Measuring and Monitoring Stream Discharge 49
    5.1. Introduction 49
    5.2. Calculating Stream Discharge 49
    5.3. Dilution Discharge Measurement 50
    5.4. Slug Injection Method For Remote Areas 50
    5.5. Stage-Discharge Relationships, Outflow and Inflows 1 & 2 51
    5.6. Outlet Rating Curve 52
    5.7. Inlet 1 Rating Curve 53
    5.8. Inlet 2 Rating Curve 53
    5.9. Discharge Into and Out of Emerald Lake 54
    5.10. References 55
6. Weather and Climate 65
    6.1. Data Recording and Instrumentation 66
    6.2. Air Temperature 68
    6.3. Humidity 69
    6.4. Wind 70
    6.5. Snow and Soil Temperatures 71
    6.6. References 71
7. Rapid Calculation of Terrain Parameters from Digital Elevation Data 84
    7.1. Use of Digital Elevation Models in Radiation Calculations 84
    7.2. Data Representation 84
    7.3. Boundary Conditions for Radiation Models 84
    7.4. Algorithms for Rapid Calculation 85
    7.5. Conclusion 87
    7.6. Code Listings 88
    7.7. References 96
8. Snow Accumulation and Distribution 100
    8.1. Introduction 100

8.2. Previous Work on Snow Distribution 100
8.3. Measurement of Snow-Water Equivalence 101
8.4. Factors Affecting Snow Distribution 101
8.5. Field Methods 104
8.6. Preliminary Results 105
8.7. Future Work 105
8.8. References 106
9. Energy Exchange at the Snow Surface 112
9.1. Net Radiation at the Snow Surface 112
9.2. Turbulent Transfer at the Snow Surface 116
9.3. Conduction and Advected Heat Transfer to the Snowcover 118
9.4. Snowcover Energy and Mass Balance 120
9.5. References 121
10. Modeling Snowmelt At a Point 144
10.1. An Energy Balance Snowmelt Model 145
10.2. Preliminary Test of the Snowmelt Model 151
10.3. References 152

LIST OF FIGURES

2.1. Topographic Map of Emerald Lake Basin. 4
2.2. Ortho-photo of Emerald Lake Basin. 5
2.3. Terrain Characteristics. 6
3.2. Snow Water Equivalent (SWE) Input Volumes 14
4.1 Snow Collection Sites 42
4.2 Cumulative Event vs Snowpit Anion Loading, Inlet 43
4.3 Anion Loading and SWE Time-Series, Inlet 44
4.4 Snowpit Chemistry at 6 Sites, May 23 1985 45
4.5 NO_3^-, SO_4^{2-} and Discharge, Inflow #2, Spring 1986 46
4.6 NO_3^- and SO_4^{2-} Time-Series, EML Outflow, June 1984 to July 1986 47
4.7 NO_3^- and SO_4^{2-} Concentrations of Inflow Streams, 1986 Melt Season 48
5.1 Outflow Discharge, 1984 Water Year 62
5.2 Outflow Discharge, 1985 Water Year 63
5.3 Outflow Discharge, 1986 Water Year 64
6.1. Daily Mean, Maximum, and Minimum Air Temperature 77
6.2. Wind Speed vs. Air Temperature 78
6.3. Daily Average Snow Surface Temperature 79
6.4. Daily Mean, Maximum, and Minimum Vapor Pressure 80
6.5. Snow Surface Vapor Pressure Gradient 81
6.6. Daily Mean, Maximum, and Minimum Wind Speed 82
6.7. Daily Average Soil and Snow Cover Temperatures 83
7.1 Horizon Angle H_ϕ for Direction ϕ 97
7.2 Orientation of Digital Elevation Model 98
7.3 A Single Horizon Profile 99
9.1 Two-Band Albedo Model 130
9.2 Computed vs. Measured Albedo 131
9.3 Computed Albedo, Emerald Lake Watershed 132
9.4 Daily Net Visible, Near-Infrared, and Solar Radiation, Ridge Site 133
9.5 Daily Net Visible, Near-Infrared, and Solar Radiation, Lake Site 134
9.6 Diurnal Solar Irradiance, Winter and Spring 135
9.7 Diurnal Net Solar Radiation, Winter and Spring 136
9.8 Daily Thermal Radiation 137
9.9 Daily Net All-Wave Radiation, Ridge Site 138
9.10 Daily Net All-Wave Radiation, Lake Site 139
9.11 Daily Turbulent Transfer 140
9.12 Daily "Net" Turbulent Transfer 141
9.13 Daily Net Radiation and "Net" Turbulent Transfer 142
9.14 Daily Energy Balance 143

LIST OF TABLES

2.1. Characteristics of Emerald Lake Watershed 2
3.1 Precipitaion and SWE for Tulare region and Kaweah basin – 50-Year Mean 11
3.2 Precipitaion from Lodgepole Ranger Station – 50-Year Mean 11
3.3. Average Snow Deposition. 11
3.4. Snow Deposition. 11
3.5 Snowboard Event Data From Emerald Lake Basin 13
3.6 Snowpit Data From Emerald Lake Basin 13
4.1 Precision and Detection Limits of Chemical Methods 30
4.2 1985 Snow Season Charge Balance 30
4.3 1986 Snow Season Charge Balance 31
4.4 Cation Contamination From Filters 31
4.5 Event Synopsis, January 9 1986 32
4.6 1985 Event Snow Chemistry Summary 32
4.7 85 Snow Pack Profile Summary 33
4.8 1986 Event Snow Chemistry Summary 34
4.9 1986 Snowpack Chemical Profile Summary 36
4.10 Winter Season Ion Concentration and Loading, from Snowfalls 37
4.11 Comparison, by Precipitation Type, of Seasonal Ion Concentration 37
4.12 Comparison, by Precipitation Type, of Seasonal Ion Loading 38
4.13 Comparison, by Precipitation Type, of Percent Flux of Ion Loading 38
4.14 Ion Loading to the Catchment during Snowmelt: 1985 and 1986 39
4.15 Snowpack Chemical Profile Time Series, Inlet 1986 40
4.16 1986 Snowpack Meltwater Chemical Concentration Data 40
4.17 One-Way ANOVA of NO_3^- and SO_4^{2-}, January 09, 1986 Storm Event 41
5.1 Monthly Water Flux, Emerald Lake Outflow, 1984-1986 56
5.2 Monthly Water Flux Into and Out of Emerald Lake, 1986 56
5.3 Daily Discharge Volume, Emerald Lake Outflow, 1984 57
5.4 Daily Discharge Volume, Emerald Lake Outflow, 1985 58
5.5 Daily Discharge Volume, Emerald Lake Outflow, 1986 59
5.6 Daily Discharge Volume, Emerald Lake Inflow 1, 1986 60
5.7 Daily Discharge Volume, Emerald Lake Inflow 2, 1986 61
6.1. Micro-Meteorological Instrument Sites. 65
6.2. Recorded Parameters and Instrumentation 73
6.3. Air and Snow Surface Temperature. 73
6.4. Air and Snow Surface Vapor Pressure. 74
6.5. Wind Speed. 75
8.1 Previous Studies on Snow Accumulation and Distribution 109
8.2. Measured Physical Snow Properties 110
8.3 Summary of Snow Depth Statistics From 1986 Water Year Surveys 111
8.4 Summary of Basin Snow Water Equivalent From Each Survey 111
8.5 Depth Statistics From Northeast Wall and Entire Basin 111
8.6 *F*-Test Results From Northeast Wall and Entire Basin 112
9.5 Soil Heat Transfer Summary. 119
9.6 Advected Heat and Mass Transfer. 119
9.7 Advected Heat and Mass Transfer Summary. 120
9.1. Selected Studies of Climate, Energy Exchange, and Snowmelt 124
9.2 Solar Radiation Summary 126
9.3 Net All-Wave Radiation Summary 126
9.4 Turbulent Transfer Summary 126
9.8 Snowcover Energy and Mass Balance Summary 127

9.9 Snowcover Energy Balance Percentage Summary 129
9.10 Snowcover Mass Balance Percentage Summary 129
9.11 Estimated Parameter Uncertainty 129
10.1 Snowmelt Model Units 146
10.2 Snowmelt Model Input Requirements 154
10.3 Output from Snowmelt Model 154
10.4 Average Snowcover Characteristics 155
10.5 Snowmelt Model Test Run 156

1. General Introduction

Alpine watersheds in the Sierra Nevada, like Emerald Lake, are weakly buffered and are thus extremely vulnerable to damage from acid deposition. Evidence indicates that acid precipitation falls in the higher elevations of the Sierra Nevada during portions of the year, but at present little information exists to determine the current or long-term effects that acidic deposition may have on these watersheds. During most years, more than 95% of the precipitation in the alpine Sierra Nevada falls as snow. While the concentration of solutes in this snow is usually very low, the large accumulations of water stored in the snowcover cause chemical loading to be moderate. If the solute concentration in snow deposited in the Sierra Nevada were to increase, the effects on aquatic systems, like those at Emerald Lake, could possibly be detrimental. To determine whether this would occur, we must improve our understanding of the processes of snow deposition, metamorphism, melt, and runoff, which determine the concentration and the rate of release of solutes to an alpine watershed.

Investigations of the snowcover require detailed monitoring of the surface climate, precipitation volume and chemistry, runoff volumes, areas of snowmelt, snow and runoff chemistry, and stream discharge and chemistry. Snow metamorphism, melting, and runoff are controlled by the magnitude of energy available to drive these processes. This energy flux is determined by the combination of local meteorological inputs of precipitation and energy, which control the release of melt water to and chemical cycling rates through the watershed. Detailed observations of alpine climates are very limited. Most of those that do exist come from locations at lower elevations, or are from non-alpine locations, or have been limited to a single, though well-instrumented measurement site. To accomplish our goals at Emerald Lake we required not only a detailed understanding of the climate at a few points, but an evaluation of the spatial variation of critical meteorological parameters over the watershed.

This study, *Snow Deposition, Melt, Runoff, and Chemistry in a Small Alpine Watershed, Emerald Lake Basin, Sequoia National Park*, began during the winter of 1985, as part of the California Air Resources Board's Integrated Watershed Study, initiated to evaluate the current status and sensitivity of high-elevation, alpine watersheds in the Sierra Nevada to damage from acid deposition. This effort represents the most detailed evaluation of alpine climate, hydrology, and hydrochemistry that has been undertaken in the Western Hemisphere. We have established and tested measurement procedures and quality control measures, instrumentation, and laboratory procedures required to evaluate the physical and chemical condition of the seasonal snowpack and the distribution of that snowpack over the watershed.

This document represents the final report on 32 months of study (July 1984 through March 1987) of snowcover deposition, processes, properties, and chemistry, and the effects of these on the aquatic systems in the Emerald Lake watershed. We present and analyze the following data collected in the Emerald Lake watershed:

1) Maps of terrain, geology, stream channels, and an evaluation of the distribution of terrain features and structure for the Emerald Lake watershed;
2) Meteorological parameters used to evaluate the climate of the watershed;
3) Snow deposition in the watershed, from both event and snow pit measurements, with an evaluation of measurement procedures used, and a comparison to snow deposition over the Sierra Nevada;
4) Chemical composition of snowfall events, the seasonal snowcover and meltwater in the watershed;
5) Stream discharge into and out of Emerald Lake.
6) Develop accurate and efficient methods for calculation of terrain parameters from a high-resolution, digital elevation model (DEM);
7) Estimate snow distribution and volume over the watershed;
8) Calculate energy exchange at the snow surface and at the ridge and lake sites, to estimate the effect of energy transfer on the mass balance of the snowcover at those sites;
9) Develop an energy-balance snowmelt model that can be used to make a detailed evaluation of energy transfer and snowmelt, and evaluate the sensitivity of snowmelt calculations to errors in the input data and to model assumptions.

Most of this analysis emphasizes the 1986 water year (October 1, 1985 to September 30, 1986), because for that year few gaps occur in the data record.

2. The Emerald Lake Watershed

TABLE 2.1: Characteristics of Emerald Lake Watershed
Sierra Nevada, California

Location (approx. center)	Geodetic: 36°36'N, 118°40'W UTM, Zone 11: 4,051,000 N; 350,500 E
Emerald Lake Elevation	2800 m
Alta Peak Elevation	3416 m
Total Relief	616 m
Lake Area	2.85 ha
Lake Volume	1.8×10^5 m^3
Basin Area	120 ha
Basin Geology	Plagioclase Granite

The Emerald Lake watershed in Sequoia National Park is the test basin for this study. It is located in the upper Marble Fork of the Kaweah River drainage, approximately 8 km from and 700 m above the nearest road. Because the watershed is in a wilderness area, travel to it is on foot or on skis. The basin is a small (120 ha) high-altitude cirque, with a stream system that drains into Emerald Lake, which is a tarn. Table 2.1 presents general topographic statistics for the watershed.

Climatically, Emerald Lake is an "alpine" or "upper subalpine" watershed. Some confusion exists over the classification of regions in this climatic zone in North America [Love, 1970; Troll, 1973a]. The watershed is well above the forestline, with a few trees on lower elevations mainly in southwestern exposures. Ives and Barry [1974] define "forestline" as the upper limit of the closed conifer forest. This term is used to differentiate that limit from the "alpine treeline", which denotes the upper limit of all "trees" (defined by Ives and Barry as "perennial woody plants with a single central stem at least 2 m tall"). (For further information see Table 1.3, pg. 9, in the Introduction of *Arctic and Alpine Environments*, edited by Ives and Barry [1974]). The majority of the watershed is above the alpine treeline, with grasses and tundra vegetation types predominating which puts it in the "alpine" classification according to Troll [1973b]. In this report the study area is referred to as an alpine watershed, after the convention established in *Arctic and Alpine Environments*, edited by Ives and Barry [1974]. They point out that "subalpine" is a subdivision of the alpine region, and not a "zone below alpine." As such, the boundary between the two is vague and can be difficult to define. Both subalpine and alpine conditions exist in the Emerald Lake watershed, but the majority of the watershed would be defined as alpine.

2.1. Topographic Data

Figure 2.1 is a topographic map of the study area, showing the watershed boundaries and our major measurement sites. The highest point in the watershed is Alta Peak (3416 m), 616 m above Emerald Lake (2800 m). While most of the watershed is bare granitic rock and talus, small patches of organic soil and vegetation occur. The basin is large enough to represent typical alpine snowmelt regimes found in the southern Sierra Nevada, but small enough to permit a sampling density adequate for this study.

At the initiation of the Integrated Watershed Study, the best map of the drainage basin was the USGS 1:62,500 scale Triple Divide Peak quadrangle. An advance copy of the USGS 1:24,000 scale map was received during the first year of work, but even at that scale, many details of the basin's topography or drainage network were not discernible. We therefore prepared a map at 1:2500 scale, along with an ortho-photo (Figure 2.2) and a high-resolution digital elevation model (DEM). The 100 m grid on the topographic map (Figure 2.1) can be used to better locate measurement sites and features in the watershed.

Maps of stream channels and sub-drainage basins, and basin geology were prepared from a field survey by Clow [1987]. Accurate location of stream channels is possible, but the boundaries of the sub-drainages are sometimes arbitrary, because the hydrologic topography is not always equivalent to the surface topography, and talus many meters deep masks ridge lines and hides water flowing through it. Channel flow is not well developed in the watershed. Few channels exist away from the lake, and many of those that do carry water only at peak flows during snowmelt. At high flows, many of the channels flow at more than bank-full stage and mix together. The accurate delineation of sub-drainage boundaries is a function of both topography and flow volume in some areas.

Base map products were prepared to our specifications by Chickering/Green Empire, Inc., in Eugene, Oregon, under a separate California Air Resources Board contract. Both the original topographic map and ortho-photo are high quality, precision products. The 100 m grid is a transparent overlay that can be removed if desired. All map products are available at a variety of scales and qualities depending on the application. The DEM is a 5 m grid of elevations covering the area shown on the map and ortho-photo.

These map products, particularly the DEM, are used to locate features and measurement sites in the watershed and to improve sampling strategies. They are essential for quantification of spatial features such as soils, geology, snowcover, vegetation, drainage areas, and stream networks. By establishing these maps on the DEM coordinate structure, it will be possible to integrate these parameters into an information system and to use them to model or calculate the distribution over the watershed of critical meteorological parameters, such as radiation, temperature, humidity, wind, and precipitation.

2.2. Terrain Structure of the Emerald Lake Watershed

The DEM can be used to determine the distribution of elevations, slopes, and exposures found in the watershed. Figure 2.3 presents a summary of these characteristics. The Area–Elevation and Area–Slope curves show that there is a fairly even distribution of slopes and elevations over the 616 m elevation range of the watershed. The watershed is steep, with half the area containing slopes greater than 30°. The mean elevation in the watershed is 3050 m, and the mean slope is 31°. The micro-meteorological instrumentation sites, marked on the Area–Elevation curve, are in the lower half of the watershed. Exposure-distribution is biased toward the north, typical of cirques in the Sierra Nevada. West-facing slopes are slightly more common than east-facing. The spikes at the NW and W exposures in the exposure-distribution curve reflect features of the terrain structure.

2.3. References

Clow, D., Geologic controls on the neutralization of acid deposition and on the chemical evolution of surface and ground waters in the Emerald Lake watershed, Sequoia National Park, California, M. S. Thesis, 216 pp., Dept. Geol., Calif. State Univ., Fresno, CA, 1987.

Ives, J. D. and R. G. Barry, eds., *Arctic and Alpine Environments*, 999 pp., Methuen, London, 1974.

Love, D., Subarctic and subalpine: where and what?, *Arctic Alpine Res.*, *2*, 63-73, 1970.

Troll, C., High-mountain belts between the polar caps and the equator: their definition and lower limit, *Arctic Alpine Res.*, *5*, A19-A28, 1973a.

Troll, C., The upper timberlines in different climatic zones, *Arctic Alpine Res.*, *5*, A3-A18, 1973b.

Figure 2.1. Topographic map of Emerald Lake watershed and surrounding area. Meteorological instrumentation sites are shown by dots 1 to 4: (1) outflow from the lake; (2) inflow to the lake; (3) pond; (4) ridge.

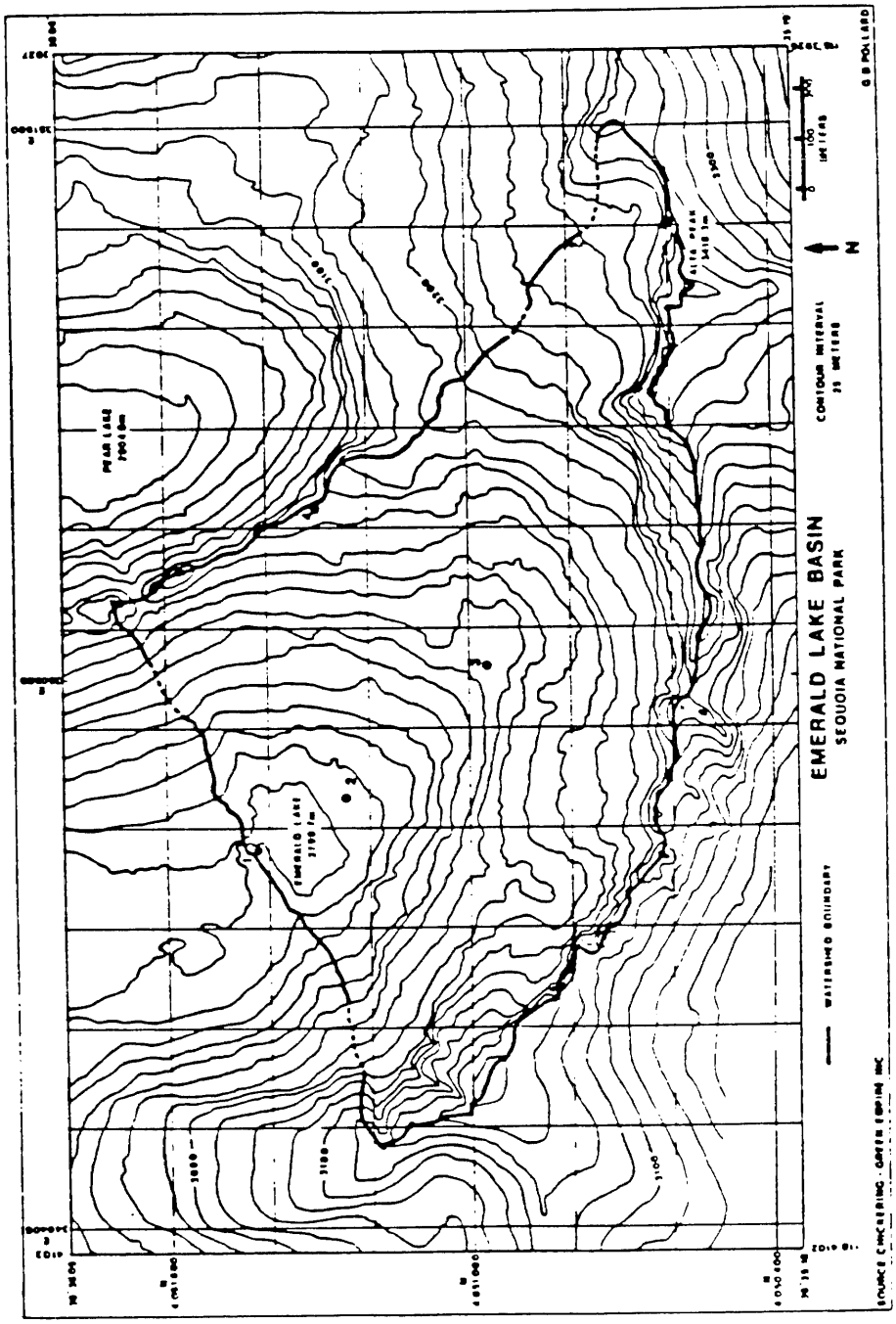

Figure 2.2. Ortho-photo of Emerald Lake watershed and surrounding area with watershed boundary, sub-drainage areas, and stream channels indicated.

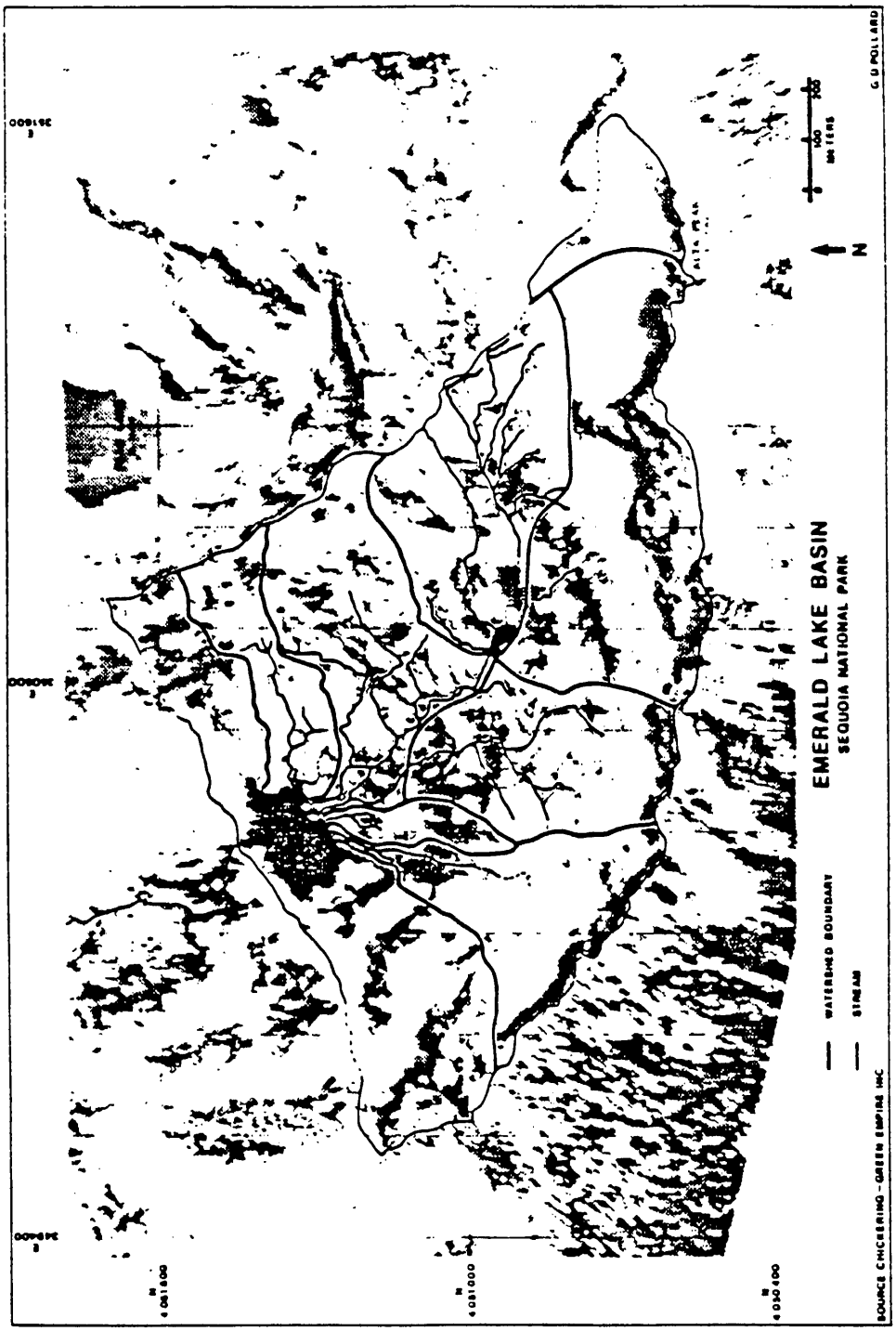

Figure 2.3. Terrain characteristics of the Emerald Lake watershed, from DEM data. Area–Elevation and Area–Slope curves are over cumulative areas, while Exposure Distribution is for absolute area.

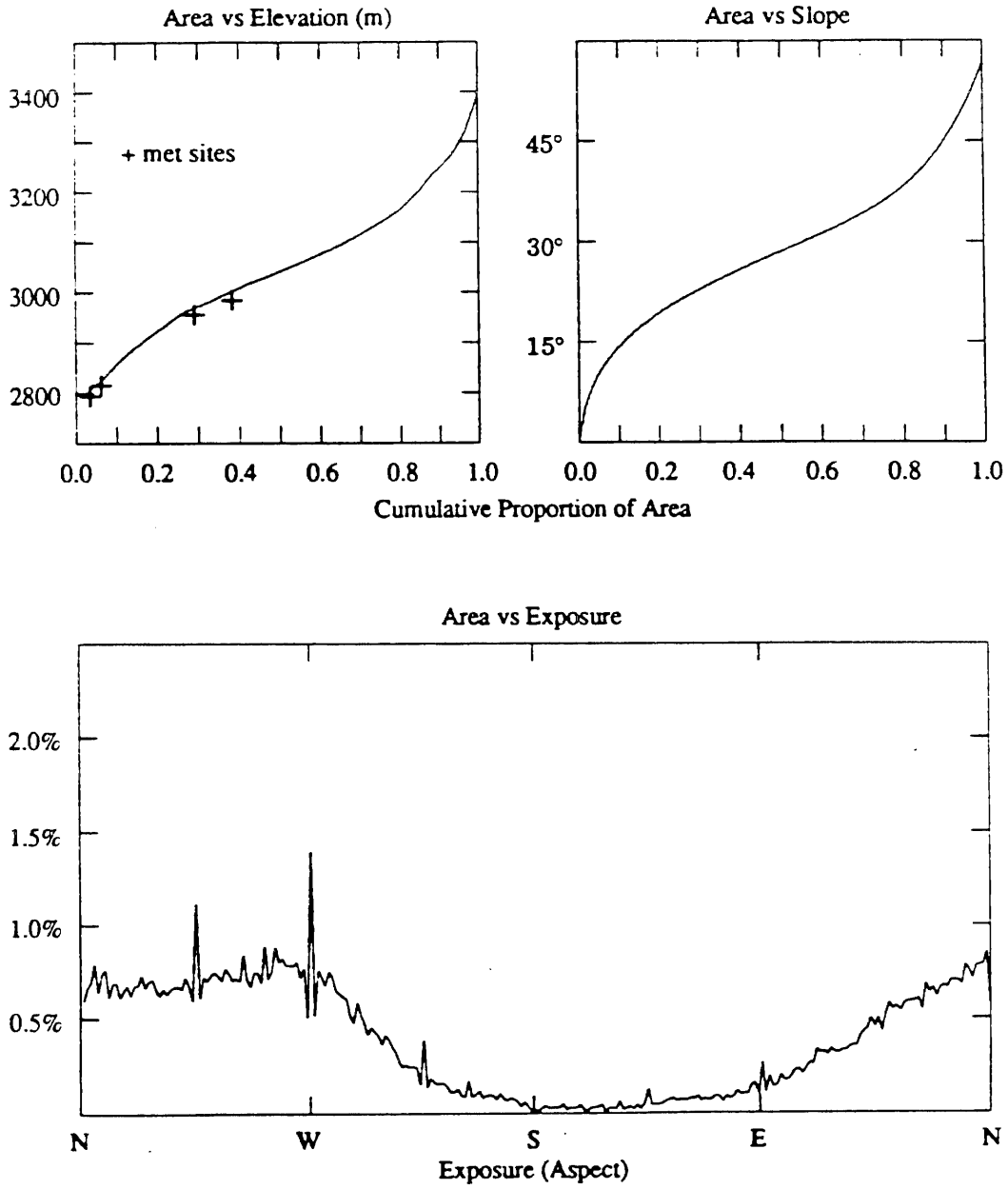

3. Summary of Snowfall - 1986 Water Year

3.1. Introduction

The following is a summary of the winter precipitation and the snowpack that developed in the winter of 1986. Depth, density, and SWE data collected from storms and snowpits in the Emerald Lake basin are presented. Data from Lodgepole, Kaweah basin, and the Tulare region are used as an index of the seasonal snowfall and are also discussed. Examination of these supplementary data serves two purposes: (1) it indicates whether the Emerald Lake data are representative of a larger area than the small basin itself, and (2) the regional data indicate that systematic errors are unlikely in the Emerald Lake data since the trends there corroborate the regional condition. It is important to determine the representativeness of the Emerald Lake data. For this study to be useful, we need to be able to apply the results to larger regions. These indices are also valuable in looking at long-term trends because both the Kaweah and Lodgepole records exceed 50 years. "Normal" in the following discussion refers to the mean value from these 50 year records. In summarizing the winter precipitation record, a discussion of the Emerald Lake data will follow a summary of regional conditions and the Lodgepole data.

Snow course data from the California Cooperative Snow Survey (CCSS) has served as an index of snowpack conditions in California for many years. The snowpack data are collected using a Federal or Mount Rose sampler and represents snow already accumulated on the ground. CCSS data does not exist for Emerald Lake, but precipitation and SWE from snow courses are summarized for the Tulare Region in Table 3.1. Precipitation is also recorded for the Kaweah Basin subregion of which Emerald Lake is a part. The precipitation data are collected from precipitation gages as it accumulates. Cumulative precipitation is the sum of the individual precipitation events. By the end of January, the regional cumulative precipitation reached 108% of the 50-year average for the date, although January precipitation was only 50% of normal for the month. Snow surveys on 73 regional snow courses showed the snowpack to be 82% of the normal for the date. February brought the regional snowpack to 140% of the 50-year mean and the precipitation to 143%. This month changed the statewide condition from deficit to surplus. A number of state records for February discharge, precipitation, and temperature were broken. The Kaweah basin received 175% of the normal precipitation by March 1 and 180% by April 1. The regional snowpack maximum was measured at 150% on April 1 [California Cooperative Snow Survey, 1986].

Table 3.2 summarizes the precipitation measured at Lodgepole Ranger Station, Sequoia National Park, which is located about 5 km from and 600 m elevation below Emerald Lake. Precipitation at Lodgepole tends to be much lower than the precipitation at Emerald Lake, but serve as an index of the long-term winter trends. The season began with higher than normal precipitation in October and November. By the end of November, Lodgepole had received 248% of the 50-year mean for the date. It is important to recognize that these months are not particularly significant to the yearly precipitation as can be seen from the 50-year mean values. The percentage values are misleading in this respect and the actual precipitation must be examined as well. December through March are traditionally the most significant precipitation months in the Sierra Nevada. December was a below normal month with only 77% of the normal precipitation for the month and January was slightly above normal with 106%. February was an extreme precipitation month with nearly 400% of the normal monthly precipitation falling between February 12 and 21. This increased the yearly cumulative value to 200% in spite of the low December input. March still showed higher than normal input followed by a dry spring with April through June being below normal.

3.2. Snowfall

Precipitation in the Emerald Lake Basin is principally snowfall. Typically, in the higher elevations of the Sierra Nevada, 90% of the annual precipitation falls as snow [Smith and Berg, 1982]; in the Emerald Lake watershed during the 1986 water year nearly 98% of the total precipitation fell as snow. Rates and volumes of falling snow are very difficult to evaluate from precipitation gage records because they are affected not only by wind, site characteristics, and precipitation intensity, but by variations in the density and structure of the snow crystals as they fall. There is uncertainty in all precipitation data [Israelson, 1967; Larson, 1971; Sevruk, 1986], but because rainfall is of higher and constant density, rainfall data are not as difficult to analyze [Harris and Carder, 1974]. Since Pagliuca [1934] first developed snow gaging techniques on Mt. Washington, and Alter [1937] worked to standardize wind shields for snow gaging on the high desert of Utah, many investigators have tried to improve gage design, calibration, placement, and wind correction [e.g. Garstka, 1944; Codd, 1947; Wilson, 1954; Allis et al., 1963; Struzer, 1969; Hamon, 1972; Osborn et al., 1972; WMO, 1973; Rawls et al., 1975]. Peck [1972] summarizes the problem of monitoring snowfall, stating that most measurements of snowfall rates and volumes are the least accurate of the meteorological measurements used in hydrologic modeling. Larson and Peck [1974] state that while it may not be possible to remove the uncertainty from snow collection gage data, with careful gage placement and calibration, these data could be used as an index to true snowfall under some circumstances. This was similar to the findings of Goodison [1978], Goodison and Metcalfe [1982], and Sturges [1984], who did detailed analysis of the ratio of gage catch to true snowfall over a period of years using several types of gages, gage placements, and types of wind shields. Goodison was very careful to use actual measurements of snow on the ground and from snow boards in his comparisons, but Sturges did not. Therefore, his results are suspect, as his true snowfall is actually snow collection gage data from a reference site in a stand of trees.

Only four of the studies cited above make any effort to evaluate precipitation data from mountainous regions [Pagliuca, 1934; Garstka, 1944; Chadwick, 1972; Hamon, 1972]. These studies clearly show that prob-

lems of wind during deposition are increased in rugged, high-altitude regions where gage placement can significantly alter gage catch. In alpine regions, volume alone will overwhelm most snow collection systems. Reynolds [1972] states that at high-altitude, high-volume snowfall sites, gage capacity must be at least 180 cm of water. The problem of keeping the gage at a fixed height above the surface or from being buried during large events is not addressed. During the 1986 snow season at Emerald Lake, 270 cm of water fell as snow, leaving serious questions about gage maintenance, anti-freeze recharge, and utility if a snow collection gage had been used. In a remote alpine environment like Emerald Lake, snow collection gages cannot be relied upon for snowfall data. Instead, detailed ground measurements of snow were made, both on an event basis and at regular intervals in snow pits.

We had planned to measure snowfall on pairs of snowboards at three sites in the Emerald Lake watershed during the 1986 snow season (Inlet, Pond, and Ridge). Avalanche danger rendered the Pond and Ridge sites inaccessible immediately after storms, and a very large storm in mid-February buried all of the snowboards at all sites, so that replacements had to be used. Table 3.3 below presents a comparative summary of snow deposition and volume at three sites in the watershed during the 1986 snow season.

Both snowboard and snow pit data from the first part of the winter show that while deposition depths varied between sites during a snowfall event, deposition of snow water equivalent (SWE) was consistent between the three sites. Snow pit data show that, in general, SWE was very similar between sites during the prior to the storm of February 18-19. During that event, significant redeposition occurred due to avalanches, wind scour, and redeposition. After mid-February, snowfall event measurements were made only at the lake site. Deposition from the mid-February storm buried the Inlet site under a very large avalanche and produced a major wind-caused redeposition drift at the Ridge site. Avalanche hazard and logistic problems from the volume of snow deposited during that event delayed comparative pits for two months. By that time, snow volume at the three sites was distinctly different.

Table 3.4 below shows a summary of snowfall at the Inlet site in the Emerald Lake watershed during the 1986 snow season. These data represent our best estimate of snow deposition volume over the watershed during the 1986 water year. Only 17 events were recorded, 9 of which were only a few cm of SWE in magnitude. Of the others, two (February 18-19 and March 19) account for nearly 60% of the season's precipitation. The mid-February event accounted for nearly 40% of the season's precipitation, and was one of the largest snowfall events on record in California. This storm initiated a major avalanche cycle throughout the Sierra Nevada [Wilson, 1986]. Avalanches that occurred during or immediately following this storm in the Emerald Lake watershed buried the inlet instrument site, and added enough mass to the ice on Emerald Lake to cause a displacement flood that depleted the lake of 50% or more of its liquid volume in a few hours. Concern about stability of the snowcover prevented access to the upper watershed for several weeks.

New snow densities during the 1986 snow season were high. In all, 9.0 m of snow fell in the watershed, accounting for 2.622 m of SWE.

Figure 3.1 presents event SWE volumes and totals and pit totals through the 1986 snow season at Emerald Lake. While snow board data from the ridge site do not indicate excess deposition during events, the pit totals suggest that the ridge site is a drift or deposition site for snow re-deposition during wind events between storms. Snow pits at the ridge site in May were 6.0 m deep, with average densities exceeding 500 kg m^{-3}. The large volume and high densities of snow deposition during the 1986 snow season made digging snow pits difficult and lengthened the intervals between pits at the two sites.

3.3. Emerald Lake Basin Event Summary

The objective of the field program was to sample each precipitation event for SWE and chemistry, with periodic sampling of pits to examine these same parameters in the accumulated snowpack. Event sampling was carried out at three locations: inlet, pond, and ridge. Snowboards were used for event sampling following established protocols [Perla and Martinelli, 1978]. A 1-m square plywood board placed on the old snow surface insures that the observer will not confuse the old snow with the new snow. The boards used were painted with chemically inert paint to minimize chemical contamination and a PVC tube was attached orthogonally to the board so it could be located after a heavy snowfall.

Two snowboards were placed several meters apart a each site on flat surfaces. As soon after each event as possible, each board was sampled. Melting and wind may remove snow from the boards; this leads to erroneous estimates of precipitation. Several samples were collected from each board using clear, graduated, PVC tubes. These tubes were inserted vertically until they reached a clean spatula inserted at the board surface. The sample was transferred to a clean plastic bag and weighed using a spring scale. Stepped samples were taken when the new snow depth exceeded the length of the tube (50 cm). Multiple samples were taken from both boards to get a mean value for the site. Depth was read from the graduations on the tube after insertion. Sample volume was calculated by multiplying tube cross-sectional area by the depth. The weight of the sample divided by the density of water, multiplied by the volume gave sample density.

The tubes worked well for obtaining chemical samples. They were acid washed periodically, and care was taken not to contaminate them in the field. Both ends were capped with acid washed PVC caps when not in use. Unfortunately, the tubes proved to be inadequate for measuring density. The tubes were thick-walled so the ends were outwardly beveled to minimize oversampling. The tubes were carefully calibrated using both sand and water for volume estimates, rather than relying on a diameter measurement. In spite of these precautions, the tubes were inconsistent in their ability to measure density. For a given type of snow they appeared precise, but their accuracy was highly suspect. Later in the season we adopted a better system for sampling density, which will be discussed below. In comparing the two methods, the tubes clearly exhibit an

unacceptable variance, which is unrepresentative of even a naturally heterogeneous snowpack. The tubes appear to over-sample in some types of snow and under-sample in others. The tubes deal poorly with even the smallest ice lenses because the lens is collapsed by the beveled edge, which then pushes snow out of the way as the tube is inserted further. It is desirable to have a sampling technique that minimizes sampling time, but our experience indicates strongly that chemistry and density must be sampled separately to maintain the individual integrity of either measurement. After May 3, all density and chemical samples were obtained separately.

No acceptable, commercially-available method of sampling snow density existed at that time. The conventional method involves inserting a 500 mL metal tube (also called a CRREL or SIPRE tube) into the pit wall, isolating the sample and weighing it [Goodison et al., 1981; Avalanche Research Centre, 1981]. This technique is extremely labor intensive and slow [Dexter, 1986] and is not feasible for continuous sampling of deep pits. Wedge-shaped cutters have the advantage of extracting a sample without requiring additional excavation, which makes them a great deal faster. The only commercially-available, wedge-shaped cutter at the time worked well in low-density, continental snowpacks, but its large surface-area-to-volume ratio of 1.44 leads to edge effect errors and the thin fabrication material deforms or is destroyed in dense snowpacks. Edge effects are important because they may be the largest source of error in density calculations. When a cutter is inserted, the edge isolates the sample by breaking the bonds or the grains separating it from the rest of the snowpack. The cutter edge may force the broken grains into the sampler or exclude them from the sample. This may result in under- or over-sampling. This error source is unquantifiable, but as the volume of the sample increases, this error diminishes. The surface-area-to-volume ratio is important because as the ratio decreases, the error because of edge effect decreases. Another widely used method is the Mount Rose (or Federal) sampler. It extracts a core of snow equal to the entire depth of the snowpack, thus only a mean density of the profile is obtained. The accuracy of this instrument has also been questioned although it is sufficient for its purpose as an index tool Work et al., 1965].

The cutter instrument and technique adopted was developed by Dr. Ron Perla of Environment Canada. The sampler is a wedge-shaped cutter 20-cm long, 10-cm wide, and 10-cm high giving a 1000-mL volume. To minimize deformation, 14 gage stainless steel was used. Occasionally it was necessary to pound the cutter into the pit wall with a rubber mallet and a less robust design would not withstand this treatment. The large volume gives a reasonable surface-area-to-volume ratio of 0.72, that minimizes under- or over-sampling. Edges are beveled to further reduce the edge effect. All cutters were carefully calibrated and found to have less than 1% volume error. In spite of the small error, the calculated correction was applied to all data. The 1000-mL cutter was used in conjunction with a top-loading digital scale. This allowed the sample to be weighed in the cutter as the tare weight of the cutter could be removed before sampling, making the process fast, precise, and accurate. A 6-m pit could be sampled for density in approximately 1 hour with one person sampling and the other recording the data (not including excavation time).

The event snowfall data are summarized in Table 3.5. Values listed represent the mean of all samples taken from both boards at each site. October storms produced little accumulation. The first major event occurred in the second week of November, followed by one more storm. December storms produced less than 0.5 m SWE and January had only one storm that brought the cumulative precipitation close to 1 m SWE. During the third week of February, a large storm deposited over 2 m of new snow (greater than 1 m SWE). The excessive loading over a short period of time produced an unstable snowpack and a major avalanche cycle followed. All snowboards were lost. Estimates of the event precipitation from this storm were obtained by sampling to the old snow surface and in this case are probably as accurate as the other values in Table 3.5. Replacement boards were used at the inlet site for the duration of the season and no further event samples were taken at the pond or ridge sites. One significant precipitation event followed in March, depositing 0.43 m SWE. The rest of the season produced a cumulative sum of less than 0.10 m SWE.

Table 3.5. shows early season variability in accumulation between the inlet, pond, and ridge sites. This may be a real difference resulting from variable precipitation in the basin or it may be due, in part, to sampling. A snowboard in one part of the basin may be scoured by wind before it is sampled while another location is not. It is impossible to sample all locations immediately after a storm terminates because of safety considerations. Accumulation in the watershed is not uniform but no discernible pattern is identifiable from the measurement sites. As the season progresses, between-site variability diminishes. By the second week in January, cumulative differences in all three sites have smoothed out, varying by a maximum of 4% on January 8 and by less than 5% by February 3.

3.4. Snow Pit Summary

Snow pits were excavated at the tower, inlet, pond, ridge, hole, cirque, east joint and southeast gully. Only the inlet, pond, ridge and hole were sampled intensively. Chemistry, density and temperature were measured at each pit. Pit data are summarized in Table 3.6. Samples for chemical analysis were collected as described above with dual profiles taken at each site. Density was determined using the tube measurements until early May, after which time density and chemistry were sampled independently as described above. The excessive amount of snow precluded taking dual density samples in the deeper pits but continuous profiles were obtained for the entire pit in all cases. Temperature was taken using digital thermometers at 10-cm increments until the temperature stabilized at 0° C, and it was checked periodically in the remaining profile to insure that the isothermal condition persisted. All values represent the mean values for each site. The data in Table 3.6 shows the 1986 water year was a large precipitation year, with snowpits up to 6 m deep and over 3 m of SWE at some locations. The overburden caused by excessive accumulation, coupled with the

warm temperatures, produced a deep, high density, snowpack.

3.5. Summary

The cumulative SWE measured from event samples and the total SWE from pits at corresponding dates agree relatively well Table 3.5 nd 3.6). The variation for date differences of two days or less ranges from 8 to 20%. These errors may be explained by the following. Pits and boards were not located at exactly the same points and the spatial heterogeneity of the snow cover may explain some of the variation. Losses from the boards before they could be sampled or sublimation at the pit location are error sources. These errors are unquantifiable. Another source for error is that the tubes led to spurious estimates of SWE.

In assessing the data and the field methods, several points should be noted. Snowboards work well if the locations are carefully selected. They must be placed at points not subject to scouring by wind and that are easily accessible so sampling may be carried out during, or immediately after a storm. Snowboards are effective in isolating the new snow from previously deposited snow; this makes them useful in chemical sampling. Snowpits are valuable for measuring SWE, stratigraphy, and mechanical and thermal properties of the snowpack. An advantage of snowpits is that they may be dug at any time; the disadvantage is that they require more time and effort than snowboards. Either method may be adequate in measuring seasonal SWE at a point. The decision should be based on the application of the data: if event data are needed then clearly the snowboards are preferable; if access is limited and time considerations are not critical, snowpits may be better.

3.6. References

Allis, J. A., B. Harris, and A. L. Sharp, A comparison of performance of five rain-gage installations, *J. Geophys. Res., 68*, 4723-4729, 1963.

Alter, J. C., Shielded storage precipitation gages, *Monthly Weath. Rev., 65*, 262-265, 1937.

Avalanche Research Centre, *Guidelines for Weather, Snowpack, and Avalanche Observations*, Tech. Mem. 132, 60 pp., Natl. Res. Council Canada, Ottawa, Ontario, 1981.

California Cooperative Snow Surveys, *Bull. 120-86, Fall Rep.*, Calif. Dept. Water. Resour., Sacramento, CA, 1986.

Codd, A. R., Seasonal storage precipitation gages, *Eos, Trans. Amer. Geophys. Union, 28*, 899-900, 1947.

Dexter, L. R., Aspect and elevation effects on the structure of the seasonal snowcover in Colorado, Ph. D. Thesis, 228 pp., Univ. Colorado, Boulder, CO, 1986.

Garstka, W. U., Hydrology of small watersheds under winter conditions of snow-cover and frozen soil, *Eos, Trans. Amer. Geophys. Union, 25*, 838-874, 1944.

Goodison, B. E., Accuracy of Canadian snow gage measurements, *J. Appl. Meteorol., 17*, 1542-1548, 1978.

Goodison, B. E., H. L. Ferguson, and G. A. McKay, Measurement and data analysis, in *Handbook of Snow*, edited by D. M. Gray and D. H. Male, pp. 191-274, Pergamon Press, New York, 1981.

Goodison, B. E. and J. R. Metcalfe, Canadian snow gauge experiment: recent results, *Proc. Western Snow Conf., 50*, 192-195, 1982.

Hamon, W. R., Computing actual precipitation, in *Distribution of Precipitation in Mountainous Areas*, Geilo Symp. No. 1, pp. 159-174, WMO, 1972.

Harris, R. E. and A. C. Carder, Rain and snow gauge comparisons, *Can. J. Earth Sci., 11*, 557-564, 1974.

Israelson, C. E., Reliability of can-type precipitation gage measurements, *Tech. Rep. 2*, 74 pp., Utah Water Res. Lab., Utah State Univ., Logan, UT, 1967.

Larson, L. W., Precipitation and its measurement, a state of the art, *Ser. 24*, 74 pp., Water Resour. Res. Inst., Univ. Wyoming, Laramie, WY, 1971.

Larson, L. W. and E. L. Peck, Accuracy of precipitation measurements for hydrologic modeling, *Water Resour. Res., 10*, 857-863, 1974.

Osborn, H. B., L. J. Lane, and J. F. Hundley, Optimum gaging of thunderstorm rainfall in southeastern Arizona, *Water Resour. Res., 8*, 259-265, 1972.

Pagliuca, S., The measurement of precipitation on a windy mountain summit, *Eos, Trans. Amer. Geophys. Union, 15, part II*, 385-393, 1934.

Peck, E. L., Snow measurement predicament, *Water Resour. Res., 8*, 244-248, 1972.

Perla, R. and M. Martinelli, Jr., *Avalanche Handbook*, Agric. Hbk. 489, rev. ed., 254 pp., U.S. Dept. Agric., Washington, DC, 1978.

Rawls, W. J., D. C. Robertson, J. F. Zuzel, and W. R. Hamon, Comparison of precipitation gage catches with a modified Alter and a rigid Alter type windshield, *Water Resour. Res., 11*, 415-417, 1975.

Reynolds, G. W., Weight capacity requirements for precipitation measurements in the Wasatch Mountains, *Water Resour. Res., 8*, 249-254, 1972.

Sevruk, B., Correction of precipitation measurements: Summary report, in *Correction of Precipitation Measurements*, edited by B. Sevruk, Züricher Geogr. Schr. No. 23, pp. 13-26,

TABLE 3.1. 1986 Precipitation and Snow Water Equivalent - Percent of 50-Year Mean

Area	February 1		March 1		April 1		May 1	
	PPT	SWE	PPT	SWE	PPT	SWE	PPT	SWE
Tulare region	108%	82%	140%	143%	150%	142%	140%	125%
Kaweah	125%	*	175%	*	180%	*	165%	*

PPT - precipitation
SWE - snow water equivalent
* no information
data source: California Cooperative Snow Survey, 1986

TABLE 3.2. 1986 Water Year Precipitation (cm) - Lodgepole Ranger Station (1943 m elevation)

	Oct	Nov	Dec	Jan	Feb	Mar	April	May	June	July	Aug	Sept
1986 water year	4.4	30.7	15.5	23.6	80.4	27.7	6.9	1.5	0.0	1.5	0.3	7.4
50-year mean	4	10	20	22	21	17	11	4	1	0	1	2
% of mean	109	302	77	106	389	162	63	37	0	407	55	397
1986 cumulative	4.4	35.2	50.7	74.2	154.6	182.2	189.2	190.7	198.7	192.1	192.4	199.8
50-year mean	4	14	34	56	77	94	105	109	110	111	111	113
% of mean	109	248	148	131	200	193	180	174	173	173	173	177

data source: California Cooperative Snow Survey, 1986

TABLE 3.3: Snow Volume Comparison
Emerald Lake Watershed, 1986 Water Year

Deposition: 10/06/85 - 02/03/86 (9 events)

Site	Samples	Snow Deposition Depth (m)	Cumulative SWE (m)
2. Inlet	10	4.34	1.04
3. Pond	4	2.97	1.01
4. Ridge	5	3.83	1.06

Concurrent Snow Pit Totals:

Date	Site	Snow Pit Depth (m)	Total SWE (m)
02/05/86:	2. Inlet	2.30	0.84
	3. Pond	2.25	0.88
	4. Ridge	2.45	0.90
05/06/86:	2. Inlet	4.05	2.40
	3. Pond	2.90	1.38
	4. Ridge	5.90	3.17

TABLE 3.4: Basin Snow Deposition
Emerald Lake Watershed, 1986 Water Year

Date	New Snow (m)	ρ_{pp} (kg m^{-3})	New SWE (m)	Cumulative SWE (m)	Percent Total	Cumulative Percent
06 Oct	0.060	267	0.016	0.016	0.006	0.006
08 Oct	0.040	275	0.011	0.027	0.004	0.010
21 Oct	0.301	126	0.038	0.065	0.015	0.025
11 Nov	0.788	150	0.118	0.183	0.045	0.070
20 Nov	0.460	250	0.115	0.298	0.044	0.114
03 Dec	1.415	270	0.378	0.676	0.144	0.258
11 Dec	0.118	300	0.035	0.711	0.013	0.271
08 Jan	0.375	410	0.152	0.863	0.058	0.329
03 Feb	0.779	230	0.178	1.041	0.068	0.397
06 Feb	0.092	55	0.005	1.046	0.002	0.399
18 Feb	2.015	410	0.826	1.872	0.315	0.714
19 Feb	0.600	400	0.240	2.112	0.092	0.806
19 Mar	1.467	290	0.427	2.539	0.163	0.969
10 Apr	0.105	328	0.035	2.574	0.013	0.982
16 Apr	0.090	151	0.014	2.588	0.005	0.987
04 May	0.110	215	0.024	2.612	0.009	0.996
07 May	0.040	241	0.010	2.622	0.004	1.000

TABLE 3.5. Snow Board Data Summary - 1986 Water Year

Site	Date		Depth (m)	Density ($kg\,m^{-3}$)	SWE (m)	Cum. SWE (m)
inlet	6	Oct	0.06	267	0.02	0.02
	8	Oct	0.04	275	0.01	0.03
	21	Oct	0.30	126	0.04	0.07
	11	Nov	0.79	150	0.12	0.19
	20	Nov	0.46	250	0.12	0.31
	3	Dec	1.42	270	0.38	0.69
	11	Dec	0.12	300	0.04	0.73
	8	Jan	0.38	410	0.15	0.88
	3	Feb	0.78	230	0.18	1.06
	6	Feb	0.09	55	0.01	1.07
	18	Feb	2.02	410	0.83	1.90
	19	Feb	0.60	400	0.24	2.14
	19	Mar	1.47	290	0.43	2.57
	10	Apr	0.11	328	0.04	2.61
	16	Apr	0.09	151	0.01	2.62
	4	May	0.11	215	0.02	2.64
	7	May	0.04	241	0.01	2.65
pond	20	Nov	0.43	271	0.13	0.13
	18	Dec	1.37	380	0.52	0.65
	8	Jan	0.45	410	0.18	0.83
	3	Feb	0.72	240	0.17	1.00
ridge	20	Nov	1.10	235	0.26	0.26
	11	Dec	1.38	290	0.40	0.66
	8	Jan	0.47	380	0.18	0.84
	3	Feb	0.89	250	0.22	1.06

TABLE 3.6. Snowpit Data Summary - 1986 Water Year

Site	Date		Depth (m)	Density ($kg\,m^{-3}$)	SWE (m)
tower	18	Feb	2.48	422	1.05
	3	Mar	3.70	485	1.79
	4	Mar	3.50	429	1.50
inlet	18	Jan	1.65	461	0.76
	6	Feb	2.30	365	0.84
	5	Mar	3.20	461	1.48
	2	May	4.05	593	2.40
	21	May	3.57	554	1.98
	27	June	2.03	590	1.20
pond	5	Feb	2.25	392	0.88
	12	Apr	3.17	524	1.66
	6	May	2.90	475	1.38
	24	May	2.10	520	1.09
	26	June	2.20	588	1.29
ridge	17	Jan	1.98	411	0.81
	4	Feb	2.45	365	0.90
	13	Apr	6.00	548	3.29
	6	May	5.90	520	3.17
	23	May	4.65	572	2.66
	27	June	2.50	578	1.44
hole	3	May	3.50	497	1.74
	7	May	4.80	485	2.33
	24	May	3.90	513	2.00
	26	June	2.00	557	1.11
cirque	11	Jan	3.05	400	1.22
east joint	5	May	2.80	487	1.36
north joint	22	May	2.40	509	1.22

Figure 3.2. Event and cumulative snow water equivalent (SWE) volumes from snowboard measurements for the Emerald Lake watershed, 1986 water year.

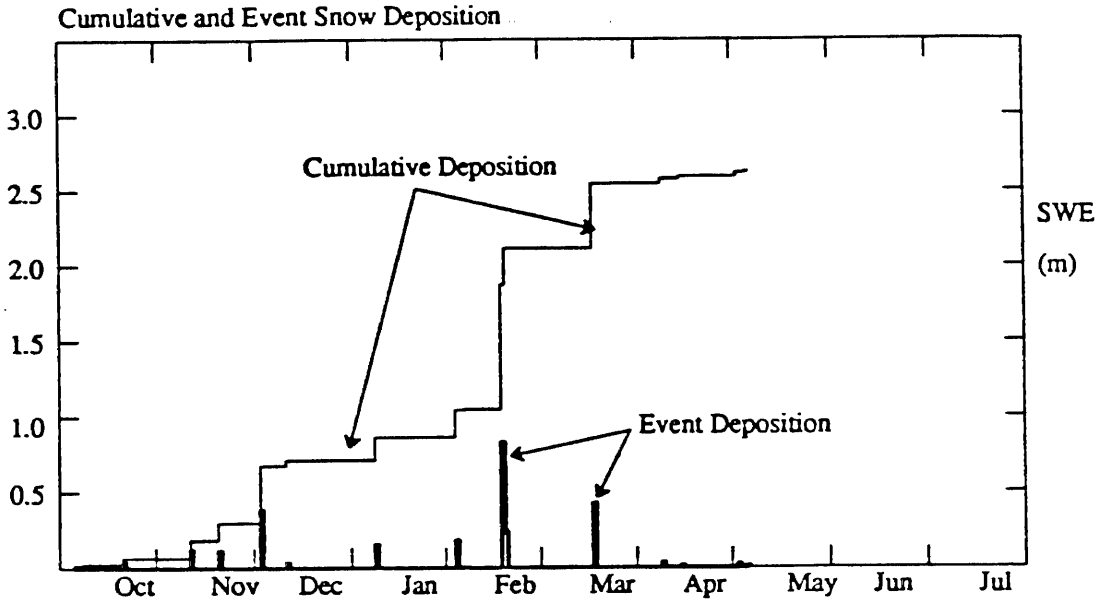

4. Chemical Characteristics of the Seasonal Snowpack

4.1. Introduction

Snowfall is the major pathway for fluxes of water and ions from the atmosphere to terrestrial and aquatic ecosystems in montane basins of the Sierra Nevada. The montane snowpack accumulates and integrates wet and dry deposition throughout the snow season. During this storage period many physical, chemical and biological transformations occur, which can lead to the release of relatively high concentrations of solutes from the snowpack in a short time period [Johannessen and Henriksen, 1978]. Understanding of snowpack contributions to the surface water chemistry of California montane basins is further complicated by the rugged and variable terrain. Large topographic differences over short distances result in spatial variation in snow accumulation, and in temporal differences in the timing of melt, within a given watershed.

Objectives

The objectives of the hydro-chemical portion of this project are:

1) Characterize the chemistry of snow deposition by separate storms, and of the accumulated snowpack through the winter.
2) Calculate chemical loading to the Emerald Lake watershed on a seasonal basis.
3) Evaluate the significance of spatial or temporal variations in snow chemistry within the basin.
4) Determine if an ionic pulse of concentrated solutes leaves the snowpack at the initiation of melt runoff.

General Approach

To assess the impact, or to evaluate the potential impact, of atmospheric acidity on an alpine environment requires measurements of the areal load of solutes (mass per unit area or volume) to the drainage basin. Measurements of subsequent chemical load to streams and lakes, as modified by snowmelt and soil buffering processes, are then necessary to understand and evaluate the effects of acidic inputs on surface waters within the basin [Rascher et al., 1987]. For the Emerald Lake watershed during two snow accumulation and snowmelt seasons, we describe the chemical composition of snowfall, the snowpack and snowmelt.

Sampling in the Emerald Lake watershed (ELW), covered the periods from October 1984 to May 1985 and from October 1985 to June 1986. Snow samples were collected intensively at one site (the inlet), and periodically at other locations in the basin to obtain an indication of the magnitude and importance of spatial and temporal variability in snow chemistry throughout the watershed (Figure 4.1). Sample collection, analytical equipment, and procedures applicable to alpine environments in the winter season were developed, refined, and then combined with depth and density measurements of the seasonal snow cover to measure the spatial distribution of snow chemistry over the watershed. Stream inflows, Emerald Lake, and the Emerald Lake outflow were sampled [Melack et al., 1987] to determine chemical loading to the lake and to evaluate the chemical response of surface waters to snowpack runoff.

Chemical data for the 1985 and 1986 snow seasons are presented in several sections. Background information on acidic snow deposition and snowpack runoff is included to provide a summary of the current state of knowledge, and to provide a framework in which to interpret the results of our research. Sampling and analytical methods, as well as quality control procedures, are described in the methods section. Results are presented in the next section. Following the results is a discussion which interprets the results in the context of the information presented in the background section.

4.2. Background

Snowfall Chemistry

Snowfall chemistry appears to be significantly different from that of rain [Raynor and Haynes, 1983; Reynolds, 1983]. It is worthwhile to explore the physics of cloud formation to understand the reasons for this difference. Snow and rain transport solutes from the atmosphere to the earth's surface through two main processes, nucleation scavenging within the cloud (rainout or snowout) and below-cloud scavenging by attachment of particles to existing hydrometeors (washout) [Davidson and Honrath, 1987].

Hydrometeors in clouds begin as ice nuclei or condensation nuclei. Heterogeneous ice nucleation by atmospheric aerosols is template specific and consequently inefficient. These ice nuclei are generally composed of clay particles derived from the earth's crust [Mason, 1975]. Only about one in 10^9 aerosols are active as ice nuclei at –10°C [Schemenauer et al., 1981], whereas all hygroscopic particles in the atmosphere with diameters greater than 0.2μm make good condensation nuclei [Dennis, 1980]. The dissimilar nucleation processes between snow and rain can generate different ionic ratios between the two types of nuclei, *e.g.* anthropogenic sulfur-containing aerosols make poor ice nucleating agents, while many forms of particulate sulfate are active condensation nuclei [Davidson and Honrath, 1987].

Nucleated ice crystals grow by two methods: water vapor diffusion or by accretion of cloud droplets in warmer clouds. Cloud droplets grow by continued vapor diffusion and by coalescence with other liquid droplets. Droplets can interact with acidic precursor gases, such as SO_2, to form acidic (e.g. H_2SO_4) droplets [Kumar, 1986]. Since the supersaturation of water vapor with respect to liquid water is always smaller than that with respect to ice, ice crystals often grow at the expense of cloud droplets. Growth of an ice crystal by diffusion is thus similar to a distillation process. Vapor diffusion concentrates the solutes in cloud drops and dilutes the solutes in ice crystals. Borys et al. [1983] found that in an alpine area of northwest Colorado, cloud water contains three times the acidity and four to five times the conductivity of unrimed snow crystals. Nucleation differences and subsequent growth differences may partially explain why, at present, solute concentrations of snow falling in the Sierra Nevada are relatively low when compared with rain falling on the same

watersheds.

Across the Canadian Precambrian Shield of eastern Canada approximately twice as many sulfate ion equivalents are deposited annually as are nitrate ion equivalents [Barrie and Sirois, 1982]. Seasonally, the relative contribution of the two ions to acidity is quite different [Barrie et al., 1983]. Nitrate ion equivalents exceed sulfate ion equivalents in the Canadian Precambrian Shield snowpack during winter by 60% [Barrie and Vet, 1984]. Similar findings have been reported during winter in southwestern Quebec [Frantisak et al., 1980] and in the Adirondacks [Galvin and Cline, 1978].

This seasonal variation in the sulfate-to-nitrate ratio appears to be the result of differences in the chemistry of rain and the chemistry of snow. Topol [1986] found that in winter precipitation at nine sites in northeastern United States, there was a significant difference in concentrations of sulfate and nitrate in rain versus snow. The sulfate-to-nitrate molar ratio was 0.48 for snow, but 1.02 for winter rain. Woo and Berg [1986] report significant differences in nitrate concentrations between rain events and snow events at their mountain research site near Lake Tahoe, California. Similar results are reported for a high-elevation site (3000 m) in Colorado by Hubert et al. [1983]. These data suggest that the high nitrate-to-sulfate ratio in snowfall is due to the more effective capture of HNO_3 vapor by snow during below-cloud scavenging. Nitric acid vapor, with a higher diffusion rate than aerosols and a high affinity for surfaces, is rapidly scavenged from the atmosphere by falling snow, five times as fast as the incorporation of aerosol NO_3^- or SO_4^{2-} into snow or rain [Hubert et al., 1983; Chang, 1984; Chan and Chung, 1986].

Theory and experimental evidence strongly indicate that nucleation differences in clouds, and washout scavenging differences below clouds, cause the chemistry of recently deposited snow to differ from that of rain. Flux of atmospheric acidity at a particular location therefore depends on precipitation type. The relatively high nitric acid input by snow to the mountain snowpack is of particular concern. Nitric acid becomes most prevalent as an acidifier of aquatic ecosystems during spring snowmelt, when the neutralization by biological reduction of nitrate is thought to be low [McLean, 1981].

Chemistry of the Seasonal Snowpack

Snow on the ground is a dynamic material that changes markedly in response to heat and mass transport [Colbeck, 1982]. Once a layer of snow is deposited in a mountain snowpack, individual snow crystals are immediately deformed by metamorphic processes. In the time span of days to weeks, snow crystals within the mountain snowpack are transformed, usually into rounded grains characterized by increasing size and a decreasing surface-to-volume ratio. Deformation and recrystallization of snow crystals within the snowpack are a consequence of snow's fine-grained texture, high specific surface area, and existence at or near its melting point. As with any solid near its melting point, snow is thermodynamically active.

After snow is deposited in the mountain snowpack it can be considered a matrix of ice particles. Following Sommerfeld and LaChapelle [1970], most researchers call these ice particles, grains. Considering snow as a thermodynamic system, metamorphic processes within the snowpack are the result of transformation of snow grains toward a state of equilibrium, where free energy is minimized. Water vapor relocates to decrease both the surface energy per unit area and the surface energy per unit volume [Male, 1980]. Metamorphism controls the properties of snow within the snowpack. Changes in density, crystal size and shape, the growth and decay of bonds between grains, and the rejection of dissolved impurities at crystal surfaces are all influenced by the type and rate of snow metamorphism [Raymond and Tusima, 1979; Colbeck, 1981; Sommerfeld, 1983].

Dry snow metamorphism within the mountain snowpack is a function of differential water vapor diffusion [Seligman, 1936]. Vapor movement is the consequence of local vapor density differences in the vicinity of grains. Vapor density gradients within the snowpack generate the preferential sublimation of water molecules from grain surfaces that have relatively high free energy. Through sublimation, water vapor molecules are recrystallized to the ice phase on grain sites that have relatively lower free energy [Langham, 1981].

These vapor density gradients are mainly caused by temperature gradients. Mass transport within the snowpack is also influenced by grain surface geometry, crystal structure, snow density and atmospheric deposition conditions [Colbeck, 1983]. The relevant temperature gradient is that in the ice matrix pores, because the thermal conductivity of the ice matrix is about 100 times that of pore air, generating a much greater thermal gradient across pore space than across grains [Akitaya, 1974]. The magnitude and timing of temperature gradients within the snowpack determines whether metamorphic processes will be kinetic, equilibrium, or a serial combination of the two [Colbeck, 1986]. The shape, size and solute chemistry of snow grains found in the mountain snowpack are largely a product of the thermal history of the snowcovered area.

Thus water molecules within the snowpack are continuously transferred by sublimation between the solid and the gaseous phase. Each snow grain acts as both a water molecule source and sink [Yosida et al., 1955]. In most alpine snowpack conditions the recrystallization can be complete, with most or all snowpack water molecules passing through the vapor phase at least once [Colbeck, 1982; Sommerfeld, 1983].

Recrystallization of snowpack ice molecules generates a physical fractionation of ionic species within the mountain snowpack. Impurities within the ice crystal lattice are segregated on the outer surface of snow grains because the impurities are not readily incorporated into the crystalline lattice during recrystallization. Snow grains are continuously purified during the snow accumulation season by the constant sublimation of smaller particles and the migration of grain boundaries on larger particles. These processes concentrate the impurities on the snow grain surface and in pore air spaces between grains [Colbeck, 1981]. Liquid water moving through the snowpack readily leaches the soluble impurities.

Percolation of liquid water through the snowpack, either by melt or rain, accelerates grain growth [Colbeck, 1979]. Where only a small amount of liquid water is available, as is generally the situation in mountain snowpacks of temperate regions, the advancing water freezes in place until the next melt or rain cycle. During this refreezing process the snow impurities are further segregated onto the surface of the newly formed ice [Mizuno and Kuroiwa, 1969], where they are available to enrich the next wave of infiltrating water. Multiple melt-freeze cycles, occurring before the percolating water reaches the base of the snowpack (and runoff commences), results in the highest concentration of ionic species in the first fraction of meltwater [Colbeck, 1981]. Dry snow metamorphism and melt-freeze cycles thus prepare the mountain snowpack for rapid removal of the soluble ions accumulated and stored over the winter snow season.

Not all chemical species are distributed identically at the percolating meltfront. Experimental work in the field and in the laboratory has established that mountain snowpacks generally exhibit preferential elution of ions [Tranter et al., 1986; Brimblecombe et al., 1985]. Preferential elution of ions, as defined by Davies et al. [1982], is the removal of some ions from the snowpack, more quickly than others, by rain or meltwater.

The order of preferential elution of the ions in a snowpack is consistent with some ions and inconsistent with others. Chloride is consistently the most slowly eluted ion, and sodium is almost as slow. Sulfate ions are eluted first and nitrate ions are generally eluted second. The order of elution is not consistent for hydrogen. The general elution sequence of ions from the mountain snowpack, as deduced by Brimblecombe et al. [1985], is $SO_4^{2-} > NO_3^- > NH_4^+ > K^+ > Ca^{2+} > Mg^{2+} > H^+ > Na^+ > Cl^-$. However, research on the preferential elution of ions from lower elevation sites, where winter rain is common, provides no evidence for the selective loss of ions [Cadle et al., 1984; Rascher et al., 1987].

Physicochemical reasons for this phenomenon are unknown. Preferential elution of ions may be the result of many factors: ionic species have different solubilities in ice; solutes are inhomogeneously distributed within snow grains; ionic solubility depends on the rate of freezing; chromatographic separation may occur during meltwater percolation through the ice matrix [Tranter et al., 1986]. The atmospheric history of snow may also influence the selective removal of ions from a snowpack. Initial nucleation and growth of ice crystals in clouds, and subsequent scavenging during the precipitation process, may determine whether specific ions are generally incorporated inside the crystal lattice, or attached to the outside of snow crystals. Atmospheric pollutants, such as NO_3^-, can be expected to be adsorbed to the outer surface of snow crystals by washout, and to be readily available in the mountain snowpack for removal early in the melt process.

The interaction of snowpack processes, such as snow metamorphism and preferential elution, with any initial pollutant, is critically important in evaluating the impact of meltwaters on the environment. The environmental impact of ions collected in the snowpack during the winter storage period is intensified by the ionic pulse, which causes ions to be released in the first fraction of meltwater at concentrations significantly higher then their bulk concentrations. Preferential elution of acidic anions further intensifies the fractionation mechanism that can lead to an acidic pulse of meltwater.

Ionic Pulse

In California and much of western North America, montane snow accumulates in deep snowpacks from about November to mid or late April. The montane snowpack is a long-term integrator of wet and dry atmospheric deposition, which is held in storage until release during a melt period. While the concentration of solutes in the montane snow of western North America is usually very low [Melack et al., 1982; Laird et al., 1986; McBean and Nikleva, 1986; Michaels et al., 1987], the large flux of water to the snowpack can produce significant chemical loading.

Snow metamorphism, as well as chemical and biological transformations, can alter the chemical concentration and distribution of ionic solutes in the snowpack, and lead to the release of relatively high concentrations of solutes in the first fraction of snowpack runoff. Field and laboratory experiments demonstrate that initial stages of melt often have ionic concentrations many times higher than averages for the whole snowpack [Colbeck, 1981; Cadle et al., 1984; Rascher et al., 1987]. Ionic concentrations in the initial melt are generally 6-12 times higher than the average concentration of the snowpack [Johannessen and Henriksen, 1978; Seip, 1980], and increases of 20× are not uncommon [Suzuki, 1982; Stein et al., 1986].

Meltwater that is highly concentrated for a short period of time is generally termed an ionic pulse. If the snowpack is acidic, the ionic pulse will also be acidic. Given a concentration factor of 6, a snowpack with negative alkalinity and a pH of 5.46 will generate meltwater with a pH of 4.91. If concentrated by a factor of 15, the snowpack will generate an ionic pulse of meltwater with a pH of 4.52.

This fractionation of the ionic solutes in the initial stages of snowmelt appears to be the main cause of sharp drops in the pH of surface waters during the spring melt period [Haapala et al., 1975; Henrikson and Wright, 1977; Skartveit and Gjessing, 1979; Seip et al., 1980; Morris and Thomas, 1985]. Kelso et al. [1986] report that acid loading from snowmelt waters in the spring of 1981 caused serious declines in alkalinity in all 30 headwater lakes of Ontario that were investigated. Snowmelt waters depressed pH values in three central Ontario lakes intensely studied by Jeffries et al. [1979], who report that these low pH values were passed on to littoral zones and tributary spawning and nursery grounds for fish.

A short-term increase in acid concentration (episodic acidification) during spring melt may cause severe physiological stress to fish and other aquatic organisms and has led to massive fish kills in Norway [Leivestad and Muniz, 1976; Leivestad et al., 1976]. Adult rainbow trout *(Salvo gairdneri)* exposed to water at pH ≤ 4.9 for time periods that approximate that of snowmelt in temperate regions of North America experience a substantial impairment of plasma electrolytic regulation and

osmotic balance, and exhibit various hematological and cardiovascular abnormalities [Giles et al., 1984].

Similar physiological and mortality responses to pH levels commonly associated with an acidic pulse in water from snowpack runoff are reported in laboratory experiments by Brown et al. [1984] for rainbow trout *(Salvo gairdneri)*, by Gunn and Keller [1984] for lake trout *(Salvelinus nanaycush)*, and by Jones et al. [1987] for arctic char *(Salvelinus alpinus)*. Young brook trout *(Salvelinus fontinalis)* in the spawning and nursery grounds in and near Emerald Lake emerge from gravels in late winter or early spring, immediately before or during snowmelt. If snowmelt water input is acidic, the emergent alevins will be subjected to a sharp pH gradient between interstitial and surface waters, which they may be unable to withstand [Peterson, 1982].

Water from snowmelt runoff flowing below lake ice is generally not diluted with lake water [Charette et al., 1986]. This lack of meltwater mixing, a consequence of thermal stratification in ice-covered lakes, passes snowmelt waters directly across lakes into downstream aquatic ecosystems [Bergmann and Welch, 1985].

Prediction of meltwater chemistry from bulk snowpack concentrations or cumulative snow event concentrations is not straightforward. The original distribution of ions in the snow grains, the magnitude and type of snowpack metamorphism, the degree of mechanical dispersion at the advancing waterfront, and the number and intensity of melt-freeze cycles prior to runoff all play important roles in determining meltwater solute concentrations [Colbeck, 1981]. Therefore, understanding the dynamics of snowmelt runoff through the Emerald Lake watershed is thus imperative when assessing the sensitivity of this alpine environment to atmospheric deposition.

Spatial and Temporal Variations in the Chemistry of Snow Covered Area

Chemical inputs from the mountain snowpack to alpine basins, such as the Emerald Lake watershed, vary spatially and temporally in a complex and interactive manner. The large topographic variations over short distances, which are so typical of alpine catchments, result in large differences in snow accumulation, ionic load, and the timing of melt within the basin. Objectively quantifying the chemistry of snow covered area to calculate chemical load for an alpine watershed is difficult.

It is essential to determine the total chemical content of snow covered area in studies on the impact of acid deposition on aquatic ecosystems. Regional levels of pollution have been determined by using the chemical composition of snowcover [Johannessen and Henriksen, 1978; Barrie and Vet, 1984]. These studies were forced to make the assumption that snow cover is chemically homogeneous over an arbitrary scale, dictated by logistical considerations.

However, obtaining a representative sample of snow chemistry from samples collected at one location is unlikely. Barrie and Vet [1984] report that in a survey of snowpack chemistry on the Eastern Canadian Shield, the coefficients of variation (ratio of the standard deviation to the mean, expressed as a percentage) were 12-41%, differing for individual ions. Cadle et al. [1984] and Jones and Sochanska [1985] each report that snow cover in forested areas is chemically heterogeneous. Variability between snow cores at a single site often exceeded variability between sampling sites in the Wasatch Mountains of Utah [Messer et al., 1982]. And in a small, remote Scottish catchment, Tranter et a' [1987] report that fresh snow is chemically heterogeneous on a scale of 50 m, and again on an intense sampling scale of 1 m. Aged snow was also chemically heterogeneous at the same scales. Both the vertical and horizontal chemical content of the Scottish snowpacks were significantly heterogeneous at a scale of 1 m.

Spatial variability in many of the physical properties of snowcover, *e.g.* snow depth, density, snow water equivalence and temperature, have been discussed earlier in this report, in the chapter on the characteristics of snow covered area. These physical properties all affect the ionic concentration and/or chemical loading in alpine watersheds [Richards, 1973]. Spatial variability in processes such as changes in wind direction and snow type during storms [Langham, 1981], mechanical changes during deposition [Adams, 1981], and variations in the type and rate of snowpack metamorphi [Colbeck, 1981] can also effect the chemical composit of the mountain snowpack to an unknown degree.

Altitude, solar aspect, slope angle and meteorology determine where, when and how rapidly melt occu [Martinelli, 1965; Meiman, 1968; Richards, 1973; Woo and Slaymaker, 1975; Granger and Male, 1978; Dozier and Outcalt, 1979]. The date melt commences may affect the chemical composition of snow meltwater if there are seasonal differences in the chemical composition of snowfall. Meltwater can percolate through the snowpack as a film, increasing the scavenging ability of advancing meltwaters and consequently increasing the ionic concentration of runoff waters from the snowpack [Suzuki, 1982]. Conversely, channels or macropores in the snowpack at the onset of runoff route flow quickly from the snow surface to the ground [Kattelmann, 1985], decreasing the scavenging ability of meltwater and leading to relatively lower ionic concentrations of runoff waters from the snowpack.

At the present state of knowledge it is not possible to quantify the relative amounts of solute held within and adsorbed on the surface of snow crystals. Very little is known on how chemical transformations occur, and little is known on how concentrations are changed within the mountain snowpack by differing rates and types of snow metamorphism. What is known about the chemistry of snow covered area is that deeper snowpacks generally have different temperature regimes than do shallow snowpacks, that deeper snowpacks undergo different types of snow metamorphism at different rates than do shallow snowpacks, that deeper snowpacks generally have a larger ionic accumulation budget than do shallow snowpacks, and that deeper snowpacks generally melt at a different rate and a different time scale than do shallow snowpacks. Therefore, to evaluate and predict the potential impact of acidic deposition on alpine aquatic ecosystems, it is vital to understand and quantify the spatial and temporal distribution of chemical inputs by the mountain snowpack to the ecosystem.

Maximum Effect Scenario

The simple analysis of the average chemical composition of a particular snowpack cannot be directly used as a surrogate for meltwater chemical composition. Fractionation and preferential elution of ions from the mountain snowpack can cause meltwater chemistry to deviate strongly from the average bulk concentration of the snowpack. Furthermore, in montane basins such as the Emerald Lake watershed, topographic differences generate substantial spatial differences in snow accumulation (and consequent ionic loading) and the timing of melt. Moreover, strong maritime influences on Pacific Coast meteorological processes can produce winter rain storms as high as the crest of the central Sierra Nevada, further complicating the prediction of meltwater chemistry [Berg, 1986]. Predicting the ionic concentrations of spring meltwater requires a thorough knowledge of the physical and atmospheric inputs to the mountain snowpack, as well as knowledge of the seasonal metamorphic evolution of the snowpack prior to the onset of melt.

With this background information, it is possible to construct a scenario for the maximum effects of snowmelt runoff on aquatic ecosystems. Cold temperatures during winter storage result in kinetic snowpack metamorphism, recrystallizing all water molecules in the snowpack many times [Colbeck, 1982; Sommerfeld, 1983]. Snowpack solutes will be highly concentrated on grain surfaces and in pore air spaces. A lack of warm storms from maritime air masses will insure that ions are not scavenged from the snowpack by rain-on-snow events prior to spring melt.

A sequence of repeated melt-freeze cycles will remove solutes from the upper portion of the snowpack and concentrate them in the lower portion of the snowpack. The first fractionation of meltwater from the snowpack will contain a high concentration of solutes. Then slow, uneven melting of the basin's snowcovered area will insure that the initial runoff waters are not diluted with lower concentration meltwaters from other portions of the watershed, or from dilute higher portions of the snowpack. Basal ice will isolate the limited buffering ability of the thin alpine soils from snowmelt runoff, and will transfer this acidic meltwater rapidly to aquatic systems.

Aquatic systems which are characterized by poor buffering, minimal groundwater flow and rapid turnover, such as Emerald Lake, will suffer the most biological and physical change, as a result of episodic acidification during spring runoff.

4.3. Methods

Careful cleaning, collection, storage, processing, and analysis are required to insure reliable chemical measurements of the very dilute snow and snowmelt that occur in the Sierra Nevada. Only plasticware (usually PVC, polyethylene, or polycarbonate) containers were used. Prior to use the containers were soaked in 10% HCl and fastidiously rinsed at least five times with deionized water (conductance 0.2–0.5 $\mu S\,cm^{-1}$). If liquid samples were to be obtained, the containers were rinsed with the sample also.

Snow samples were obtained on an event basis for most storms that deposited more than 1 cm of water. Duplicate, vertical sections were collected from snow boards with carefully cleaned clear PVC coring tubes (5-cm diameter, 50-cm long, with a sharp, beveled cutting edge) and deposited in clean polyethylene bags. If snow depths were greater than 30 cm, multiple sections were taken and deposited in separate bags to insure the veracity of the profile. During the winter of 1985 most samples were taken from snow boards located near the inlet to Emerald Lake (Figure 4.1). During the winter of 1986 multiple samples were taken from pairs of snow boards located near the inlet, pond, and on the ridge between Emerald and Pear lakes. During both years the frequency of sample collection in the watershed during winter was dictated by snow conditions and avalanche hazard. Usually immediately following a snow deposition event sites above the lake could not be visited safely, and under some conditions even the site at the inlet could not be reached. When this occurred, samples were taken near the outflow of the lake.

Exceptionally heavy snowfall during February 17-19, 1986, resulted in nearly 3 m of snow deposition ($\simeq$ 1.34 m SWE), along with several large avalanches, which irretrievably buried all snow boards in the watershed. Samples of this event were taken from a snow pit dug to a stratum recognizable as the snow surface prior to the storm. Two new snow boards were placed at the inlet, and event sampling was limited to this site for the remainder of the 1986 snow season.

Snow samples of the whole snowpack were obtained by digging pits to the ground and collecting duplicate, contiguous, vertical sections each about 30 cm in length for the entire profile, using the same PVC sampling tube described above. Each 30-cm segment was deposited into a separate, cleaned polyethylene bag. During the early winter of 1985 a few profiles were obtained with a 75-cm PVC coring sampler fitted with extension rods, which allowed profiles to be removed without digging a pit. This procedure was abandoned because the continuity of the sample collection could not be checked directly in deeper snow. All bagged samples were placed inside a second cleaned bag to avoid abrasion of the inner bag during transport from the watershed. Chemical profiles of the snowpack were obtained at intervals of 4-6 weeks during the winters of 1985 and 1986. During 1985 winter profiles were limited to the inlet or outlet of Emerald Lake; during 1986 winter profiles were obtained at the inlet, outlet, pond and ridge sites (Figure 4.1). During the snowmelt season for both years, profiles were also obtained at a variety of additional locations in the watershed.

Meltwater samples were collected by two methods. During spring 1985 meltwater was extracted from saturated snow by spinning in a cleaned, hand operated, plastic lettuce dryer with a 200 μm nylon mesh insert to better separate liquid water from debris and snow crystals. All samples obtained from this device were found contaminated. During spring 1986 linear polyethylene funnels inserted into 2L linear polyethylene bottles were placed on shelves cut into the shaded side of snow pits at several locations near Emerald Lake. This allowed collection of water dripping through the snowpack to the level of the shelf.

All snow samples were kept frozen in the bags in which they were collected at the field site and transported to Santa Barbara for analysis. In the laboratory individual samples were placed in a covered, acid-washed polyethylene bucket, and melted at room temperature (20°C). The mass of the melted snow sample was determined by weighing the tared bucket. As soon as the sample was melted, pH and conductivity were measured on unfiltered samples. Subsamples were filtered through pre-rinsed, 47 mm Gelman A/E glass fiber filters. One set of subsamples was immediately analyzed for ammonium and phosphate. A second set was stored in the dark at 4°C for subsequent cation and anion determinations. A third set was frozen for total dissolved N (nitrogen) and P (phosphorus) analysis. An unfiltered subsample was also frozen for total N and P analysis.

Meltwater samples were subsampled in the field into unfiltered and Gelman A/E glass fiber filtered aliquots. These subsamples were treated exactly as the snow samples, except that total and total dissolved N and P portions were not taken.

The pH measurements were made with combination electrodes suitable for use in dilute waters (Sargent Welch S-30072-15 or Ross 8104) and a Fisher Acumet 805 pH meter. For each series of measurements the electrode was calibrated with pH 7.00 and pH 4.00 reference buffers and washed twice for 3 minutes with stirred deionized water. The electrode was rinsed with an aliquot of sample, and the temperature compensated pH determination made on a fresh, quiescent sample after 5 minutes. Other precautions in our protocol include standardization before and after with $10^{-4}N$ and $10^{-5}N$ solutions of HCl [Galloway et al., 1979], equilibrating samples and buffers to ambient temperature, and thorough rinsing of the electrode with deionized water between readings. Conductance was measured with a Yellow Springs Instruments Model 32 meter and glass electrode with a 0.1 cell constant. Simultaneous temperature measurements were made, and conductivity was standardized to 20°C using a coefficient of 2% per °C. The conductivity cell was calibrated with dilute solutions of KCl.

Ammonium and phosphate were determined spectrophotometrically by the indophenol-blue and molybdenum-blue methods [Strickland and Parsons, 1972]. Total and total dissolved N and P were determined as nitrate and phosphate after digestion in an autoclave with persulfate [Valderrama, 1981]. Nitrate and phosphate were measured by the cadmium reduction [Strickland and Parsons, 1972] and molybdenum-blue methods respectively.

Calcium, magnesium, sodium, and potassium were analyzed with a Varian AA6 atomic absorption spectrophotometer. An air-acetylene flame was used; addition of lanthanum chloride suppressed chemical and ionization interferences during calcium and magnesium determinations. Especially dilute samples were also analyzed with a graphite furnace and manual 20-μL injections. Chloride, nitrate, and sulfate were measured by ion chromatography (Dionex Model 2010i) employing chemical ion suppression and conductivity detection.

Our program for quality assurance and quality control incorporated the following features: A standard protocol was followed for sample collection, processing, and analysis. At least duplicate samples were obtained and analyzed in most cases. Care was taken to avoid touching any surface that was to contact the sample; this was especially important for the snow samples, because the sampling tubes, bags, and bottles were often used under difficult field conditions. Filter blanks were done with varying amounts of rinse water. Results were scrutinized for any evidence of contamination (e.g. high Na^+ and Cl^- in one sample of a duplicate set) and deleted if clearly in error. Freshly prepared calibration standards and reagent blanks were used in every array. Precision and detection limits were determined; known additions were analyzed to check accuracy (Table 4.1). Samples prepared by USGS and NBS labs were periodically analyzed.

4.4. Results

During the 1985 snow season, 10 samples from 9 events and 19 samples from 14 snowpack profiles (including two sets of duplicates) were obtained; one of each type was judged contaminated. The 29 samples collected involved a total of 330 analyses. During the 1986 snow season, 85 samples were collected from 11 events. After analyses, 18% of the samples were judged contaminated and not incorporated into subsequent data analysis. Twenty-three snowpack profiles generated 438 individual samples, which were combined into 180 samples for analysis; 8% of these were judged contaminated. Fourteen snowmelt samples were collected; only one appeared contaminated. A total of 4408 analyses were performed for this snow season. On no date were data lost to contamination in either snow season. Our protocol of duplicate sampling insured that at least one sample from each snowpack layer was suitable for analysis.

Almost all the chemical analyses of snow and snow meltwater had an excess of positive charge (Tables and 4.3). Ion percent difference (IOD) (difference cations minus anions divided by the sum of cations plus anions, times 100) ranged from -3.4% to 43.4% in 1985, and from 0.1% to 46.5% in 1986, except for snowpit samples collected on June 27 1986, which had a maximum of 82.9%. Except for the June 27 samples, these IOD percentages are well within the chemical reanalysis criteria of ± 60% set by the NADP quality assurance guidelines for charge totals less than 50 $\mu eq\ L^{-1}$ [Campbell, 1983]. Similar analyses performed on the summer inflows to Emerald Lake (charge totals 90–120 $\mu eq\ L^{-1}$) ranged from a 10% negative excess to a 10% positive excess, but were usually within 5% of balance. Several factors contribute to the bias of positive charge in snowpack samples. One is leaching of sodium and occasionally other cations from glass fiber filters. Table 4.4 indicates the extent of contamination possible as a function of the volume rinse. In almost all cases, over 100 mL was used. Hence, ca. 1–2 $\mu eq\ L^{-1}$ of sodium is a likely contamination value. A secondary contribution to the charge imbalance could be a slight overestimate of calcium, which is frequently near its detection limit. However, re-analysis of some of these samples with the graphite furnace made only slight improvements.

Another contributor may be an unmeasured ion. Bicarbonate was not measured, because at the pH of the samples it is below detection by the Gran titration method, *i.e.* $< 1\,\mu eq\ L^{-1}$. Organic acids are known to occur in western snow at very low levels [Laird et al., 1986], and our measurements of dissolved organic N and P further support the likelihood of dissolved organic carbon, and hence organic acids. Analysis of snow from 1987 found an average of about 2 $\mu eq\ L^{-1}$ of weak organic acids in each sample. The presence of weak organic acids thus explains the majority of the charge imbalance, not caused by Na^+ contamination.

Precipitation-weighted concentrations for each ion, calculated by the relation

$$\bar{C} = \frac{\Sigma P_i C_i}{\Sigma P_i}$$

were used to compute profile, board, site and event sample averages. Here $\bar{C}$ is the precipitation-weighted mean of the ion, P_i is the snow water equivalent (SWE) for sample i, and C_i is the concentration of the ion in sample i. The ionic concentrations of each event were determined by calculating the precipitation-weighted means for each vertical profile, then a weighted average was computed for each board, then for each site, and finally a precipitation-weighted mean concentration for the snow event was computed by combining means from all sites. An example of the this volume-weighted averaging procedure used to produce event summaries is shown in Table 4.5. A similar procedure was followed to calculate a volume-weighted mean concentration for each snow pit.

Treating profile, snowboard and site samples as replicates results in chemical concentrations for each event having increased reliability, by decreasing the standard error (s.e. $= S / \sqrt{n}$). The precipitation-weighted sample averages for each event yield results that can be used to represent the entire watershed. Summaries of chemical composition for event and snowpack samples from the 1985 and 1986 snow seasons are presented in Tables 4.6, 4.7, 4.8, and 4.9.

From November 11 through March 27 of 1985, a total of 1.046 m of SWE was collected for event analysis, having a volume weighted pH of 5.29, conductivity of $4.0\,\mu S\ cm^{-1}$, and total ionic content of $21.6\,\mu eq\ L^{-1}$ (Table 4.10). From November 20 through May 7 of 1986, a total of 2.567 m of SWE was collected for event analysis, having a volume weighted pH of 5.34, conductivity of $3.3\,\mu S\ cm^{-1}$, and total ionic content of $15.7\,\mu eq\ L^{-1}$. These are the first event measurements of high-altitude snowfall in the southern Sierra Nevada. They indicate an exceptionally dilute snowpack, with a trace of non-carbonic acid acidity.

The precipitation-weighted standard deviation for the mean concentrations was calculated by a modification of the relation proposed by Miller [1977], and used by Liljestrand and Morgan [1979] and by Topol [1986]

$$S = [(1 / \Sigma P_i)\, \Sigma P_i (C_i - \bar{C})^2\,]^{1/2}.$$

Here S denotes the precipitation-weighted standard deviation of the mean for a snow season, P_i is the volume of water for the i th event, C_i is the concentration of the i th event, and $\bar{C}$ is the mean concentration of the ion for the snow season. The standard deviations (Table 4.10) of event measurements are generally small, indicating low variation between storms. Differences in concentration between the two years sampled is also small.

The relative concentration of the various ions did not vary much from year to year. Cations ($\mu eq\ L^{-1}$) followed the general pattern $H^+ > Ca^{2+} > Na^+ = NH_4^+ > K^+ > Mg^{2+}$ (Table 4.10). Anion abundance followed the general pattern $Cl^- > NO_3^- = SO_4^{2-} >> PO_4^{3-}$. Since PO_4^{3-} concentrations are consistently much lower than the concentrations of the other anions, they are not reported for snowpit profiles.

The ratio of SO_4^{2-} to NO_3^- equivalents, was 1.30 in the 1985 snow season, and 0.89 in the 1986 snow season. The molar ratios of SO_4^{2-} to NO_3^- were 0.65 in 1985, and 0.44 in 1986.

Comparison of the seasonal volume-weighted ion concentrations, by precipitation type, is presented in Table 4.11. Solute concentrations in rainfall were consistently 5-10 times greater than those in snowfall during winter, for all the major ions, for water years 1985 and 1986. Solute concentrations in autumn snow were intermediate in magnitude between those of rainfall and snowfall in winter. For example, the H^+ concentration in rainfall was about 16 $\mu eq\ L^{-1}$, 7 $\mu eq\ L^{-1}$ in autumn snowfall, and 4 $\mu eq\ L^{-1}$ in winter snowfall. Rain and autumn snow samples for chemistry analysis were collected at the inlet site as part of the California Air Resource Board's CADMP network (California Air Resources Board, 1988), using an Aerochem Metrics Model 301 sampler. Volume-weighted chemistry for snowfall from the winter season is from Table 4.10.

Ionic flux to the ELW was predominately in the form of snowfall. Snowfall in winter supplied about 1000 mm of water over the basin in 1985, and about 2300 mm of water in 1986 (Table 4.12). Rain supplied about 16 and 32 mm of water for those respective water years. Snowfall in winter was generally responsible for 10 times the ionic loading to the watershed, expressed as meq m^{-2} (mass/unit area), than was rain. For example, the H^+ deposition to the watershed, by rain, was 0.3 meq m^{-2} for each water year, while the H^+ deposition by winter snow was 5.5 meq m^{-2} in 1985, and 10.9 meq m^{-2} in 1986. For all measured cations in 1986, rain deposited 2.0 meq m^{-2}, autumn snow 8.9 meq m^{-2}, and winter snow 21.7 meq m^{-2}. The relative anion deposition in 1986 was similar, with rain depositing 1.5 meq m^{-2}, autumn snow 6.2 meq m^{-2}, and winter snow 15.5 meq m^{-2}. Water year 1985 followed a similar pattern of cation and anion deposition by precipitation type.

In general ion deposition from fall snow was intermediate in magnitude between winter snow and rain, with the exception of NH_4^+ (Table 4.12). In 1985 autumn snow supplied 1.4 meq m^{-2} of NH_4^+ to the basin, while winter snow deposited 0.9 meq m^{-2} and rain 0.7 meq m^{-2}. For the 1986 water year, autumn snowfall deposited 4.6 meq m^{-2} of NH_4^+ over the basin, while winter snow deposited 3.3 meq m^{-2} and rain 0.8 meq m^{-2}.

Ionic loading values in Table 4.12 are calculated by multiplying the seasonal volume-weighted ion concentrations in Table 4.11, by areal estimates of seasonal water inputs to the basin. Since the estimation of areal precipitation from point measurements is a persistent problem, precipitation amounts are the best estimates

of precipitation over the entire basin available, and are from Dracup et al. (1988), except for the 1985 snowfall from November to March, which is based on point measurements of events (Tables 4.6 and 4.10).

Converting the values in Table 4.12 to percentages provides additional insight into the relative contribution of each precipitation type to the annual flux of ions and water to the ELW, from wet deposition. Snowfall (autumn and winter), supplied about 99% of the precipitation input to ELW, rainfall only about 1% (Table 4.13). In general, about 90% of solutes deposited in the ELW, by wet deposition from the atmosphere, were in the medium of snow. Rain deposited about 3% of the H^+ flux from wet deposition to the basin, while autumn snow deposited about 12%, and winter snow about 85%.

Dry deposition to the Emerald Lake basin can be evaluated by the difference in ionic loading (mass/unit area) between cumulative snowfalls and snowpits. If dry deposition is an important source of solute flux to the watershed, snowpit loading should be greater than that from cumulative snowfall to that date at the same site. Figure 4.2 shows that for anions and SWE at the inlet site prior to the onset of melt, there was little difference between event and snowpit totals. Inlet site data gathered on March 5 1986 was in a new location that was not representitive of previous samples at that site, because the inlet site was buried by approximately 5 m of avalanche debris in mid-February. Snowpit data from the tower site was substituted for the inlet site on March 5, to generate Figure 4.2. Cumulative ionic loading and snow water equivalence from events was very similar to loading values derived from snowpit analyses, prior to the onset of snowmelt.

Ionic loading to the Emerald Lake watershed was computed by multiplying the average ionic concentration of the basin by the total volume of snow water equivalence in the basin (W_T). Since cumulative event chemistry appears to be similar to snowpit chemistry prior to the onset of melt, the volume-weighted mean concentrations from snow events were used to calculate the average chemical composition of the basin at maximum snow accumulation. The large sample size that is a consequence of numerous replicates from various collection sites for event chemistry generates a chemical average that is more representitive of the entire watershed than that from limited snowpit data. October snowfalls (and the November 11 1985 snowfall) were considered non-accumulating. Event chemistry from these snowfalls were excluded from the calculation of ionic concentration in the basin, at maximum snow accumulation. After the April onset of melt in the 1985 and 1986 snow seasons, snowpit data were used to calculate the average chemical concentration of the watershed's snowpack. Calculation of the volume of snow water equivalence for the basin is explained in Chapter 8.

At maximum snow accumulation for the 1985 snow season there was 1.2×10^6 cubic meters of snow water equivalence in the Emerald Lake watershed, with a basin-wide loading for all major ions of 2.6×10^4 equivalents (Table 4.14). At maximum snow accumulation in the 1986 snow season there was 2.4×10^6 cubic meters of snow water equivalence in the basin, containing 3.6×10^4 equivalents of ions. After the onset of melt several trends are evident. Conductivity of the snowpack generally decreases with time, while pH increases with time. Base cation concentrations generally remain the same. Anion concentrations in the snowpack decrease with time.

Comparison of anion loading to SWE, in Figure 4.3, clearly demonstrates the removal of anions from the inlet snowpack at a faster rate than SWE decreases, subsequent to the April onset of melt in the spring of 1986. Movement of anions from the upper layers of the snowpack to lower depths, and then to runoff is presented in Table 4.15. At the inlet site, in 1986, nitrate concentrations in the snowpack layer at the snow surface decreased from 1.5 $\mu eq\ L^{-1}$ to 0.1 $\mu eq\ L^{-1}$ between March 5th and May 23, while nitrate concentrations at the snowpack layer next to the ground changed from 1.6 $\mu eq\ L^{-1}$ to 0.9 $\mu eq\ L^{-1}$ during the same time period. Following a similar pattern over this time period was pH, which increased from 5.33 to 5.49 at the snow surface, but only changed from 5.36 to 5.37 at the ground layer. However, meltwater collected from the snowpack between May 1st and June 11th, 1986 did not exhibit higher concentrations of solutes than the snowpack from which the meltwater was sampled (Table 4.16).

Spatial and temporal variability of snow chemistry from snow events during the snow accumulation season is very small (Tables 4.5, 4.6 and 4.8). Comparison of within site variability (4 replicates) to between site variability by a one way analysis of variance (SAS statistical package), for NO_3^- and SO_4^{2-} from the January 9th, 1986 snow event at the inlet, tower, pond and ridge, yielded no significant differences between sites for either nitrate ($Pr > 0.65$) or sulfate ($Pr > 0.740$) (Table 4.17). However, after the onset of melt in the spring, event chemistry differed markedly with time. The concentration and loading of snowpit profiles also exhibited a distinct spatial difference after the onset of spring melt. Snow events on and after April 10 1986, were characterized by low SWE, with a 5-10 fold increase over winter snowfall, in the concentrations of NH_4^+, Na^+, NO_3^- and SO_4^{2-} (Table 4.8). Comparison of snowpack profiles from six sites on May 23 1985 (Figure 4.4), demonstrates the large spatial variability in both anion concentration and loading after the onset of melt in the basin. Base cations exhibited similar variability. Near the end of the snowmelt season snowpit profiles again show little variability (Table 4.9).

4.5. Discussion

Mean concentrations of the major ions in the seasonal snowpack of the Emerald Lake Watershed (ELW) for 1985 and 1986 were very low. Individual ions had concentrations less than 5 $\mu eq\ L^{-1}$ for the 1985 and 1986 snow seasons. Snowfall was slightly acidic, with a volume-weighted pH of about 5.3.

Few event samples spanning an entire winter are available with which to compare our data. The measurements by Melack et al. [1982] at Mammoth Mt., in the eastern central Sierra Nevada, are comparable in measured constituents except pH, which was slightly higher (5.7). Snowpack chemistry in the Gem Lake watershed, located high (3595 m) on the eastern slope of the Sierra Nevada, was similar to that of Emerald Lake,

with a pH of 5.43, and with all major ions having concentrations less than 5.0 $\mu eq\ L^{-1}$ [Stoddard 1986]. Michaels et al. [1987] found similar concentrations in an alpine snowpack in the Colorado Rockies.

Integrated snowpack chemistry from other periods and sites on the west coast is in general agreement with our Emerald Lake results, with the difference that Emerald Lake watershed pH values are slightly lower. A transect of snowpack chemistry in the Cascade-Sierra Nevada Mountains from the U.S.-Canadian border to a point northeast of Bakersfield, CA. [Laird et al., 1986], generated a median pH of 5.6, with a H^+ concentration of 2.0 $\mu eq\ L^{-1}$. Snowpack chemistry from the Alpine Lakes Wilderness Area east of Seattle had an average pH of 5.6 [Welch et al., 1984], though the pH of snow along the Pacific Coast of Canada was found by McBean and Nikleva [1986] to be 5.4. Similar pH values are reported by Feth et al. [1964] for 51 sites in the Sierra Nevada (pH 5.8), and by Brown and Skau [1975], who observed an average pH of 5.6 for 26 sites in the Sierra Nevada.

Comparison of acidity values from the Emerald Lake watershed with the precipitation from remote areas of the world is useful when trying to assess the impact of anthropogenic emissions on the local environment. Measurements of the acidity of ice cores taken from the Agassiz ice cap and Mt. Oxford areas in the Canadian high Arctic, by Barrie et al. [1985] at an elevation of ≈1600 m, represent a natural background apparently unaffected by man-made pollution. This background level of acidity has remained relatively constant throughout this century at a level corresponding to a background H^+ concentration of 5.8 $\mu eq\ L^{-1}$. However, the seasonal acidity of the wintertime's snowpack at these remote sites has increased from a H^+ concentration of 8 $\mu eq\ L^{-1}$ between 1925 and 1956, to 14 $\mu eq\ L^{-1}$ from 1957 to 1977. Barrie et al. attribute this snowpack increase in acidity during the Arctic winter to European emissions of SO_2 and NO_x. Hydrogen ion concentrations of 5.3 and 4.6 $\mu eq\ L^{-1}$ for the snow seasons of 1985 and 1986 at Emerald Lake are comparable to the background acidity of the Arctic, and less than the acidity of winter snowfall in the Canadian Arctic.

The acidity of snowfall in the ELW appears to be unaffected by anthropogenic sources. Analysis of sediment cores from Emerald Lake indicates that the current pH of the lake is within the historical range for the basin [Melack et al., 1987]. This suggests that the pH of snowfall in 1985 and 1986 did not cause the pH of Emerald Lake to change from past values. Since snowmelt runoff provides the majority of water input to Emerald Lake, by inference it appears that the present pH (about 5.3) of snowfall is similar to that of the pH from snowfall for the past 100 years. Additionally, there is little difference when pH from snowfall at the ELW is compared to the pH of Arctic snow, where the Arctic snow is apparently unaffected by anthropogenic sources.

The H^+ concentration of snowfall (≈ 5 $\mu eq\ L^{-1}$) at ELW is lower than the H^+ concentration of rainfall (≈ 12 $\mu eq\ L^{-1}$) in the basin (Table 4.11). All major ions follow a similar pattern. Volume-weighted concentrations of solutes in snowfall events from late November through May were 5-10 times lower than those of rainfall. However, ionic flux to the watershed, from wet deposition, occured predominately from snowfall.

The importance of snowfall as a source of ionic flux to the watershed cannot be overemphasized. Snow (autumn and winter combined), supplied almost 99% of the annual precipitation input for water years 1985 and 1986, rain only 1% (Table 4.13). This snowfall accounted for about 90% of the wet deposition of all major solutes to the watershed. Rainfall, though more concentrated than snowfall, generally provided less than 10% of the ionic flux (Table 4.13). Snow is the major pathway for fluxes of water and ions to the ELW.

Apparently there is little temporal or spatial variation in the chemistry of snowfall from December through March, the snow accumulation season, at ELW. For example, comparison of NO_3^- and SO_4^{2-} concentrations from the storm event on January 9th, 1986, yield no significant differences between the inlet, tower, pond and ridge sites (Table 4.17). The chemistry of any particular snowfall during winter, at a specific site in the watershed, appears to be similar to the chemistry of that snowfall at other locations in the watershed, and similar to the chemistry of snowfalls at different dates and even different years, at this time (Tables 4.5, 4.6 and 4.8).

However, the chemistry of snowfall from storms after the onset of melt in the spring of 1986 was very different than the chemistry of storms before the start of spring melt that year. Storms from April through May 1986, had a 12-fold increase in the volume-weighted concentrations of NH_4^+, and a 5 to 6-fold increase in NO_3^- and SO_4^{2-}, relative to the volume-weighted mean concentrations for that snow season. Two of the snowfalls in spring had pH values of 5.11 and 5.17 (Table 4.8). Snow temperatures of these spring storms were warm (Chapter 6), but the consequent increase in riming does not entirely explain the higher chemical concentrations, as storms in January and February of the same year were also characterized by snowfall temperatures near 0°C (Chapter 6), yet had very dilute solute concentrations (Table 4.8). A possible explanation for the differences in chemical concentrations of these storms may have been a change from frontal systems of marine origin in the winter to convective storms in the spring.

Solute concentrations in snowfall from October through November (autumn), were also very different than the solute concentrations in snowfall during winter (Table 4.11), and were similar to the chemistry of spring snowfall (Table 4.8). Again, a possible explanation for this pattern may be a seasonal difference in the origin of the storm airmass.

Autumn snowfalls are important for several reasons. Precipitation input from autumn snowfall, in water years 1985 and 1986, was about 8% of the annual total (Table 4.13), or 8 times the water flux from rain. Autumn snowfalls at this time supplied a large percentage of the annual ionic flux to the ELW from wet deposition (Table 4.13). Autumn snowfalls deposited about 30% of the annual NO_3^- and SO_4^{2-} flux from wet deposition, and about 50% of the NH_4^+. For the base cations, autumn snowfall supplied about 40% of the Ca^{2+} flux, and about 15% of the remaining cations. Monitoring precipitation and ionic flux from autumn snowfalls is

important.

The fate of autumn snowfall, once deposited in the ELW, varies spatially and temporally. Some snow melts immediately, causing a rise in stream discharge. More snow melts slowly through October and November. Streams maintain an elevated concentration of solutes through this time period, particularly the strong acid anions (Cl^-, NO_3^- and SO_4^{2-}) [Melack et al., 1987], since this snow has relatively high concentrations of solutes compared to winter snow (Table 4.11). The chemistry of stream water is further complicated by overland flow from snowmelt runoff rinsing dry deposition (deposited during the summer) from rock and vegetation surfaces. Snowmelt runoff from autumn snowfalls also flushes the products of biological activity from soils. Additional solutes are added to snowpack runoff by these processes, before the runoff reaches the basin's streams.

Spatial distribution of the snowpack formed by autumn snowfalls is difficult to quantify. Uneven melting of this snowpack can be caused by large spatial differences in ground temperature and incoming insolation (Chapter 6). The result is that spatial distribution of the snowpack formed by autumn snowfall is not uniform over the catchment when the snow accumulation season starts in late November or early December. Large areas of the watershed have no snow at this time, other areas have accumulated snow characterized by relatively high ionic concentrations.

The molar ratios of SO_4^{2-} to NO_3^- at Emerald Lake, for snowfalls from December through March, are comparable to the 0.48 sulfate to nitrate ratio Topol [1986] reports for snowfall at 9 sites in the northeastern United States. The 0.65 and 0.44 SO_4^{2-} to NO_3^- molar ratios at Emerald Lake from the 1985 and 1986 snow seasons, respectively, are comparable to the annual molar ratios of sulfate to nitrate at Giant Forest in Sequoia National Forest (elevation 1856 m), which ranged from 0.55 to 0.90 for the years 1981 through 1984 [Stohlgren and Parsons, 1987]. However, these values are very different from the 2.6 and 2.9 SO_4^{2-} to NO_3^- ratios reported by Berg [1986] and by Woo and Berg [1986], respectively, for snow at the CSSL research site near Lake Tahoe (elevation 2103 m). These molar ratios suggest that acidic deposition from snowfall may be very different between the northern and southern Sierra Nevada. Alternatively, these differences may be due to methodological differences in analytical technique.

Dry deposition does not appear to be an important contributor of soluble ions to the chemical loading of the watershed during the snow accumulation season. There exists little difference between cumulative event and snowpack chemistry, in either chemical concentrations or ionic loading of solutes (Figure 4.2), prior to the onset of spring melt. Particulates were excluded from the chemical analyses by filtering; therefore, the contribution of particulates to dry deposition cannot be ascertained. The importance of dry deposition after the onset of spring melt is ambiguous. Inspection of Table 4.15 suggests that cation concentrations increase in the surface layer of the snowpack with time after the initiation of snowmelt at the inlet. Cation concentrations from integrated snowpack profiles sampled after the onset of melt are often similar, or even higher, than cation concentrations sampled before the onset of melt, for both the 1985 and 1986 snow seasons (Tables 4.7 and 4.9). Anion concentrations consistently decrease with time after the onset of spring melt. Inconsistencies with the analytical precision associated with measuring these extremely low concentrations of cations necessitate a cautious approach to interpreting these apparent cation trends.

The representativeness of event samples to the event storm is subject to complicating factors such as wind scouring and redeposition (see Chapter 3). However, the consistent agreement of SWE and ionic concentration between cumulative event samples and snowpit samples strongly supports the suggestion that the winter snowpack in alpine regions does act as a storage reservoir of deposition through this time period. Chemical characterization of the snowpack, and calculation of ionic loading to the watershed during the winter storage season, are described in a similar fashion by either cumulative event chemistry or by the chemistry of snowpack profiles sampled at maximum snow depth. Determination of ionic loading (mass/unit area), at a point in the ELW, appears to be measured equally well by either cumulative snow boards or by snowpits, before the onset of snowmelt.

The integrated chemistry of snowpack profiles prior to the onset of melt are difficult to interpret with respect to the spatial variability in ionic concentration, but appear to support the hypothesis that there is little spatial variability in the snowpack chemistry of ELW, before the onset of snowmelt (Tables 4.7 and 4.9). Ionic loading of the major ions in the snowpack was different between sites, at this time, as a consequence of differences in SWE between sites. Once snowmelt begins there appears to be large spatial and temporal variation in the chemistry of the snowpack (Figure 4.4). Snowpack chemistry appears to become more uniform towards the end of snowmelt (Table 4.9).

Spatial and temporal variations in snowpack chemistry have important implications for estimations of ionic load and mass balance in watersheds. If small alpine basins have a relatively homogeneous snow chemistry at maximum snow accumulation, and again towards the end of snowmelt, then ionic content and changes in mass balance can be calculated from a small number of chemistry samples, provided SWE is accurately measured. However, the apparent heterogeneity in chemical composition of the snowpack during the peak snowmelt season makes it difficult to estimate areal loading of solutes in the snowpack at this time. Determination of ionic content or chemical mass balance during the main snowmelt season requires a large number of sample sites. A time series of snowpit profiles from representitive areas of the watershed, starting at maximum snow accumulation and continuing through the melt season, is necessary to answer this hypothesis.

The importance of ionic flux to alpine watersheds, from snowfall, is compounded by the storage ability of the snowpack. The large volume of water that was deposited to the ELW as snowfall resulted in significant ionic loading to the watershed. H^+ load to the watershed at maximum snow accumulation was 6.4×10^3 equivalents (eqs) in 1985 and 11×10^3 in 1986, while the

sum of base cations was 8×10^3 eqs and 10^4 eqs for the respective years (Table 4.14). The load of strong acid anions to the watershed was 3×10^3 eqs and 4×10^3 eqs for NO_3^- in 1985 and 1986, while SO_4^{2-} load was 3.7×10^3 and 3.4×10^3 for those years (Table 4.14).

Ionic content of the snowpack may be important to the surface water chemistry of the Emerald Lake watershed. The combination of the temporary storage of snow, snow metamorphism, and the low buffering capability of the basin may cause the low concentration of solutes in the snowpack to produce runoff that episodically acidifies surface waters.

Two approaches were taken to evaluate the existence of an ionic pulse during the initial stages of snowmelt at Emerald Lake. One was to determine the difference between the percentage decrease in water content of the snowpack and the percentage decrease in ionic content for a succession of snowpit chemical profiles taken at the same site during spring. Results of these calculations for the period from April 14 to May 23 1986, for chemical profiles taken at the ridge site, indicated no enhanced loss of H^+, a 2.5-fold increase in SO_4^{2-} and Cl^- loss, and a 4-fold increase in NO_3^- loss. Calculations for the period from May 5 to May 23 1986, for chemical profiles taken at the inlet site showed no enhanced H^+ loss, and a 2-2.5-fold increase in NO_3^- and SO_4^{2-} losses. At the inlet and bench sites from May 10-23 1985, NO_3^- loss was enhanced from 3.7-1.7-fold, SO_4^{2-} loss was enhanced about 1.6-fold, and H^+ loss was enhanced about 1.7-fold.

The second approach was to compare the chemical concentrations of meltwater collected from the snow with the chemical concentration of the snowpack (snow plus meltwater). The measurements shown in Table 4.16 do not indicate elevated concentrations in the meltwater. These samples were collected late in the melt season, after considerable melt had occurred. However, indirect evidence for an ionic pulse is available. Between March 5 and May 5 of 1986, 50 cm of SWE fell at the inlet site, depositing 14.9 meq of anions (Table 4.8). Yet the anion loading in the inlet pit decreased from 13.7 meq on March 5 to 7.3 meq on May 5, while SWE increased from 175 cm to 244 cm (Figure 4.3).

Concentration of solutes in the first fraction of snowpack meltwater may result in runoff from the chemically dilute, but large volume snowpack, significantly increasing the ionic concentrations of surface waters. Melack et al. [1987] report elevated concentrations of NO_3^- and SO_4^{2-} from inflowing, lake and outflowing waters of the Emerald Lake watershed during the period of spring runoff from 1984 through 1986. Inflowing streams to Emerald Lake exhibit a pronounced increase in nitrate and sulfate concentrations with the first fraction of spring meltwater to enter that subdrainage. Comparison of NO_3^- and SO_4^{2-} concentrations to discharge in inflow #2 during the first six months of 1986 clearly demonstrates the increase in concentration of these two ionic species with the first fraction of meltwater to enter the drainage (Figure 4.5). Melack et al. [1987] also report that the ELW's outflow from 1984 through 1986 exhibited a pronounced cyclical increase in nitrate and sulfate concentrations during spring runoff, followed by a rapid decline in concentration (Figure 4.6). Stream waters experienced a decrease in pH and ANC, during the period of snowmelt runoff, from 1984 through 1986.

The hypothesis that pH and ANC declines result from acidification during snowmelt can be tested by evaluating two predictions. H^+ sufficient to titrate the buffering capacity of the entire lake should be present in the concentrated, early stages of snowmelt, or should be added to the snowmelt as it becomes runoff. The major ion composition of the lake, except for hydrogen and bicarbonate concentrations, should remain relatively unchanged as the lake acidifies.

Evidence provided by Melack et al. [1987] for Emerald Lake indicates that dilution may be the dominant process during snowmelt. Calculations of chemical inputs via inflowing streams show that these waters are a net source of ANC, and a small source of H^+, to the lake. Furthermore, within the lake, major cations and silica only decrease in concentration during snowmelt, and the sum of strong acid anions (Cl^-, NO_3^- and SO_4^{2-}), which experience a temporary increase, is always less than the sum of base cations. However, ANC concentrations in inflowing streams, lake water, and the outflow decrease from about 40 $\mu eq\ L^{-1}$ to 10 $\mu eq\ L^{-1}$ during spring runoff.

An anionic pulse does appear to be generated in the snowpack of the Emerald Lake watershed. This pulse causes a pronounced increase in the NO_3^- and SO_4^{2-} concentrations of the stream and subsurface lakewaters in the basin. Anions are preferentially eluted from the snowpack with the initial fraction of meltwater (Tables 4.7, 4.9, 4.11). Comparison of anion concentration to SWE at the inlet site (Figure 4.3), illustrates the accelerated loss of anions with respect to SWE from the snowpack after the April onset of melt in the spring of 1986. The nonconservative nature of H^+ makes it difficult to determine if the pulse of anions does cause acidification. It should be noted that when all nitrogen pathways are examined, the net acidification potential from nitrogen is expressed as the number of mobile NO_3^- anions [Reuss and Johnson; 1987]. This occurs regardless of the type of nitrogen input (e.g. nitric acid, ammonium sulfate, or ammonium nitrate).

Nitrate concentration in the basin's streams is elevated much more than sulfate concentration at the onset of spring runoff. Inflowing streams in 1986 had an increase in NO_3^- concentration of $\approx$120%, whereas SO_4^{2-} concentration increases $\approx$50% (Figure 4.5). After transit through the buffering medium of Emerald Lake, NO_3^- concentration in the outflow stream was raised $\approx$110%, while SO_4^{2-} concentration was increased by $\approx$40%, compared to winter values (Figure 4.6). These anions were then exported into downstream limnological systems. Preferential elution of NO_3^- from the snowpack may partially explain these relative ionic concentrations, but snow chemistry data is inconclusive. The high concentration of nitrate in surface waters at the start of spring runoff underscores the significance of the relatively high NO_3^- to SO_4^{2-} ratio of winter snow. The high nitrate concentration indicates that neither terrestrial nor aquatic systems within the watershed are able to neutralize this anion during spring runoff.

Ablation results from the complex interplay of physiographic factors such as slope, aspect, latitude and hor-

izon, with energy balance exchanges at the air/snow and snow/ground interfaces (Elder, in press). Source areas of snowmelt runoff thus vary spatially and temporally (Woo and Slaymaker, 1975). The onset of snowmelt at ELW shifts temporally from subbasins with a southwestern aspect to subbasins with a progressively more northern aspect. These ablation differences within a watershed cause a corresponding change in the chemistry of the snowpack and snowpack runoff [Williams and Melack, in press].

Streamwater from ELW subbasins sampled from January through July 1986, had the highest values of NO_3^- and SO_4^{2-}, at the onset of snowmelt (Figure 4.7). The outflow experienced the same anionic pulse with the onset of snowmelt in the watershed. If we had been able to sample the water chemistry from inflows #1 and SEG at the onset of snowmelt in their respective basins, we may have measured NO_3^- and SO_4^{2-} concentrations comparable to the maximum concentrations that were measured in inflows #2 and #4.

The NO_3^- pulse in stream water may be due to sources other than an ionic pulse from snowmelt runoff. Groundwater, soil water and organic horizons in soil may all contribute NO_3^- to snowmelt runoff. However, the small percentage of soils and high percentage of bedrock characteristic of ELW make this unlikely. Furthermore, biological activity from vegetation, soils and phytoplankton utilizes NO_3^- as a nutrient, which would tend to mask the amplitude of the NO_3^- pulse in stream waters. Also, coincident with the NO_3^- pulse is a SO_4^{2-} pulse. Moreover, the NO_3^- ion in the 1985 and 1986 snowpacks was eluted in greater magnitude than the SO_4^{2-} ion. Anionic concentrations in stream waters follow a pattern similar to snowpack elution. Maximum concentrations of NO_3^- in streams at the onset of snowmelt were about 100% greater than January concentrations, while SO_4^{2-} concentrations at this time were about 40% greater than January concentrations. Finally, measurements made in 1987 of NO_3^- concentrations in snowpack meltwater, before contact with the ground, were 5 times bulk snowpack concentrations.

There is an apparent sequential shift in the generation of a NO_3^- and SO_4^{2-} pulse through the ELW that corresponds to the onset of snowmelt in each subbasin. The period of time that the watershed experienced this anionic pulse was thus longer than any single subbasin. Lakewater concentrations of NO_3^- and SO_4^{2-} may respond by remaining elevated for a longer time period than individual subbasins, or may be unaffected because concentrated meltwater from a subbasin just starting melt may be offset by dilute meltwater from a subbasin in the later stages of snowmelt. Water from the lake's outflow indicates how the watershed as a whole was influenced by subbasin differences in anionic concentration.

Maximum concentrations of NO_3^- and SO_4^{2-} measured in inflows were about 1.5 times and 1.1 times those of the outflow. The strength of the anionic pulse generated by inflows was attenuated when integrated in the outflow. What is surprising is that the percentage increase in NO_3^- and SO_4^{2-} concentration in the outflow at the onset of springmelt was the same as the inflows, about 100% for NO_3^- and 40% for SO_4^{2-}. Furthermore, outflow concentrations remain elevated near maximum values for a much longer time period than any of the individual inflows. For the watershed as a whole, Figure 4.7 illustrates how decreases in NO_3^- and SO_4^{2-} concentrations in inflow #2 appear to be balanced by contributions from inflow #4, such that NO_3^- and SO_4^{2-} concentrations in the outflow remain elevated for a longer time span than any subbasin.

Spatial and temporal variations in the onset and intensity of snowmelt appear to alter the water chemistry of alpine basins. Inflow concentrations of NO_3^- and SO_4^{2-} during spring runoff in alpine basins are highly variable spatially and temporally, necessitating sampling from all subbasins to adequately characterize inputs to lake systems at this time. Spatial and temporal variations in the onset of snowmelt do not appear to dilute the percentage increase in NO_3^- and SO_4^{2-} pulses in alpine watersheds. Rather, these ablation differences apparently increase the time span the watersheds are exposed to elevated concentrations of NO_3^- and SO_4^{2-}, and to extend the time span that these elevated concentrations are transported to downstream aquatic systems. If the NO_3^- and SO_4^{2-} ions are associated with the H^+ during deposition to alpine watersheds, these results suggest that the effects of acidic deposition on such areas will be prolonged.

Snowmelt is perhaps the dominant event that effects alpine ecosystems on an annual basis [Melack et al., in press]. This infusion of concentrated runoff followed immediately by very dilute meltwater may be the controlling abiotic event in alpine ecosystems. Small changes in water chemistry can have dramatic effects on individual organisms, and even on entire community structures.

Artificial acidification experiments performed in enclosures placed in Emerald Lake demonstrate that decreasing Emerald Lake to a pH of 5.5 causes a major restructuring of zooplankton communities within the lake, which may in turn effect higher trophic levels [Melack et al., 1987]. Artificial acidification of stream channels demonstrate a similar effect on stream inveterbrates [Melack et al., 1987]. Snowmelt runoff lowered stream and subsurface lakewater at ELW to a pH of 5.5 in 1986, through a combination of dilution and titration. This occurred at present atmospheric deposition levels. ANC concentrations in stream and subsurface lakewaters of the ELW are annually lowered to the range of 4-12 $\mu eq\ L^{-1}$, during the spring period of snowmelt runoff.

At current levels of wet deposition, the Emerald Lake basin stands on the threshold of acidification. Any increase in the acidity of snowfall will be magnified in snowmelt runoff through the process of snow metamorphism. Spatial and temporal differences in the onset of snowmelt may increase the timespan that the Emerald Lake basin is exposed to this elevated concentration of solutes in snowpack runoff.

4.6. References

Adams, W. P., Snow and ice on lakes, in *Handbook of Snow*, edited by D. M. Gray and D. H. Male, pp. 437-466, Pergamon Press, New York, 1981.

Akitaya, E., Studies on depth hoar, *Cont. Inst. Low Temp. Sci., Ser. A*, 1-67, 1974.

Barrie, L. A., K. G. Anlauf, H. A. Wiebe, and P. Fellin, Acidic pollutants in air and precipitation at selected rural locations in Canada, in *Proceedings of the American Chemistry Society Symposium on Acid Rain*, Ann Arbor Sci., Ann Arbor, MI, 1983.

Barrie, L. A., D. Fisher, and R. M. Koerner, Twentieth century trends in Arctic air pollution revealed by conductivity and acidity observations in snow and ice in the Canadian High Arctic, *Atmos. Environ.*, *19*, 2055-2063, 1985.

Barrie, L. A. and A. Sirois, An analysis and assessment of precipitation chemistry measurements made by CANSAP: 1977-1980, *Rep. no. AQRB-82-003-T*, Atmos. Environ. Serv., Downsview, Ontario, 1982.

Barrie, L. A. and R. J. Vet, The concentration and deposition of acidity, major ions and trace metals in the snowpack of the Eastern Canadian Shield during the winter of 1980-1981., *Atmos. Environ.*, *18*, 1459-1469, 1984.

Berg, N., Snow chemistry in the central Sierra Nevada, California, *Water, Air, Soil Pollut.*, *30*, 1015-1021, 1986.

Bergmann, M. A. and H. E. Welch, Spring meltwater mixing in small arctic lakes, *Can. J. Fish. Aquatic Sci.*, *42*, 1784-1798, 1985.

Board, California Air Resources, California: acid deposition data July 1984-June 1987, *Tech. Support Div.*, 107 pp., P. O. Box 2815, Sacramento, CA, 1988.

Borys, R. D., P. J. DeMott, E. E.Hindman, and D. Feng, The significance of snow crystal and mountain-surface riming to the removal of atmospheric trace constituents from cold clouds, in *Precipitation Scavenging, Dry Deposition, and Resuspension*, edited by H. R. Pruppacher, R. G. Semonin and W. G. N. Slinn, pp. 181-189, Elsevier, New York, 1983.

Brimblecombe, P., M. Tranter, P. W. Abrahams, I. Blackwood, T. D. Davies, and C. E. Vincent, Relocation and preferential elution of acidic solute through the snowpack of a small, remote high-altitude Scottish catchment, *Ann. Glaciol.*, *7*, 141-147, 1985.

Brown, J. C. and C. M. Skau, *Chemical composition of snow in the east central Sierra Nevada*, Coop. Rep. Ser. Publ. no. AG-1, Natural Resour. Div., Univ. Nevada, Reno, NV, 1975.

Brown, S. B., J. G. Eales, R. E. Evans, and T. J. Hara, Interrenal, thyroidal, carbohydrate response of rainbow trout (*Salmo gairdneri*) to environmental acidification, *Can. J. Fish. Aquatic Sci.*, *41*, 36-45, 1984.

Cadle, S. H., J. M. Dasch, and N. E. Grossnickle, Retention and release of chemical species by a northern Michigan snowpack, *Water, Air, Soil Pollut.*, *22*, 303-319, 1984.

Campbell, S. A., Sampling and analysis of rain, *ASTM Special Tech. Publ. 823*, ASTM, Philadelphia, 1983.

Chan, W. H. and D. H. S. Chung, Regional-scale precipitation scavenging of SO_2, SO_4^{2-}, NO_3^-, and HNO_3, *Atmos. Environ.*, *20*, 1397-1402, 1986.

Chang, T. Y., Rain and snow scavenging of HNO_3 vapor in the atmosphere, *Atmos. Environ.*, *18*, 191-197, 1984.

Charette, J. Y., H.G. Jones, W. Sochanska, and J. M. Gauther, Changes in lake water quality during spring runoff in a northern boreal forest subjected to acidic precipitation, in *Canadian Hydrology Symposium Proceedings*, Natl. Res. Council Canada, Ottawa, 1986.

Colbeck, S. C., Grain clusters in wet snow, *J. Colloid Interface Sci.*, *72*, 371-384, 1979.

Colbeck, S. C., A simulation of the enrichment of atmospheric pollutants in snow cover runoff, *Water Resour. Res.*, *17*, 1383-1388, 1981.

Colbeck, S. C., An overview of seasonal snow metamorphism, *Rev. Geophys. Space Phys.*, *20*, 45-61, 1982.

Colbeck, S. C., Theory of metamorphism of dry snow, *J. Geophys. Res.*, *88*, 5475-5482, 1983.

Colbeck, S. C., Classification of seasonal snow cover crystals, *Water Resour. Res.*, *22*, 59S-70S, 1986.

Davidson, C. I., R. E. Honrath, J. B. Kadane, R. S. Tsay, P. A. Mayewski, W. B. Lyons, and N. Z. Heidam, The scavenging of atmospheric sulfate by Arctic snow, *Atmos. Environ.*, *21*, 871-882, 1987.

Davies, T. D., C. E. Vincent, and P. Brimblecombe, Preferential elution of strong acids from a Norwegian ice cap, *Nature*, *300*, 161-163, 1982.

Dennis, A. S., *Weather Modification by Cloud Seeding*, Academic Press, New York, 1980.

Dozier, J. and S. I. Outcalt, An approach toward energy balance simulation over rugged terrain, *Geogr. Anal.*, *11*, 65-85, 1979.

Dracup, J. A., J. M. Melack, D. Marks, R. Kattelmann, and J. O. Sickman, The hydrologic mass balance of the Emerald Lake Basin Integrated Watershed Study, Sequoia National Park, California, *Final Rep., Contr. A4-123-32*, 78 pp., Calif. Air Resour. Board, Sacramento, CA, 1988.

Elder, K. J., Spatial and temporal variation of net snow accumulation in a small alpine watershed, Emerald Lake Basin, Sierra Nevada, California, USA, *Ann. Glaciol.*, in press.

Feth, J. H., S. M. Rogers, and G. E. Roberson, Chemical composition of snow in the northern Sierra Nevada and other areas, *Water Supply Pap. 1535J*, U.S. Geol. Survey, 1964.

Frantisak, F., G. H. Pelletier, M. Bedard, and G. Castonguay, Precipitation quality in northwest Quebec, Canada, *Prepared for presentation at the 73rd Annual Meeting of the Air Pollution Control Association, Montreal, Quebec, 22-27 June*, 1980.

Galloway, J. N., B. J. Crosby, and G. E. Likens, Acid precipitation: measurement of pH and acidity, *Limnol. Oceangr.*, *24*, 1161-1165, 1979.

Galloway, J. N., C. L. Shofield, G. R. Hendrey, N. F. Peters, and A. H. Johannes, Lake acidification during spring snowmelt, in *Proceedings ILWAS Annual Review Conference*, 1980.

Galvin, P. J. and J. A. Cline, Measurement of anions in the snowcover of the Adirondack Mountains, *Atmos. Environ.*, *12*, 1163-1167, 1978.

Giles, M. A., H. S. Mayewski, and B. Hobden, Osmoregulatory and hematological responses of rainbow trout (*Salmo gairdneri*) to extended environmental acidification, *Can. J. Fish. Aquatic Sci.*, *41*, 1686-1694, 1984.

Granger, R. J. and D. H. Male, Melting of a prairie snowpack, *J. Appl. Meteorol.*, *17*, 1833-1842, 1978.

Gunn, J. M. and W. Keller, Spawning site water chemistry and lake trout (*Salvelinus namaycush*) sac fry survival during spring snowmelt, *Can. J. Fish. Aquatic Sci.*, *41*, 319-329, 1984.

Haapala, H., P. Sepponen, and E. Meskus, Effects of spring floods on water acidity in the Kiiminkijoki area, Finland, *Oikos*, *26*, 26-31, 1975.

Henriksen, A. and R. F. Wright, Effects of acid precipitation on a small acid lake in southern Norway, *Nordic Hydrol.*, *8*, 1-10, 1977.

Hubert, B. J., F. C. Fehsenfels, R. B. Norton, and D. Albritton, The scavenging of nitric acid vapor by snow, in *Precipitation Scavenging, Dry Deposition, and Resuspension*, edited by W. G. N. Slinn, pp. 293-302, Elsevier, New York, 1983.

Jefferies, D. S., C. M. Cox, and P. J. Dillon, Depression of pH in lakes and streams in central Ontario during snowmelt, *Can. J. Fish. Res. Board Can.*, *36*, 640-646, 1979.

Johannessen, M. and A. Henriksen, Chemistry of snow meltwater: changes in concentration during melting, *Water Resour. Res., 14*, 615-619, 1978.

Jones, H. G. and W. Sochanska, The chemical characteristics of snow cover in a northern boreal forest during the spring runoff period, *Ann. Glaciol., 7*, 176-174, 1985.

Jones, K. A., S. B. Brown, and T. J. Hara, Behaviorial and biochemical studies of onset and recovery from acid stress in Arctic char (*Salvelinus alpinus*), *Can. J. Fish. Aquatic Sci., 44*, 373-381, 1987.

Kattelmann, R. C., Macropores in snowpacks of the Sierra Nevada, *Ann. Glaciol., 6*, 1985.

Kelso, J. R. M., C. K. Minns, J. H. Lipsit, and D. S. Jeffries, Headwater lake chemistry during the spring freshet in north-central Ontario, *Water, Air, Soil Pollut., 29*, 245-259, 1986.

Kumar, S., Reactive scavenging of pollutants by rain: a modeling approach, *Atmos. Environ., 20*, 1015-1024, 1986.

Laird, L. B., H. E. Taylor, and V. C. Kennedy, Snow chemistry of the Cascade–Sierra Nevada Mountains, *Environ. Sci. Technol., 20*, 275-290, 1986.

Langham, E. J., Physics and properties of snowcover, in *Handbook of Snow*, edited by D. M. Gray and D. H. Male, pp. 275-337, Pergamon Press, Toronto, 1981.

Leivestad, H., G. Hendrey, I. P. Muniz, and E. Snekvik, Effects of acid precipitation on freshwater organisms, in *Impact of Acid Precipitation on Forest and Freshwater Ecosystems in Norway*, edited by F. H. Braekke, SNSF Proj. 1432 As, Res. Rep. FR 6/76, pp. 87-111, Oslo, 1976.

Leivestad, H. and I. P. Muniz, Fish kill at low pH in a Norwegian river, *Nature, 259*, 391-392, 1976.

Liljestrand, H. M. and J. J. Morgan, Error analysis applied to indirect methods for precipitation acidity, *Tellus, 31*, 421-431, 1979.

Male, D. H., The seasonal snowcover, in *Dynamics of Snow and Ice Masses*, edited by S. C. Colbeck, pp. 305-390, Academic Press, New York, 1980.

Martinelli, M. Jr., Accumulation of snow in alpine areas of central Colorado and means of influencing it, *J. Glaciol., 5*, 625-636, 1965.

Mason, B. J., *Clouds, Rain and Rainmaking*, pp. 34-37, 50-53, Cambridge Univ. Press, Cambridge, 1975.

McBean, G. A. and S. Nikleva, Composition of snow in Pacific coastal mountains, *Atmos. Environ., 20*, 1161-1164, 1986.

McLean, R. A. N., The relative contributions of sulfuric and nitric acids in acid rain to the acidification of the ecosystem: implications for control strategies, *J. Air Pollut. Control Assoc., 31*, 1184-1186, 1981.

Meiman, J. R., Snow accumulation related to elevation, aspect and forest canopy, in *Snow Hydrology, Proceedings of a Workshop Seminar*, pp. 35-47, Can. Natl. Comm. Intl. Hydrol. Decade, Ottawa, Ontario, 1968.

Melack, J. M., S. D. Cooper, R. W. Holmes, J. O. Sickman, K. Kratz, P. Hopkins, H. Hardenbergh, M. Thieme, and L. Meeker, Chemical and biological survey of lakes and streams located in the Emerald Lake watershed, Sequoia National Park, *Final Rep. to the Calif. Air Resour. Board , contract A3-096-32*, 1987.

Melack, J. M., J. L. Stoddard, and D. R. Dawson, Acid precipitation and buffer capacity of lakes in the Sierra Nevada, California, in *Proceedings of the International Symposium on Hydrometeorology*, edited by A. I. Johnson and R. A. Clarke, pp. 35-41, Amer. Water Resour. Assoc., Bethesda, MD, 1982.

Melack, J. M., M. W. Williams, and J. O. Sickman, Episodic acidification during snowmelt in waters of the Sierra Nevada, California, in *Proceedings of the First International Symposium on Mountain Watersheds*, in press.

Messer, J. J., L. Slezak, and C. I. Liff, Potential for acid snowmelt in the Wasatch Mountains, *Water Quality Ser. Rep. UWRL/Q-82/06*, Utah Water Res. Lab., Utah State Univ., Logan, 1982.

Michaels, H. A., A. Bradman, C. L. Blanchard, and J. Harte, Investigation of snow pack chemistry on the western slope of the Colorado Rockies, *Rep. No. ERG-87-1*, 55 pp., Energy Resour. Group, Univ. Calif., Berkeley, CA, 1987.

Miller, J. M., A statistical evaluation of the U. S. precipitation network, in *Precipitation Scavenging (1974)*, edited by R. B. Semonin and R. W. Beadle, pp. 639-659, Tech. Info. Ctr., Energy Res. Devel. Admin., Springfield, VA, 1977.

Mizuno, Y. and D. Kuroiwa, Solute segregation in ice observed by autoradiography, *Cont. Inst. Low Temp. Sci., Ser. A*, 41-51, 1969.

Morris, E. M. and A. G. Thomas, Preferential discharge of pollutants during snowmelt in Scotland, *J. Glaciol., 31*, 190-193, 1985.

Peterson, R. H., P. G. Daye, G. L. Lacroix, and E. T. Garside, Reproduction in fish experiencing acid and metal stress, in *Proceedings of an International Symposium on Acidic Rain and Fishery Impacts on Northeastern North America*, edited by R. E. Johnson, pp. 177-195, Amer. Fish. Soc., Bethesda, MD, 1982.

Rascher, C. M., C. T. Driscoll, and N. E. Peters, Concentration and flux of solutes from snow and forest floor during snowmelt in the West-central Adirondack region of New York, *Biogeochemistry, 3*, 209-224, 1987.

Raymond, C. F. and K. Tusima, Grain coarsening of water-saturated snow, *J. Glaciol., 22*, 83-105, 1979.

Raynor, G. S. and J. V. Haynes, Differential rain and snow scavenging efficiency implied by ionic concentration differences in winter precipitation, in *Precipitation Scavenging, Dry Deposition, and Resuspension*, edited by H. R. Pruppacher, R. G. Semonin, and W. G. N. Slinn, pp. 249-264, Elsevier, New York, 1983.

Reuss, J. O. and D. W. Johnson, in *Acid Deposition and the Acidification of Soils and Waters*, p. 119, Springer-Verlag, New York, 1986.

Reynolds, B., The chemical composition of snow at a rural upland site in Mid-Wales, *Atmos. Environ., 17*, 1849-1851, 1983.

Richards, T. L., Physics and chemistry of snowfall and snow distribution, in *The Role of Snow and Ice in Hydrology*, edited by J. C. Rodda, IAHS-AIHS Publ. 107, pp. 1-13, Intl. Assoc. Hydrol. Sci., Wallingford, UK, 1973.

Schemenauer, R. S., M. O. Berry, and J. B. Maxwell, Snowfall formation, in *Handbook of Snow*, edited by D. M. Gray and D. H. Male, pp. 129-151, Pergamon Press, New York, 1981.

Seip, H. M., G. Abrahamsen, N. Christophersen, E. T. Gjessing, and A. O. Stuanes, Snow and meltwater chemistry in mini-catchments, *SNSF Proj. IR53/80*, Oslo, 1980.

Seligman, G., *Snow Structure and Ski Fields*, Intl. Glaciol. Soc., Cambridge, 1936. (Reprinted 1980)

Skarveit, A. and K. T. Gjessing, Chemical budgets and chemical quality of snow and runoff during spring snowmelt, *Nordic Hydrol., 10*, 141-154, 1979.

Sommerfeld, R. A., A branch grain theory of temperature gradient metamorphism in snow, *J. Geophys. Res., 88*, 1484-1494, 1983.

Sommerfeld, R. A. and E. LaChapelle, The classification of snow metamorphism, *J. Glaciol., 9*, 3-17, 1970.

Stein, J., H. G. Jones, J. Roberge, and W. Sochanska, The prediction of both runoff quality and quantity by the use of an integrated snowmelt model, in *Modelling Snowmelt-Induced Processes*, edited by E. M. Morris, IAHS-AIHS Publ. 155, pp. 347-359, Intl. Assoc. Hydrol. Sci., Wallingford, UK, 1986.

Stoddard, J. L., Nutritional status, microcrustacean communities and susceptibility to acid precipitation of high elevation lakes in the Sierra Nevada, California, Ph. D. Thesis, 188 pp pp., Dept. Biol. Sci., Univ. Calif., Santa Barbara, CA, 1986.

Stohlgren, T. J. and D. J. Parsons, Variation of wet deposition chemistry in Sequoia National Park, California, *Atmos. Environ.*, *21*, 1369-1374, 1987.

Strickland, J. D. and T. R. Parsons, A practical handbook of seawater analysis, *Bull. Fish. Res. Bd. Canada*, *167*, 83, 1972.

Suzuki, K., Chemical changes of snow cover by melting, *Jap. J. Limnol.*, *43*, 102-112, 1982.

Topol, L. E., Differences in ionic composition and behavior in winter rain and snow, *Atmos. Environ.*, *20*, 347-355, 1986.

Tranter, M., P. Brimblecombe, T. D. Davies, C. E. Vincent, P. W. Abrahams, and I. Blackwood, The composition of snowfall, snowpack, and meltwater in the Scottish Highlands – evidence for preferential elution, *Atmos. Environ.*, *20*, 517-525, 1986.

Tranter, M., T. D. Davies, P. W. Abrahams, I. Blackwood, P. Brimblecombe, and C. E. Vincent, Spatial variability in the chemical composition of snowcover in a small, remote, Scottish catchment, *Atmos. Environ.*, *21*, 853-862, 1987.

Valderrama, J. C., The simultaneous analysis of total nitrogen and total phosphorus in natural waters, *Marine Chem.*, *10*, 109-122, 1981.

Welch, E. B., W. H. Chamberlain, and D. E. Spyidak, Chemical content of snow and effect of melting on Cascade mountain lakes, *Northwest Sci.*, *58*, 85-93, 1984.

Williams, M. W. and J. M. Melack, Effects of spatial and temporal variation in snowmelt on nitrate and sulfate pulses in an alpine watershed, *Ann. Glaciol.*, in press.

Woo, M. and H. O. Slaymaker, Alpine streamflow response to variable snowpack thickness and extent, *Geogr. Annaler, Ser. A*, *57A*, 201-212, 1975.

Woo, S. and N. H. Berg, Factors influencing the quality of snow precipitation and snow throughfall at a Sierra Nevada site, in *Proceedings of the Symposium: Cold Regions Hydrology*, edited by D. L. Kane, pp. 201-209, Amer. Water Resour. Assoc., Bethesda, MD, 1986.

Yosida, Z. et al., Physical studies on deposited snow 1. Thermal properties, *Cont. Inst. Low Temp. Sci., Ser. A*, 19-74, 1955.

TABLE 4.1. Precision and Detection Limits of Chemical Methods

Standard deviation (S.D.) and method detection limit† (MDL = 2 SD) of chemical methods. Replicate det tions (n) of deionized water (DIW) or analyst prepared standards† (the levels tabulated are the theoretical trations) were measured on separate days except where indicated (*) when a single trial on one day was usec

Constituent	Units	n	Standard	SD	MDL
Ammonium	μM	10	DIW	0.15	0.30
Phosphate	μM	10	DIW	0.03	0.06
Silica	μM	7	DIW	0.20	0.40
Nitrate	μeq L^{-1}	7*	0.50	0.10	0.20
Chloride	μeq L^{-1}	7*	0.50	0.19	0.38
Sulfate	μeq L^{-1}	7*	0.75	0.22	0.44
Calcium	μeq L^{-1}	4	2.50	0.50	1.00
Magnesium	μeq L^{-1}	4	2.06	0.16	0.32
Sodium	μeq L^{-1}	6	1.09	0.25	0.50
Potassium	μeq L^{-1}	6	0.64	0.22	0.45

†Limits of detection for major ions were established in accord with the Scientific Apparatus Makers Ass (SAMA) definition for detection limit: that concentration which yields an absorptance equal to twice the s deviation of a series of measurements of a solution whose concentration is detectable above, but close to th absorptance. Determination of method detection limits for ions by ion chromatography (Dionex 2010i ion ch graph, 200 μL sample loop, 3 μS attenuation or atomic absorption spectrophotometry (direct, air-acetylene) tated the use of a low level standard as DIW gave no signal under our routine operating conditions.

TABLE 4.2. 1985 Snow Season Charge Balance Data

Date	Site	SWE (cm)	Σ^+	Σ^-	Σ^+/Σ^-	$\frac{\Sigma^+ - \Sigma^-}{\Sigma^+ + \Sigma^-}$
Snowpack Chemical Profile Summary						
841212	inlet	52	11.9	9.6	1.24	10.7%
850130	inlet	38	10.4	10.6	0.98	-1.0%
850227	inlet	83	13.4	12.1	1.11	5.1%
850510	inlet	22	13.0	8.1	1.60	23.2%
850510	tower	33	7.4	4.3	1.72	26.5%
850510	bench	26	10.5	6.6	1.59	22.8%
850523	cirque	27	12.7	7.1	1.79	28.3%
850523	bench	22	9.6	5.3	1.81	28.9%
850523	ramp	47	11.8	6.7	1.76	27.6%
850523	hole	61	8.8	5.1	1.73	26.6%
850523	inlet	16	13.1	6.7	1.96	32.3%
850523	pond	31	12.1	10.0	1.21	9.5%
Snow Chemistry Event Summary						
841110	event	78	18.3	19.6	0.93	-3.4%
841119	event	13	19.5	20.8	0.94	-3.2%
841128	event	19	10.6	8.8	1.20	9.3%
841211	event	43	7.9	6.2	1.27	12.1%
850111	event	14	9.4	4.5	2.09	35.3%
850130	event	9	11.1	8.3	1.34	14.4%
850206	event	1	12.3	7.5	1.64	24.2%
850215	event	8	10.9	4.3	2.53	43.4%
850315	event	1	10.8	9.2	1.17	8.0%
850327	event	80	6.6	3.3	2.00	33.3%

Stein, J., H. G. Jones, J. Roberge, and W. Sochanska, The prediction of both runoff quality and quantity by the use of an integrated snowmelt model, in *Modelling Snowmelt-Induced Processes*, edited by E. M. Morris, IAHS-AIHS Publ. 155, pp. 347-359, Intl. Assoc. Hydrol. Sci., Wallingford, UK, 1986.

Stoddard, J. L., Nutritional status, microcrustacean communities and susceptibility to acid precipitation of high elevation lakes in the Sierra Nevada, California, Ph. D. Thesis, 188 pp pp., Dept. Biol. Sci., Univ. Calif., Santa Barbara, CA, 1986.

Stohlgren, T. J. and D. J. Parsons, Variation of wet deposition chemistry in Sequoia National Park, California, *Atmos. Environ.*, *21*, 1369-1374, 1987.

Strickland, J. D. and T. R. Parsons, A practical handbook of seawater analysis, *Bull. Fish. Res. Bd. Canada*, *167*, 83, 1972.

Suzuki, K., Chemical changes of snow cover by melting, *Jap. J. Limnol.*, *43*, 102-112, 1982.

Topol, L. E., Differences in ionic composition and behavior in winter rain and snow, *Atmos. Environ.*, *20*, 347-355, 1986.

Tranter, M., P. Brimblecombe, T. D. Davies, C. E. Vincent, P. W. Abrahams, and I. Blackwood, The composition of snowfall, snowpack, and meltwater in the Scottish Highlands – evidence for preferential elution, *Atmos. Environ.*, *20*, 517-525, 1986.

Tranter, M., T. D. Davies, P. W. Abrahams, I. Blackwood, P. Brimblecombe, and C. E. Vincent, Spatial variability in the chemical composition of snowcover in a small, remote, Scottish catchment, *Atmos. Environ.*, *21*, 853-862, 1987.

Valderrama, J. C., The simultaneous analysis of total nitrogen and total phosphorus in natural waters, *Marine Chem.*, *10*, 109-122, 1981.

Welch, E. B., W. H. Chamberlain, and D. E. Spyidak, Chemical content of snow and effect of melting on Cascade mountain lakes, *Northwest Sci.*, *58*, 85-93, 1984.

Williams, M. W. and J. M. Melack, Effects of spatial and temporal variation in snowmelt on nitrate and sulfate pulses in an alpine watershed, *Ann. Glaciol.*, in press.

Woo, M. and H. O. Slaymaker, Alpine streamflow response to variable snowpack thickness and extent, *Geogr. Annaler, Ser. A*, *57A*, 201-212, 1975.

Woo, S. and N. H. Berg, Factors influencing the quality of snow precipitation and snow throughfall at a Sierra Nevada site, in *Proceedings of the Symposium: Cold Regions Hydrology*, edited by D. L. Kane, pp. 201-209, Amer. Water Resour. Assoc., Bethesda, MD, 1986.

Yosida, Z. et al., Physical studies on deposited snow 1. Thermal properties, *Cont. Inst. Low Temp. Sci., Ser. A*, 19-74, 1955.

TABLE 4.1. Precision and Detection Limits of Chemical Methods

Standard deviation (S.D.) and method detection limit† (MDL = 2 SD) of chemical methods. Replicate deter tions (n) of deionized water (DIW) or analyst prepared standards† (the levels tabulated are the theoretical c trations) were measured on separate days except where indicated (*) when a single trial on one day was used.

Constituent	Units	n	Standard	SD	MDL
Ammonium	µM	10	DIW	0.15	0.30
Phosphate	µM	10	DIW	0.03	0.06
Silica	µM	7	DIW	0.20	0.40
Nitrate	µeq L^{-1}	7*	0.50	0.10	0.20
Chloride	µeq L^{-1}	7*	0.50	0.19	0.38
Sulfate	µeq L^{-1}	7*	0.75	0.22	0.44
Calcium	µeq L^{-1}	4	2.50	0.50	1.00
Magnesium	µeq L^{-1}	4	2.06	0.16	0.32
Sodium	µeq L^{-1}	6	1.09	0.25	0.50
Potassium	µeq L^{-1}	6	0.64	0.22	0.45

†Limits of detection for major ions were established in accord with the Scientific Apparatus Makers Assoc (SAMA) definition for detection limit: that concentration which yields an absorptance equal to twice the sta deviation of a series of measurements of a solution whose concentration is detectable above, but close to the absorptance. Determination of method detection limits for ions by ion chromatography (Dionex 2010i ion chr graph, 200 µL sample loop, 3 µS attenuation or atomic absorption spectrophotometry (direct, air-acetylene) n tated the use of a low level standard as DIW gave no signal under our routine operating conditions.

TABLE 4.2. 1985 Snow Season Charge Balance Data

Date	Site	SWE (cm)	Σ^+	Σ^-	Σ^+/Σ^-	$\frac{\Sigma^+ - \Sigma^-}{\Sigma^+ + \Sigma^-}$
Snowpack Chemical Profile Summary						
841212	inlet	52	11.9	9.6	1.24	10.7%
850130	inlet	38	10.4	10.6	0.98	-1.0%
850227	inlet	83	13.4	12.1	1.11	5.1%
850510	inlet	22	13.0	8.1	1.60	23.2%
850510	tower	33	7.4	4.3	1.72	26.5%
850510	bench	26	10.5	6.6	1.59	22.8%
850523	cirque	27	12.7	7.1	1.79	28.3%
850523	bench	22	9.6	5.3	1.81	28.9%
850523	ramp	47	11.8	6.7	1.76	27.6%
850523	hole	61	8.8	5.1	1.73	26.6%
850523	inlet	16	13.1	6.7	1.96	32.3%
850523	pond	31	12.1	10.0	1.21	9.5%
Snow Chemistry Event Summary						
841110	event	78	18.3	19.6	0.93	-3.4%
841119	event	13	19.5	20.8	0.94	-3.2%
841128	event	19	10.6	8.8	1.20	9.3%
841211	event	43	7.9	6.2	1.27	12.1%
850111	event	14	9.4	4.5	2.09	35.3%
850130	event	9	11.1	8.3	1.34	14.4%
850206	event	1	12.3	7.5	1.64	24.2%
850215	event	8	10.9	4.3	2.53	43.4%
850315	event	1	10.8	9.2	1.17	8.0%
850327	event	80	6.6	3.3	2.00	33.3%

TABLE 4.3. 1986 Snow Season Charge Balance Data

Date	Site	SWE(cm)	Σ^+	Σ^-	Σ^+/Σ^-	$\frac{\Sigma^+ - \Sigma^-}{\Sigma^+ + \Sigma^-}$
Snowpack Chemical Profile Summary						
860118	inlet	70	6.0	4.3	1.40	16.5%
860205	pond	80	8.7	5.4	1.61	23.4%
860205	ridge	89	9.2	5.6	1.64	24.3%
860305	inlet	175	10.4	7.8	1.33	14.3%
860414	pond	165	7.2	3.3	2.18	37.1%
860414	ridge	317	8.4	4.7	1.79	28.2%
860505	hole	231	7.5	3.2	2.34	40.2%
860505	inlet	243	6.4	3.0	2.13	36.2%
860523	inlet	197	7.6	2.9	2.62	44.8%
860523	ridge	264	7.7	2.8	2.74	46.5%
860627	inlet	119	7.5	0.7	10.71	82.9%
860627	ridge	141	9.2	1.9	4.84	65.8%
Event Summary Snow Chemistry						
851120	event	19	8.5	5.1	1.67	25.0%
851203	event	43	9.7	6.4	1.52	20.5%
860109	event	17	7.9	3.0	2.63	45.0%
860204	event	18	8.4	5.9	1.42	17.5%
860219	event	106	8.7	6.0	1.45	18.4%
860319	event	42	7.6	6.8	1.12	5.6%
860410	event	3	19.6	14.2	1.38	16.0%
860416	event	1	33.2	31.1	1.07	3.3%
860504	event	2	23.8	18.3	1.30	13.1%
860507	event	1	38.3	38.2	1.00	0.1%

TABLE 4.4. Cation Contamination from Filters

Desorption of cations and bicarbonate from Gelman A/E 47mm glass fiber filters determined in sequenti of deionized water. Five 50 mL aliquots of MilliQ water (specific conductance < 1 $\mu S\ cm^{-1}$, 25°C) sequentially through each of two A/E filters from different lots of filters. Additionally, the first lea filtered again through a Nucleopore .22 µm membrane filter. Leachates were analyzed for cations by at tion spectrophotometry (direct, air-acetylene). Data are tabulated in $\mu eq\ L^{-1}$, and undetectable levels ar by u. Levels of cations in re-filtered leachates are in parentheses. Method detection limits for Ca^{2+}, Mg K^+ are 1.0, 0.3, 0.5, and 0.5 $\mu eq\ L^{-1}$, respectively.

Lot #	Aliquot	Ca^{2+}	Mg^{2+}	Na^+	K^+
1498	1	(3.3)4.7	2.2	(38)37	0.6
	2	1.7	1.2	3.6	u
	3	1.3	1.0	4.0	u
	4	1.3	1.0	2.0	u
	5	1.0	0.6	(1.4)1.7	u
1498	1	(4.6)6.6	2.2	(48)46	0.6
	2	1.3	1.2	5.7	u
	3	1.0	1.2	2.7	u
	4	1.0	0.7	1.9	u
	5	(1.0)1.0	0.7	(1.3)1.4	u
2664	1	(2.3)2.8	1.6	(39)39	0.6
	2	1.0	1.0	3.0	u
	3	1.0	1.0	4.0	u
	4	u	0.5	1.4	u
	5	u	0.5	(1.4)1.4	u
2664	1	(1.6)1.7	1.3	(36)34	u
	2	1.0	1.2	7.6	u
	3	u	1.2	1.7	u
	4	u	0.5	1.4	u
	5	(1.0)u	0.5	(1.6)1.4	u

TABLE 4.5 Event Synopsis, Ion Concentrations, January 9 1986

Core	SWE (mm)	pH	µS	(Concentrations in µeq L^{-1}) H^+	NH_4^+	Na^+	K^+	Ca^{2+}	Mg^{2+}	NO_3^-	SO_4^{2-}	Cl^-	PO_4^{3-}
Inlet Site													
1A	156	5.46	2.0	3.5	0.6	1.5	0.5	0.1	0.1	1.0	0.6	0.5	0.0
1B	152	5.46	2.0	3.5	0.7	3.3	0.6	0.2	0.1	1.1	0.8	0.7	0.1
$\bar{x}1$	154	5.46	2.0	3.5	0.7	2.4	0.6	0.1	0.1	1.1	0.7	0.6	0.1
2A	152	5.46	2.6	3.5	1.4	2.5	0.6	0.2	0.2	0.6	1.0	1.3	0.1
2B	148	5.48	3.2	3.3	1.5	2.4	1.7	3.9	1.4	0.8	0.9	1.4	0.1
$\bar{x}2$	150	5.47	2.9	3.4	1.4	2.5	1.1	2.0	0.8	0.7	0.9	1.4	0.1
Site	152	5.46	2.4	3.5	1.0	2.4	0.8	1.1	0.4	0.9	0.8	1.0	0.1
Tower Site													
1A	193	5.36	2.6	4.4	1.3	1.6	0.5	0.4	0.1	1.5	1.3	1.8	0.0
1B	162	5.40	2.6	4.0	1.1	0.7	0.5	0.6	0.1	1.1	1.1	0.9	0.1
1C	172	5.43	2.2	3.7	1.2	1.6	0.5	2.5	0.6	0.9	0.6	0.8	0.1
1D	56	5.51	2.1	3.1	1.4	1.5	0.7	2.5	0.4	0.5	0.5	1.7	0.1
Site	165	5.40	2.4	4.0	1.2	1.4	0.5	1.2	0.3	1.2	1.0	1.2	0.1
Pond Site													
1A	205	5.52	4.9	3.0	0.9	1.3	1.0	1.1	0.3	0.5	0.7	1.3	0.0
1B	193	5.60	3.9	2.5	0.9	1.6	0.7	0.6	0.1	0.2	0.8	1.5	0.0
$\bar{x}1$	199	5.55	4.4	2.8	0.9	1.4	0.9	0.9	0.2	0.4	0.8	1.4	0.0
2A	167	5.40	2.6	4.0	1.1	1.0	0.3	0.1	0.1	1.1	0.7	1.3	0.1
2B	170	5.39	2.9	4.1	1.2	1.8	0.2	0.1	0.1	0.9	0.6	0.9	0.0
$\bar{x}2$	169	5.40	2.8	4.0	1.1	1.4	0.3	0.1	0.1	1.0	0.7	1.1	0.1
Site	185	5.48	3.7	3.3	1.0	1.4	0.6	0.6	0.2	0.6	0.7	1.3	0.0
Ridge Site													
1A	180	5.32	2.4	4.8	1.1	2.6	0.8	2.5	0.6	1.0	0.9	1.5	0.1
1B	180	5.15	3.4	7.1	1.7	1.7	0.7	2.5	0.8	0.3	0.9	0.8	0.2
$\bar{x}1$	180	5.22	2.9	6.0	1.4	2.1	0.8	2.5	0.7	0.7	0.9	1.1	0.1
2A	179	5.36	3.2	4.4	1.1	2.9	1.5	0.1	0.1	1.0	0.8	2.7	0.0
2B	174	5.38	2.3	4.2	0.7	1.5	0.5	0.1	0.1	1.0	0.6	0.9	0.0
$\bar{x}2$	177	5.37	2.8	4.3	0.9	2.2	1.0	0.1	0.1	1.0	0.7	1.8	0.0
Site	179	5.29	2.9	5.1	1.1	2.2	0.9	1.3	0.4	0.8	0.8	1.5	0.1
Event	171	5.40	2.9	4.0	1.1	1.8	0.7	1.0	0.3	0.9	0.8	1.3	0.1

Table 4.6. 1985 Event Snow Chemistry Summary

SWE (mm)	pH	µS	(Concentrations in µeq L^{-1}) H^+	NH_4^+	Na^+	K^+	Ca^{2+}	Mg^{2+}	NO_3^-	SO_4^{2-}	Cl^-	PO_4^{3-}
841110												
78	5.30	5.4	5.0	0.5	4.3	1.1	4.1	3.3	4.1	6.3	7.6	1.6
841119												
135	5.41	6.3	3.9	1.9	3.6	1.9	6.8	1.4	6.1	7.1	6.7	0.9
841128												
190	5.30	4.0	5.0	1.0	1.8	0.5	1.7	0.6	1.6	2.2	4.9	0.1
841211												
43	5.43	2.7	3.7	1.9	0.8	0.5	0.9	0.1	2.0	2.7	1.4	0.1
850111												
146	5.25	1.8	5.6	0.2	1.6	0.5	1.5	0.0	1.5	1.0	1.9	0.1
850130												
90	5.23	7.5	5.9	1.1	1.1	1.3	1.7	0.0	1.4	3.4	3.4	0.1
850206												
16	5.21	3.4	6.2	1.6	1.0	1.7	1.7	0.1	1.0	2.7	3.6	0.2
850215												
88	5.06	2.0	8.7	0.2	0.9	0.5	0.5	0.1	0.7	0.6	3.0	0.0
850315												
180	5.28	3.9	5.3	1.0	1.2	0.9	1.5	0.9	2.1	3.0	3.7	0.4
850327												
80	5.42	1.6	3.8	0.3	1.3	0.4	0.5	0.3	1.0	1.0	1.2	0.1

Table 4.7 1985 Snowpack Chemical Profile Summary
Ion Concentration and Ion Loading

Date	SWE (cm)	pH	µS	(Concentrations in µeq L^{-1}. Loadings in meq m^{-2}.) H^+	NH_4^+	Na^+	K^+	Ca^{2+}	Mg^{2+}	NO_3^-	SO_4^{2-}	Cl^-
Inlet:												
841212	53	5.52	3.4	3.0	2.7	1.6	0.9	2.6	1.1	3.7	2.9	3.0
		Loading		1.6	1.4	0.8	0.5	1.4	0.6	1.9	1.5	1.6
850130	38	5.46	2.8	3.5	1.8	2.1	1.4	1.3	0.3	4.1	2.6	3.9
		Loading		1.3	0.7	0.8	0.5	0.5	0.1	1.6	1.0	1.5
850227	83	5.40	3.1	4.0	3.3	2.4	0.9	1.7	1.1	5.0	3.7	3.4
		Loading		3.3	2.7	2.0	0.7	1.4	1.0	4.1	3.1	2.8
850510	22	5.34	1.8	4.6	3.5	2.4	0.7	1.3	0.5	3.3	1.7	3.1
		Loading		1.0	0.8	0.5	0.2	0.3	0.1	0.7	0.4	0.7
850523	17	5.55	2.0	2.8	1.9	4.5	0.2	2.6	1.1	1.8	1.3	3.6
		Loading		0.5	0.3	0.7	0.0	0.4	0.2	0.3	0.2	0.6
Tower:												
850510	34	6.15	2.2	0.7	1.4	1.3	0.6	2.9	0.5	1.3	1.1	1.9
		Loading		0.2	0.5	0.4	0.2	1.0	0.2	0.4	0.4	0.6
Bench:												
850510	26	5.40	1.9	4.0	2.9	2.1	0.6	0.6	0.3	3.3	1.5	1.8
		Loading		1.0	0.7	0.5	0.2	0.2	0.1	0.9	0.4	0.5
850523	22	5.52	1.9	3.0	0.7	3.5	0.5	1.2	0.7	0.6	1.2	3.5
		Loading		0.6	0.2	0.7	0.1	0.2	0.2	0.1	0.3	0.8
Pond:												
850523	32	5.64	2.7	2.3	1.1	4.0	1.3	2.4	1.0	1.1	4.0	4.9
		Loading		0.7	0.3	1.30	0.4	0.8	0.3	0.3	1.30	1.6
Ramp:												
850523	47	5.55	1.8	2.8	1.3	2.7	1.3	2.3	1.4	1.4	3.0	2.3
		Loading		1.3	0.6	1.3	0.6	1.1	0.7	0.7	1.4	1.1
Hole:												
850523	61	5.42	2.0	3.8	1.1	2.2	0.3	0.5	0.9	1.8	1.3	2.0
		Loading		2.3	0.6	1.3	0.22	0.3	0.6	1.1	0.8	1.2
Cirque:												
850523	27	5.54	2.1	2.9	0.5	3.6	1.0	1.9	2.8	0.3	3.7	3.1
		Loading		0.8	0.1	1.0	0.2	0.5	0.8	0.1	1.0	0.8

Table 4.8. 1986 Event Snow Chemistry Summary

SWE (mm)	pH	µS	(Concentrations in µeq L^{-1}) H^+	NH_4^+	Na^+	K^+	Ca^{2+}	Mg^{2+}	NO_3^-	SO_4^{2-}	Cl^-	PO_4^{3-}
851120 194	5.37	3.2	4.3	1.0	1.0	0.5	1.3	0.4	0.7	0.7	3.7	0.1
851203-1218 438	5.25	3.4	5.6	0.8	1.5	0.5	0.9	0.4	1.8	1.7	2.9	0.1
860109 171	5.40	2.9	4.0	1.1	0.8	0.7	1.0	0.3	0.9	0.8	1.3	0.1
860204 186	5.37	3.1	4.3	2.2	0.6	1.0	0.2	0.1	1.4	1.3	3.2	0.0
860219 66	5.31	3.0	4.9	0.8	1.6	0.9	0.3	0.2	1.9	1.2	2.9	0.1
860319 428	5.46	3.1	3.5	1.1	1.3	1.0	0.5	0.2	1.1	1.9	3.8	0.1
860410 35	5.54	8.6	2.9	7.5	5.0	1.0	1.6	1.6	5.3	3.6	5.3	0.3
860416 14	5.17	7.6	6.8	19.0	4.0	1.1	1.7	0.6	13.0	12.6	5.5	0.2
860504 25	5.34	5.8	4.6	15.2	1.6	0.6	1.4	0.4	6.9	8.0	3.4	0.2
860507 10	5.11	9.4	7.7	18.1	8.6	1.7	1.4	0.8	14.3	15.2	8.7	0.1

Table 4.9 1986 Snowpack Chemical Profile Summary
Ion Concentrations and Ion Loading

Core	SWE (cm)	pH	µS	(Concentrations in µeq L^{-1}. Loadings in meq m^{-2}.) H^+	NH_4^+	Na^+	K^+	Ca^{2+}	Mg^{2+}	NO_3^-	SO_4^{2-}	Cl^-
Inlet												
				Date: 860118								
A	70	5.37	2.6	4.3	0.8	0.4	0.2	0.2	0.1	1.5	1.0	0.9
B	71	5.40	2.7	4.0	0.1	1.2	0.5	0.2	0.1	1.2	1.6	2.5
Mean	71	5.39	2.6	4.1	0.4	0.8	0.4	0.2	0.1	1.3	1.3	1.7
		Loading		2.9	0.3	0.6	0.3	0.1	0.1	0.9	0.9	1.2
				Date: 860305								
A	148	5.31	3.2	4.9	1.0	2.9	0.7	0.3	0.3	1.9	1.3	4.8
		Loading		7.3	1.5	4.3	1.0	0.4	0.4	2.7	1.8	7.1
				Date: 860505								
A	241	5.43	2.0	3.7	1.0	0.9	0.3	0.1	0.1	0.5	1.3	1.2
B	246	5.43	2.2	3.7	1.1	0.9	0.6	0.1	0.2	0.8	0.7	1.7
Mean	244	5.43	2.1	3.7	1.1	0.9	0.5	0.1	0.1	0.6	1.0	1.4
		Loading		9.0	2.6	2.2	1.1	0.2	0.3	1.5	2.5	3.5
				Date: 860523								
A	197	5.46	2.1	3.5	1.1	1.4	0.3	1.3	0.3	0.6	0.7	1.8
B	198	5.42	2.1	3.8	0.8	1.8	0.7	0.4	0.1	0.5	0.7	1.6
Mean	198	5.44	2.1	3.6	0.9	1.6	0.5	0.8	0.2	0.5	0.7	1.7
		Loading		7.2	1.8	3.2	0.9	1.6	0.5	1.0	1.4	3.3
				Date: 860627								
A	119	5.46	1.8	3.5	0.7	1.2	0.2	1.3	0.4	0.4	0.1	0.5
B	120	5.52	1.4	3.0	0.7	1.6	0.2	1.8	0.6	0.3	0.1	0.1
Mean	119	5.49	1.6	3.2	0.7	1.4	0.2	1.5	0.5	0.3	0.1	0.3
		Loading		3.8	0.8	1.7	0.3	1.8	0.6	0.4	0.1	0.3
Tower												
				Date: 860305								
A	170	5.34	3.3	4.6	2.1	1.6	0.5	0.4	0.3	1.5	1.6	4.7
B	180	5.27	3.9	5.4	2.2	0.9	0.5	0.2	0.3	1.5	1.5	4.7
Mean	175	5.30	3.6	5.0	2.2	1.2	0.5	0.3	0.3	1.5	1.6	4.7
		Loading		8.8	3.8	2.1	0.8	0.5	0.5	2.6	2.7	8.2
Pond												
				Date: 860205								
A	80	5.39	2.9	4.1	1.0	2.0	1.0	0.3	0.3	1.5	1.3	2.6
		Loading		3.2	0.8	1.6	0.7	0.2	0.2	1.2	1.0	2.1
				Date: 860414								
A	166	5.41	2.3	3.9	1.1	1.2	0.3	0.2	0.1	0.9	0.6	1.6
B	166	5.44	2.2	3.6	1.1	1.8	0.6	0.3	0.1	0.9	1.0	1.6
Mean	166	5.42	2.3	3.8	1.1	1.5	0.5	0.2	0.1	0.9	0.8	1.6
		Loading		6.2	1.8	2.5	0.8	0.4	0.2	1.6	1.3	2.7

Table 4.9 (continued). 1986 Snowpack Chemical Profile Summary

Core	SWE (cm)	pH	µS	(Concentrations in µeq L^{-1}. Loadings in meq m^{-2}.) H^+	NH_4^+	Na^+	K^+	Ca^{2+}	Mg^{2+}	NO_3^-	SO_4^{2-}	Cl^-
Ridge												
				Date: 860205								
A	90	5.33	3.1	4.7	1.3	1.0	0.5	0.6	1.1	0.6	1.5	3.5
		Loading		4.2	1.1	0.8	0.4	0.5	1.0	0.6	1.3	3.1
				Date: 860414								
A	305	5.48	2.8	3.3	1.3	1.4	0.9	0.5	0.3	1.4	1.8	2.0
B	329	5.49	2.6	3.2	1.3	1.8	0.4	1.9	0.3	1.3	1.2	1.8
Mean	318	5.49	2.7	3.2	1.3	1.6	0.7	1.3	0.3	1.3	1.5	1.9
		Loading		1.0	4.1	5.1	2.1	4.0	0.8	4.3	4.7	6.0
				Date: 860523								
A	262	5.44	3.3	3.6	1.1	1.2	0.4	0.1	0.2	0.3	1.2	1.2
B	266	5.43	2.2	3.7	1.1	1.3	0.2	1.6	0.6	0.7	0.8	1.4
Mean	264	5.43	2.7	3.7	1.1	1.3	0.3	0.9	0.4	0.5	1.0	1.3
		Loading		9.7	2.8	3.4	0.8	2.3	1.0	1.4	2.7	3.5
				Date: 860627								
A	138	5.44	1.8	3.6	0.7	1.9	0.4	2.0	1.3	0.2	0.2	1.7
B	144	5.49	1.8	3.2	0.9	2.0	0.3	1.3	0.8	0.2	0.2	1.4
Mean	141	5.47	1.8	3.4	0.8	2.0	0.3	1.7	1.0	0.2	0.2	1.5
		Loading		4.8	1.2	2.8	4.5	2.4	1.5	0.3	0.3	2.1
Hole												
				Date: 860505								
A	228	5.36	2.6	4.4	2.0	1.3	0.3	0.2	0.1	1.4	1.2	1.7
B	235	5.37	2.5	4.3	1.6	0.6	0.3	0.1	0.1	1.2	1.1	1.6
Mean	232	5.37	2.5	4.3	1.8	0.9	0.3	0.1	0.1	1.3	1.2	1.7
		Loading		10.0	4.1	2.2	0.7	0.2	0.3	3.0	2.7	3.8

Table 4.10. Volume-weighted Ion Concentration and Wet Deposition, from Winter Snowfalls (Snowboards), Water Years 1985 and 1986

Year	pH	µS	H^+	NH_4^+	Na^+	K^+	Ca^{2+}	Mg^{2+}	NO_3^-	SO_4^{2-}	Cl^-	PO_4^{3-}
Seasonal volume-weighted chemical concentration (µeq L^{-1})												
WY85	5.29	4.0	5.3	0.9	1.9	0.9	2.2	0.7	2.3	3.0	4.0	0.4
S	0.03	0.6	0.4	0.2	0.3	0.2	0.6	0.3	0.5	0.7	0.6	0.1
WY86	5.34	3.3	4.6	1.4	1.4	0.8	0.6	0.3	1.8	1.6	3.1	0.1
S	0.06	0.7	0.6	1.9	0.6	0.1	0.3	0.2	1.1	1.1	0.6	0.0

Year	SWE (mm)	H^+	NH_4^+	Na^+	K^+	Ca^{2+}	Mg^{2+}	NO_3^-	SO_4^{2-}	Cl^-	PO_4^{3-}
Snow season deposition (meq m^{-2})											
WY85	1046	5.50	0.94	1.95	0.91	2.35	0.76	2.41	3.15	4.15	0.41
WY86	2567	11.88	3.55	3.72	2.09	1.52	0.70	4.52	4.01	7.96	0.25
Snow season depositon (mg m^{-2})											
WY85	1046	5.5	13.2	44.7	35.7	47.1	9.2	33.8	50.5	147.3	4.3
WY86	2567	12.0	49.8	85.5	81.8	30.4	8.6	63.3	64.2	282.1	2.6

S = precipitation-weighted standard deviation = $S = [(1 / \Sigma P_i)\, \Sigma P_i (C_i - \bar{C})^2]^{1/2}$.
P_i = volume of water for the i th event.
C_i = concentration of the i th event.
$\bar{C}$ = mean concentration of the ion for the snow season.

WY 85: snowfall events from November 11 1984 to March 27 1985 (see Table 4.6).
WY 86: snowfall events from November 20 1985 to May 7 1986 (see Table 4.8).
The November 11 snowfall of 120 mm SWE was not sampled for chemistry

Table 4.11. Comparison, by Precipitation Type, of the Seasonal Volume-Weighted Ion Concentration from Wet Deposition (point measurements), Water Years 1985 and 1986

Volume-weighted chemical concentrations (µeq L^{-1})

Type	pH	µS	H^+	NH_4^+	Na^+	K^+	Ca^{2+}	Mg^{2+}	NO_3^-	SO_4^{2-}	Cl^-	Σ^+	Σ^-
WY85													
Rain	4.93	19.1	16.7	42.8	18.1	5.6	34.1	4.7	40.4	30.6	17.1	125.0	88.0
Snow-Autumn	5.07	6.8	8.3	15.1	5.5	1.2	6.2	1.3	11.8	7.8	7.6	37.5	27.3
Snow-Winter	5.28	4.0	5.3	0.9	1.9	0.9	2.2	0.7	2.3	3.0	4.0	11.9	9.3
WY86													
Rain	4.87	13.0	10.7	23.4	5.0	2.0	17.9	3.1	22.2	18.3	5.6	62.0	46.2
Snow-Autumn	5.11	8.0	7.4	21.8	3.0	1.4	7.0	1.1	14.7	10.0	4.3	41.7	29.0
Snow-Winter	5.34	3.3	4.6	1.4	1.4	0.8	0.6	0.3	1.8	1.6	3.1	9.1	6.5

Chemistry Sources [CARB, 1988]
Rain: Aerochem Metrics model 301 sampler at the inlet site.
Snow-Autumn: Aerochem Metrics model 301 sampler at the inlet site.
Winter Snow (1985): Table 4.10.
Winter Snow (1986): Table 4.10.

Table 4.12. Comparison, by Precipitation Type, of the Seasonal Wet Deposition of Ions and Water, Water Years 1985 and 1986

Type	SWE (mm)	Deposition (meq m^{-2}) H^+	NH_4^+	Na^+	K^+	Ca^{2+}	Mg^{2+}	NO_3^-	SO_4^{2-}	Cl^-	Σ^+	Σ^-
WY 85												
Rain	16	0.3	0.7	0.3	0.1	0.5	0.1	0.6	0.5	0.3	2.0	1.4
Snow-Autumn	95	0.9	1.4	0.5	0.1	0.6	0.1	1.1	0.7	0.7	3.6	2.6
Snow-Winter	1046	5.5	0.9	2.0	0.9	2.3	0.7	2.4	3.1	4.2	12.4	9.7
WY 86												
Rain	32	0.3	0.8	0.2	0.1	0.6	0.1	0.7	0.6	0.2	2.0	1.5
Snow-Autumn	213	1.6	4.6	0.6	0.3	1.5	0.2	3.1	2.1	0.9	8.9	6.2
Snow-Winter	2380	10.9	3.3	3.3	1.9	1.4	0.7	4.3	3.8	7.4	21.7	15.5

Calculation of Wet Deposition
Ionic loading to the basin was calculated by multiplying precipitation amount by the volume-weighted concentrations in Table 4.11.

Precipitation Sources
Precipitation amount is our best estimate of the amount of water that was deposited over the entire watershed. Since areal estimates of precipitation are difficult to make, all precipitation estimates utilize the best estimate of areal precipitation available. Rain: precipitation from Dracup et al. [1988]. Autumn Snow: precipitation from Dracup et al. [1988]. Winter Snow (1985): precipitation from snowboards (Table 4.10). Winter Snow (1986): precipitation from Dracup et al. [1988].

Table 4.13. Percent Flux of Wet Deposition, by Precipitation Type, Water Years 1985 and 1986

Type	SWE	Percent Flux, by Precipitation Type H^+	NH_4^+	Na^+	K^+	Ca^{2+}	Mg^{2+}	NO_3^-	SO_4^{2-}	Cl^-	Σ^+	Σ^-
WY 85												
Rain	1	4	24	10	8	16	8	15	11	5	11	10
Snow-Autumn	8	12	46	19	10	17	13	27	17	14	20	19
Snow-Winter	91	84	30	71	82	67	79	58	72	81	69	71
WY 86												
Rain	1	3	9	4	3	17	10	9	9	2	6	6
Snow-Autumn	8	12	53	15	13	43	22	38	33	11	27	27
Snow-Winter	91	85	38	81	84	41	68	53	58	87	67	67

Water and chemistry sources are same as Table 4.12.

Table 4.14 Volume-Weighted Ion Concentrations and Ion Loading to the Basin Snowmelt: 1985 and 1986

Mean concentrations ($\mu eq\ L^{-1}$)

Date	Source	pH	Cond	H^+	NH_4^+	Na^+	K^+	Ca^{2+}	Mg^{2+}	NO_3^-	SO_4^{2-}	Cl^-
850327†	a	5.29	4.0	5.3	0.9	1.9	0.9	2.2	0.7	2.3	3.0	4.0
850523	b	5.52	2.1	3.1	1.1	3.1	0.8	1.6	1.3	1.3	2.4	2.9
860416†	c	5.34	3.2	4.6	1.2	1.4	0.8	0.6	0.3	1.7	1.4	3.1
860505	d	5.40	2.3	4.0	1.4	0.9	0.4	0.1	0.1	0.9	1.1	1.1
860523	e	5.43	2.4	3.7	1.0	1.4	0.4	0.9	0.3	0.5	0.9	1.5
860627	f	5.48	1.7	3.3	0.8	1.7	0.3	1.6	0.8	0.2	0.2	1.0

Ion Loading (10^3 Equivalents)

Date	Source	SWE (cm)	W_t ($10^6 m^3$)	H^+	NH_4^+	Na^+	K^+	Ca^{2+}	Mg^{2+}	NO_3^-	SO_4^{2-}	Cl^-	Σ Ions
850327†	a	92	1.2	6.4	1.1	2.3	1.1	2.8	0.9	2.8	3.7	4.9	26.0
850523	b	28	0.37	1.1	0.4	1.2	0.3	0.6	0.5	0.5	0.9	1.1	6.6
860416†	c	200	2.40	11.0	2.9	3.4	2.0	1.4	0.7	4.1	3.4	7.4	36.0
860505	d	197	2.36	9.4	3.3	2.1	0.9	0.2	0.2	2.1	2.6	2.6	23.0
860523	e	152	1.82	6.7	2.0	2.6	0.7	1.6	0.5	0.9	1.6	2.7	19.0
860627	f	56	0.67	2.2	0.5	1.1	0.2	1.1	0.5	0.1	0.1	0.7	6.5

SWE = mean snow water equivalence for the basin.
W_t = volume of snow water equivalence in the watershed.

Chemistry sources
- a = chemistry based on event samples through 850327
- b = chemistry from snowpits at the inlet, bench, pond, ramp, hole, cirque
- c = chemistry based on event samples through 860416
- d = chemistry from snowpits at the inlet and hole
- e = chemistry from snowpits at the inlet and ridge
- f = chemistry from snowpits at the inlet and ridge

†maximum accumulation date of the snow season

Table 4.15. Snowpack Chemical Profile Time Series, Inlet 1986

height (cm)	pH	µS	SWE (mm)	(Concentrations in µeq L^{-1}) H^+	NH_4^+	Na^+	K^+	Ca^{2+}	Mg^{2+}	NO_3^-	SO_4^{2-}	Cl^-
86 Jan 18												
167-117	5.41	2.2	225	3.9	0.1	1.8	0.5	0.3	0.1	1.4	1.2	0.9
117-67	5.48	2.2	205	3.3	0.0	1.3	0.5	0.1	0.1	0.9	0.8	1.4
67-17	5.32	3.8	225	4.8	0.0	0.8	0.6	0.2	0.1	1.2	2.5	4.8
17-0	5.40	2.1	58	4.0	0.4	0.5	0.3	0.3	0.1	1.7	2.0	3.0
86 March 05												
320-240	5.33	2.8	448	4.7	0.9	2.8	0.7	0.1	0.2	1.5	1.1	2.3
240-160	5.28	3.2	300	5.3	0.7	4.8	1.1	0.6	0.1	2.4	1.3	3.8
160-80	5.26	2.9	352	5.5	0.4	4.5	0.3	0.1	0.2	2.1	0.8	3.3
80-0	5.36	3.8	380	4.4	1.9	8.0	0.6	0.4	0.5	1.6	1.8	9.9
86 May 05												
415-345	5.46	1.9	416	3.5	0.7	0.4	0.5	0.1	0.1	0.4	0.3	0.7
345-265	5.49	2.6	444	3.2	1.3	0.6	0.1	0.0	0.2	0.9	1.0	1.4
265-185	5.39	1.9	481	4.1	0.8	1.0	0.7	0.0	0.1	0.4	0.2	1.7
185-105	5.44	2.0	471	3.6	1.1	1.3	0.6	0.0	0.2	1.0	0.9	1.7
105-0	5.40	2.6	649	4.0	1.3	0.9	1.0	0.2	0.2	1.0	1.1	2.5
86 May 23												
357-280	5.49	2.0	446	3.2	0.9	1.9	0.9	0.0	0.1	0.1	0.7	2.1
280-200	5.44	2.6	462	3.6	1.0	2.7	0.5	0.6	0.1	0.5	0.6	0.5
200-120	5.39	1.9	446	4.1	0.6	2.0	0.7	0.9	0.3	0.2	0.6	2.9
120-80	5.40	2.0	206	4.0	0.8	2.4	0.9	0.2	0.1	1.0	0.8	1.3
80-0	5.37	2.1	416	4.3	0.5	0.1	0.5	0.0	0.1	0.9	0.7	0.8
86 June 27												
203-125	5.50	1.6	496	3.2	0.4	1.7	0.2	1.1	0.5	0.1	0.1	0.7
125-40	5.50	1.8	423	3.2	0.8	0.6	0.2	1.1	0.2	0.5	0.0	0.2
40-0	5.36	2.0	267	4.4	1.0	1.4	0.3	1.8	0.4	0.8	0.4	0.6

Table 4.16. 1986 Snowpack Meltwater Chemical Concentration Data

Date	Time	Site	pH	µS	(Concentrations in µeq L^{-1}) H^+	NH_4^+	Na^+	K^+	Ca^{2+}	Mg^{2+}	NO_3^-	SO_4^{2-}	Cl^-
860501	18:30	SE gully	5.43	2.1	3.7	0.2	2.2	0.3	1.8	0.5	0.4	0.6	0.8
860502	09:15	SE gully	5.42	1.9	3.8	0.0	0.6	0.2	1.1	0.2	0.2	0.3	0.7
860502	18:30	SE gully	5.42	2.0	3.8	0.0	0.7	0.3	1.1	0.3	0.6	0.9	0.7
860518	11:30	inlet1	5.48	1.9	3.3	0.9	1.5	0.3	1.1	0.4	0.9	1.1	2.1
860519	11:30	inlet1	5.45	1.8	3.5	0.3	1.8	0.3	1.1	0.5	0.5	0.8	1.1
860518	11:15	inlet2	5.36	2.9	4.4	1.0	2.0	0.4	1.1	0.5	2.8	1.6	1.6
860519	11:30	inlet2	5.39	2.6	4.1	0.6	1.8	0.4	1.1	0.4	2.2	1.3	1.3
860519	11:30	SE gully	5.58	1.8	2.6	0.4	0.6	0.2	1.1	0.3	0.6	0.5	0.5
860525	09:20	inlet1	5.40	2.0	4.0	0.1	1.1	0.4	1.1	0.3	0.6	0.7	1.5
860525	16:30	inlet1	5.58	1.9	2.6	0.2	1.9	0.4	2.5	0.8	0.9	0.7	1.4
860525	10:10	SE gully	5.51	1.8	3.1	0.3	0.7	0.4	1.1	0.7	0.4	0.3	0.8
860525	14:00	ridge	5.42	1.9	3.8	0.2	0.7	0.3	1.1	0.7	0.9	0.4	0.3
860611	14:00	inlet1	5.44	2.7	3.6	0.9	1.5	1.5	0.3	0.5	0.7	1.9	1.5
860611	14:00	SE gully	5.51	2.1	3.1	1.0	1.7	1.0	0.3	0.3	2.0	0.9	1.6

Table 4.17. Statistical Analysis of Within- and Between-Site Variance of NO_3^- and SO_4^{2-} Concentrations from January 09, 1986 Snow Event

Nitrate				Sulfate			
Site	N	Mean	SD	Site	N	Mean	SD
Inlet	4	0.875	0.2217	Inlet	4	0.825	0.1708
Tower	4	0.675	0.4031	Tower	4	0.700	0.0817
Pond	4	0.825	0.3500	Pond	4	0.800	0.1414
Ridge	4	1.000	0.4163	Ridge	4	0.875	0.3862

One-way analysis of variance

Source	DF	Σ Squared	Mean Square	F value	Pr > F
Nitrate					
Site	3	0.1269	0.07229	0.57	0.6455
Error	12	1.5225	0.12688		
Sulfate					
Site	3	0.065	0.02167	0.42	0.7401
Error	12	0.615	0.05125		

Figure 4.1. Snow collection sites and drainage subbasins of the Emerald Lake catchment. Subbasins are as follows: A east joint, B southeast gully, C inflow #1, C+D inflow #1 and inflow #2, D inflow #2, E inflow #3, F inflow #4, G west joint. Sampling sites are as follows: 1 tower, 2 inlet, 3 bench, 4 ridge, 5 ramp, 6 pond, 7 hole, 8 cirque.

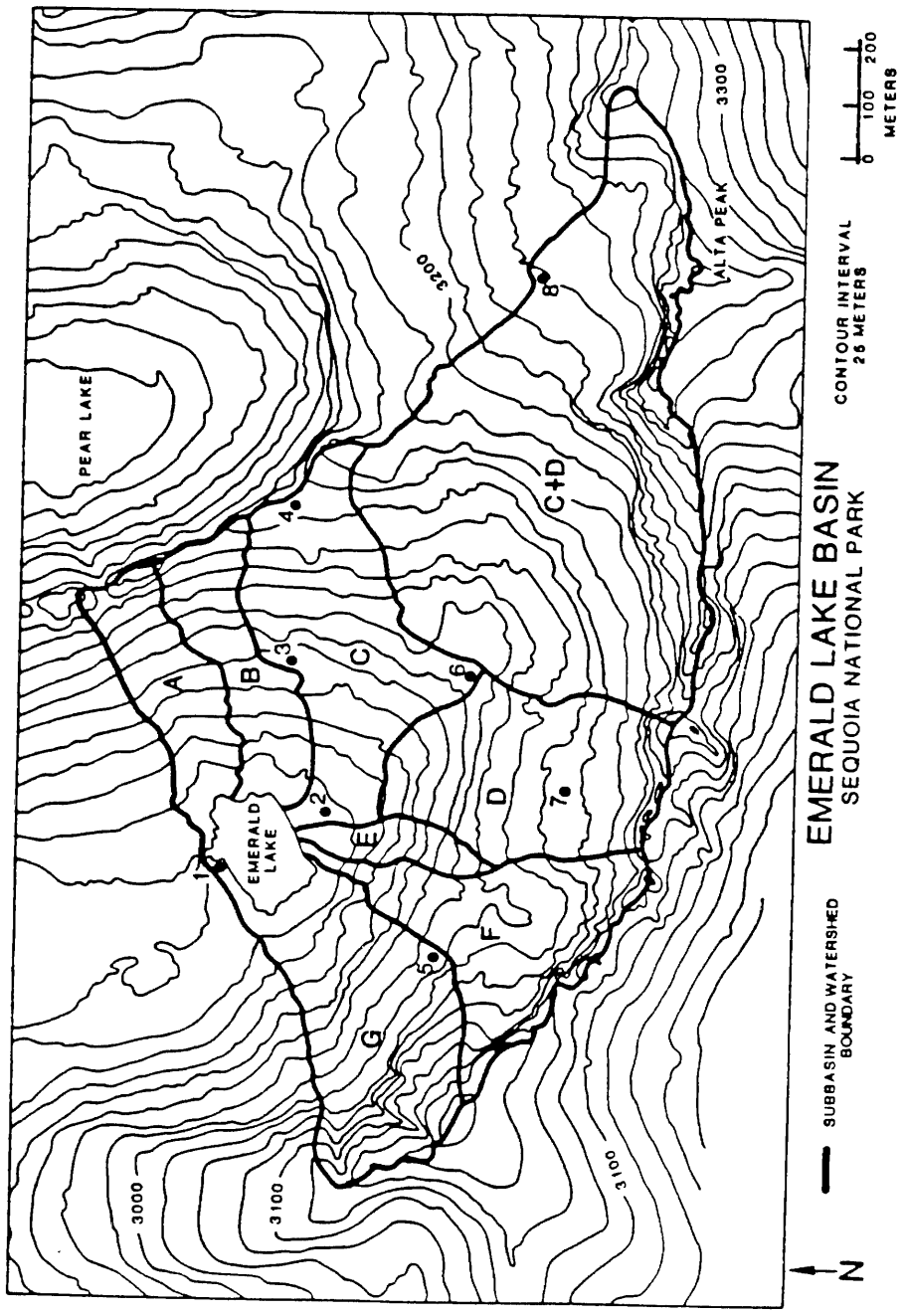

Figure 4.2. Cumulative event versus snowpit measurements for anion loading and SWE at the inlet site, 1986 snow season.

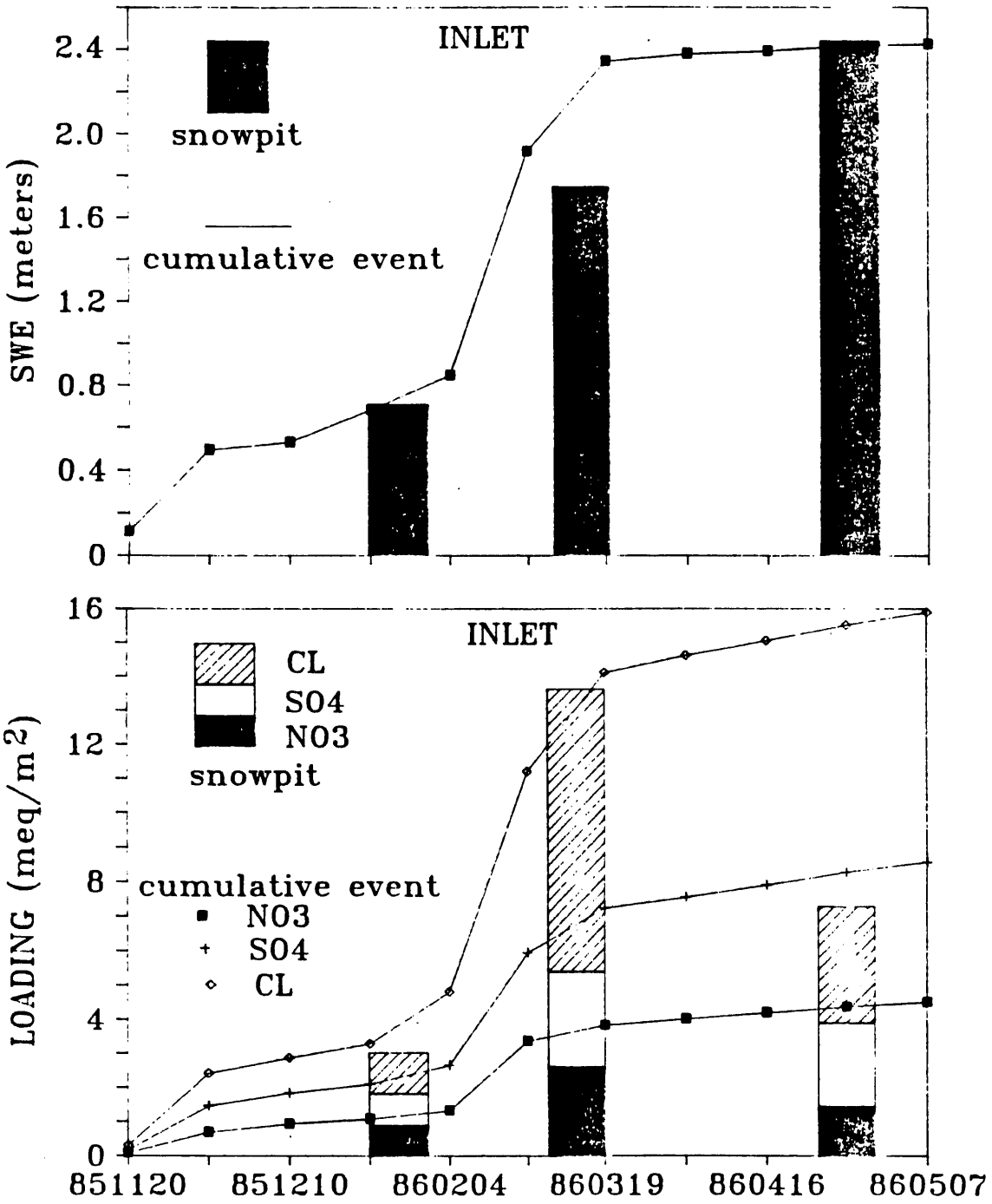

Figure 4.3. Anion loading and SWE in the snowpack as a function of time at the inlet site, 1986 snow season.

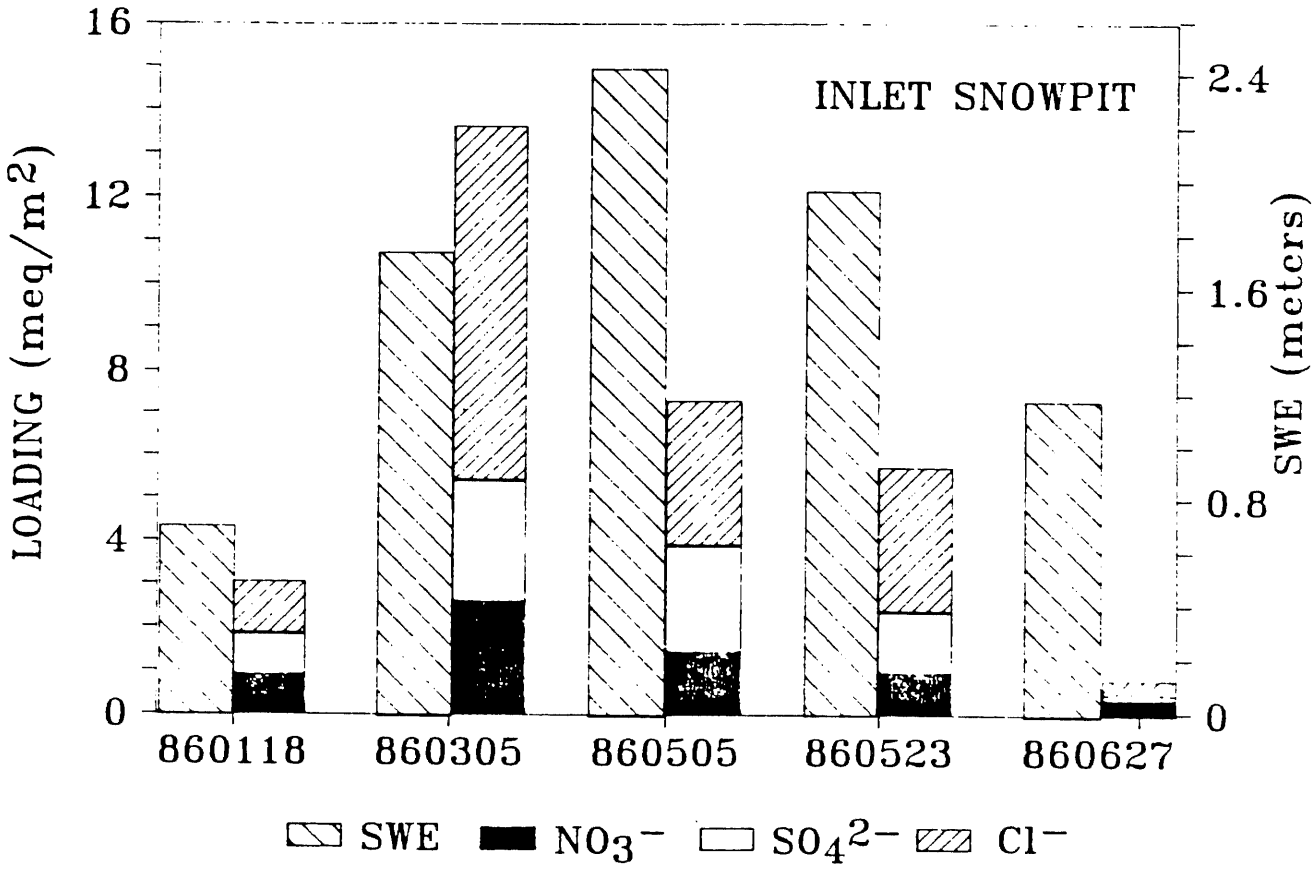

Figure 4.4. Spatial variability in anion concentration and loading at six sites in the Emerald Lake catchment on May 23, 1985.

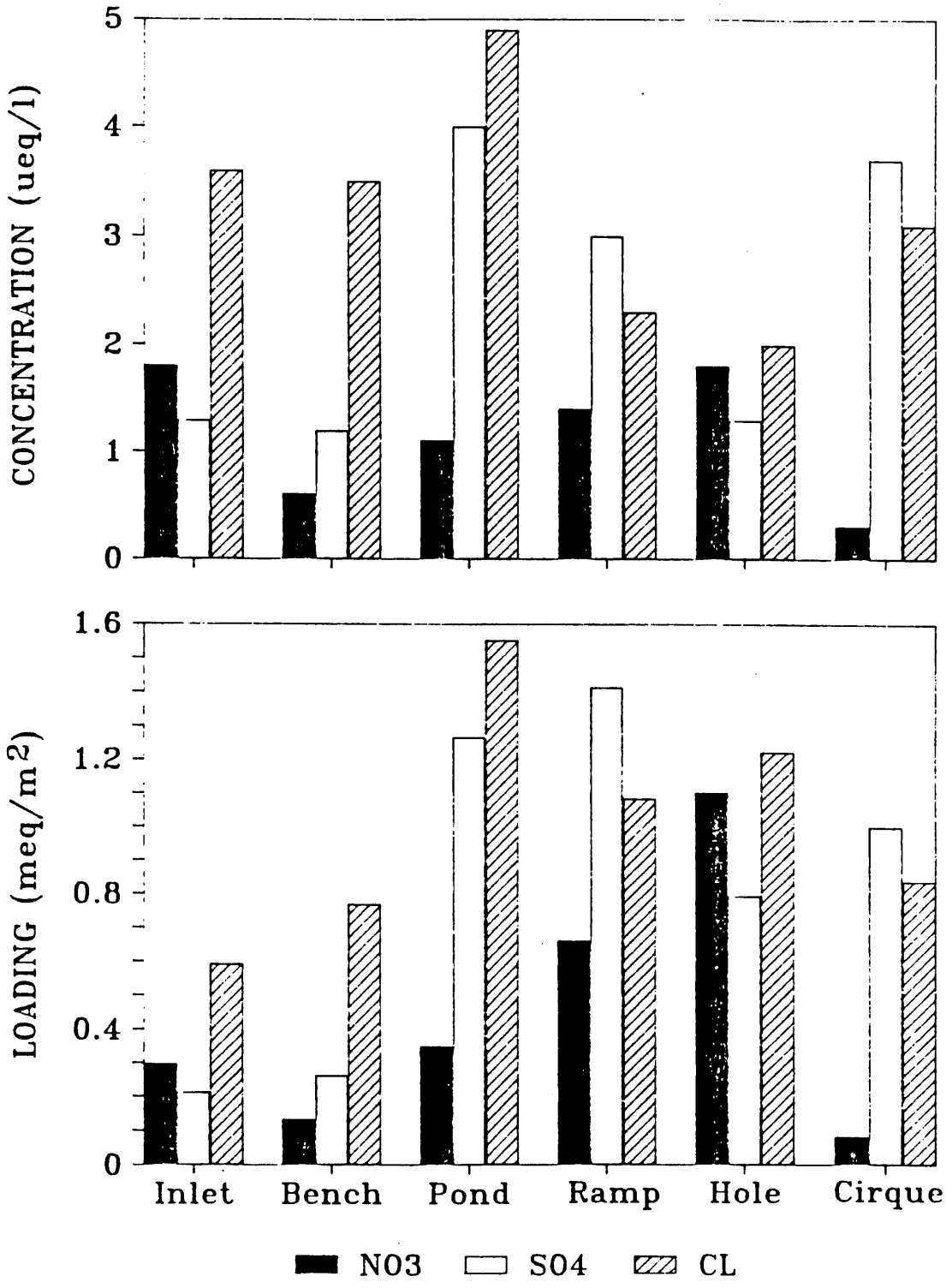

Figure 4.5. Nitrate and sulfate concentrations and discharge from inflow #2 from January 1 to July 1, 1986.

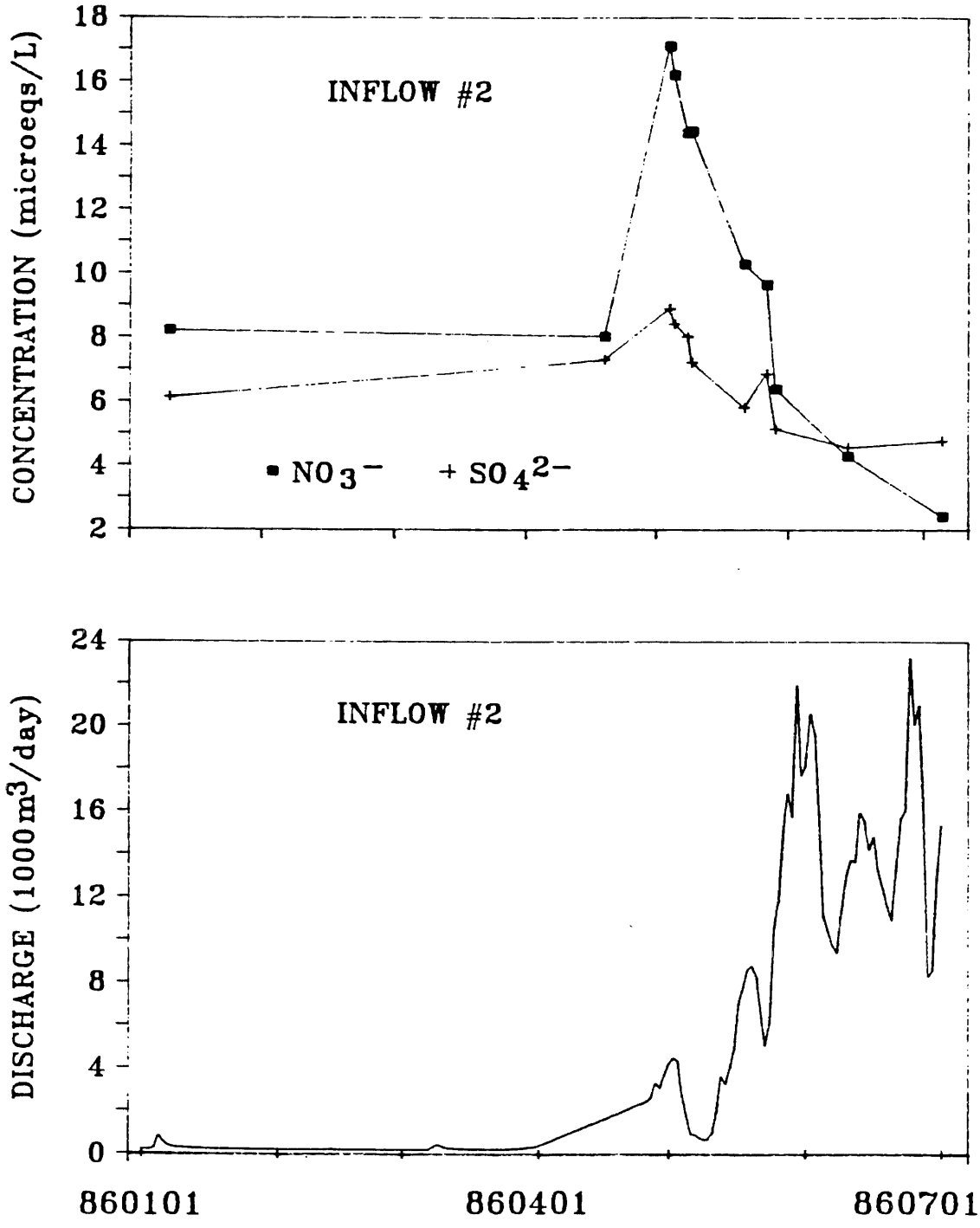

Figure 4.6. Nitrate and sulfate time series at the Emerald Lake outflow from June 1984 to July 1986.

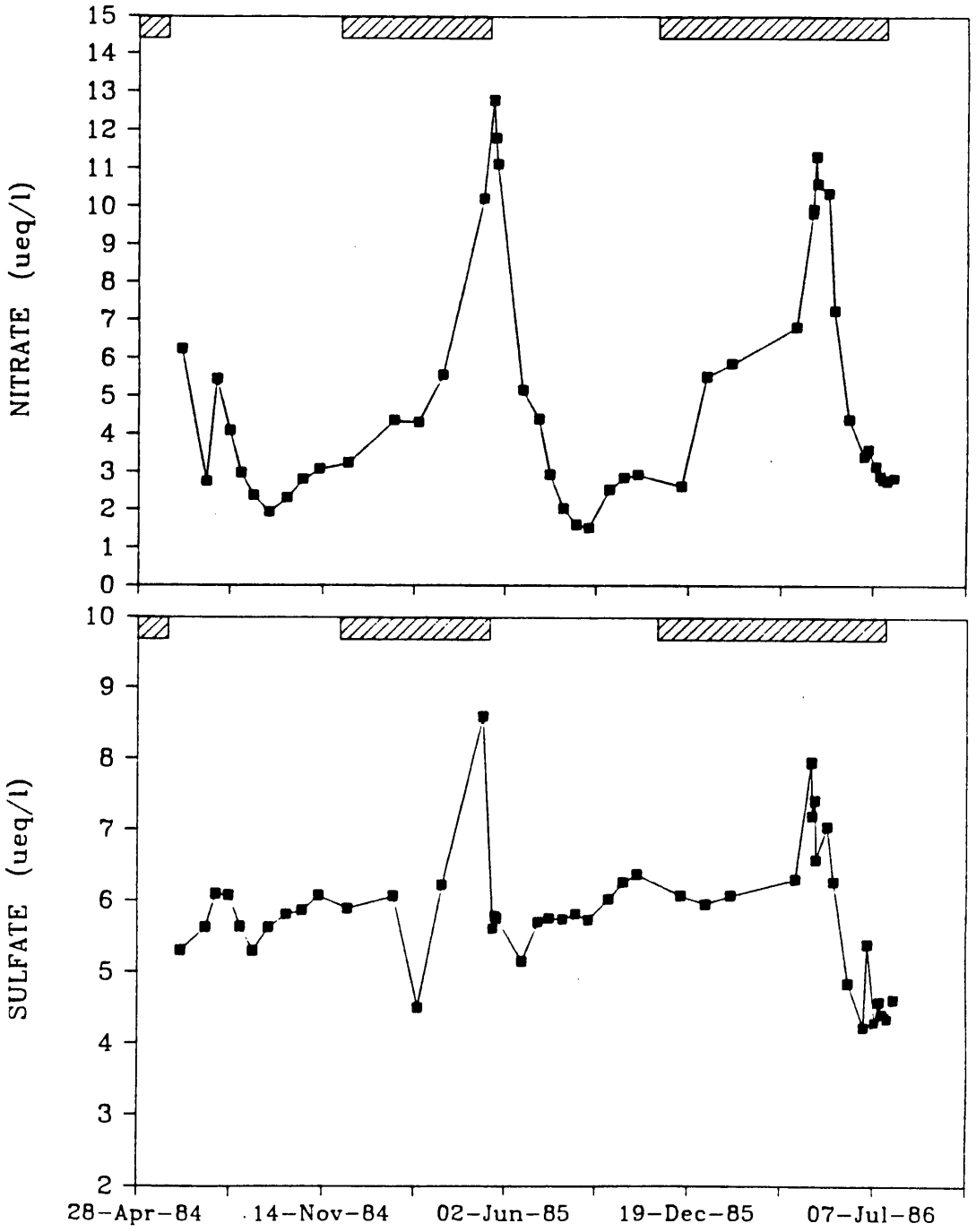

Figure 4.7. NO_3^- and SO_4^{2-} concentrations from streams are compared to snowmelt in their respective basins. Snowmelt on May 5 was 1% in the C+D subbasin and inflow #2 subbasin, with no snowmelt in the inflow #4 subbasin. OF is the outflow, SEG is the southeast gully, #1 is inflow #1, #2 is inflow #2, #4 is inflow #4.

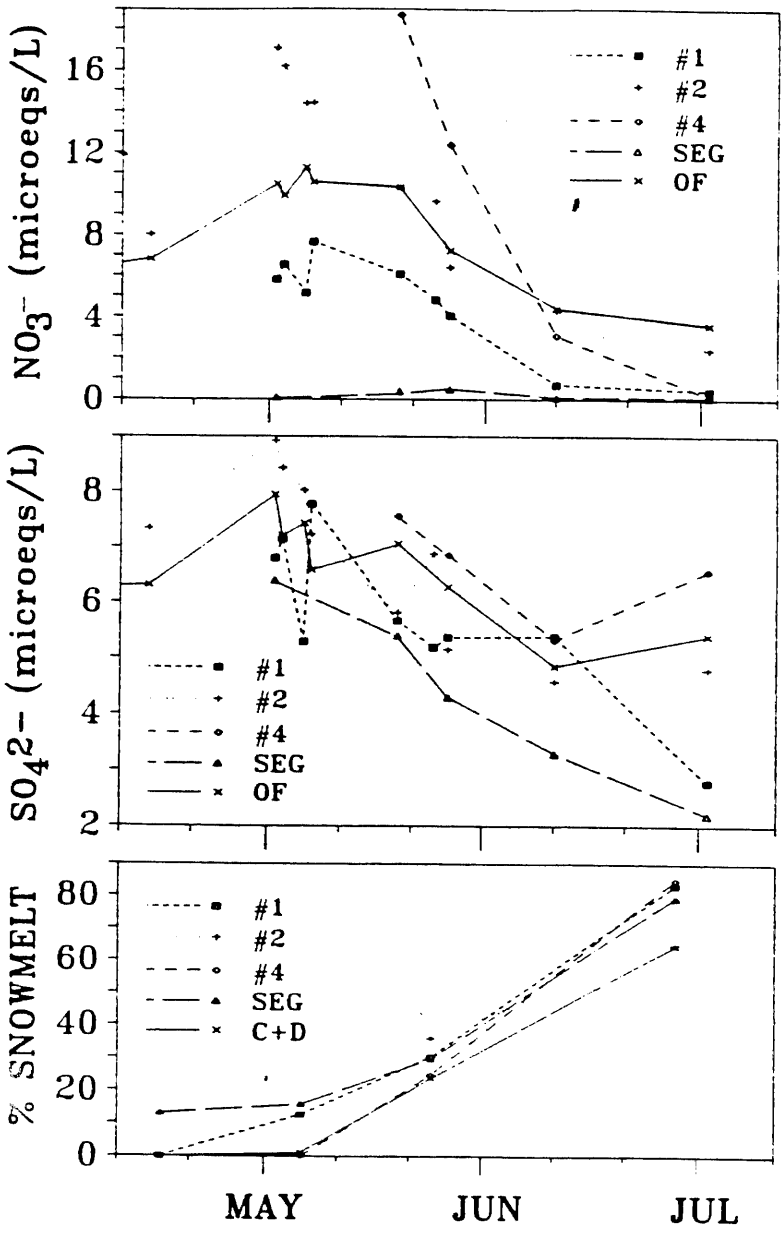

5. Measuring and Monitoring Stream Discharge

5.1. Introduction

In order to better understand the hydrology of a drainage basin we need to know the total flux of water from a basin and the spatial variation of that flux throughout the basin. The sources and magnitudes of water flux across the basin provide information which is essential to understanding variations in the hydrologic response of a drainage area to storm or snowmelt events [Eagleson, 1970]. This information is seldom available for basins or sub-basins smaller than 100 km^2 [USGS, 1971] though water flux from regions much smaller than this can be hydrologically very important.

Two examples of the importance of smaller scale variations in water flux are: (1) snowmelt runoff analysis where aspect and slope of a basin sub-region have a controlling effect on the rate melt water is generated [Dozier and Outcalt, 1979; Dozier, 1980; Frampton and Marks, 1980], and (2) detailed analysis of the hydrochemistry of the water flux through a basin system. In this case the origin of the water and the conditions under which the runoff was generated must be known [Marks et al., 1986]. Both of these problems are central to our work at Emerald Lake, which requires measuring or estimating water flux from drainage areas as small as a few hectares.

Because it is not possible to continuously monitor discharge in a natural stream, the problem is broken into two parts. The stage, or water height above a datum, is monitored, and discharge is measured at a variety of stages to establish a stage-discharge relationship, or rating curve. In the absence of high sediment transport, the channel geometry (or shape) is usually fixed, so it is assumed that at a given stage height, the discharge is constant. If discharge is measured at a full range of expected stage heights, then the rating curve can be reliably determined using either a linear or log-linear regression. However, it can be difficult to measure discharge at extreme high stages, especially in small alpine streams where such flows may be short-lived and not easy to anticipate. It is essential, therefore, to make as many measurements of discharge as possible, in order to establish the best possible rating curve for a given channel reach [Buchanan and Somers, 1968, 1969; USGS, 1977; Brakensiek et al., 1979].

Measuring discharge in small, swift flowing, alpine streams is difficult. Stream channels in such areas are poorly defined, or strewn with large boulders and falls such that conventional velocity profiling is not possible. At high flow there may be air entrainment. Turbulent or uneven flow under these conditions cannot be measured with a cup-type meter. At low flow, water depths can be so small that the size of even pygmy-type cup meters are on the order of the channel depth in many locations. Flow velocities may be so low (<15 $cm\,s^{-1}$) that the frictional resistance of the meter is on the same order as the force of the flowing water.

The normal method for measuring discharge under these conditions is to install a flume or weir. This allows direct measurement of discharge from the height of water in the weir or flume, by constricting the channel shape and slope at that place along the reach. Portable flumes can be used for this purpose, but this is not a viable alternative at Emerald Lake. We have measured discharges from 0.005–1.05 $m^3\,s^{-1}$ at the outflow of the lake; it would require 10 to 12 different size flumes to span this range of flows [U.S.D.A., 1979]. A concrete weir with several stage notches could be used, but this would be expensive, and would not be allowed in a wilderness area. At Emerald Lake we must rely on measured discharges to establish rating curves.

To solve these problems, we have developed a method that is simple but reliable, independent of channel geometry or flow characteristics, inexpensive, and ideally suited for use in a remote area such as Emerald Lake. The method requires minimal calibration, and can be performed by a lone investigator under certain circumstances. Any undivided channel reach can be used. Channel depth, turbulent flow, or low velocity flow have only minimal effect on the measurement. All of the equipment and supplies necessary to perform several field measurements weigh less than 5 kg. The method has a precision of better than 5% and an accuracy of better than 10% under most circumstances.

5.2. Calculating Stream Discharge

The flux of water through a channel is in general represented as a volume over time:

$$Q = A\,V \tag{1}$$

where Q is discharge ($m^3\,s^{-1}$), A is cross sectional area (m^2), and V is mean channel velocity ($m\,s^{-1}$) Hydraulic continuity requires that the discharge Q be the same along any cross section of the channel in the absence of branching or tributaries. This assumption is justified along a channel length of several hundred meters, as long as reasonably constant evaporation, infiltration, and ground water influx occur along the reach in question. For purposes of discharge measurement, continuity along a few tens of meters is sufficient.

For open channel reaches where channel geometry is not irregular, channel depth is greater than 10–15 cm, flow velocities are greater than 1 $m\,s^{-1}$, and flow regimes are not highly turbulent, Q can be measured by several conventional methods. A can be measured by hand or surveying techniques, and V can be estimated using a cup-type flow meter following the technique described by King and Brater [1963]. These conditions, however, are not likely to be met by most of the smaller streams draining small alpine watersheds. The difficulty with the above equation is that in many cases, both A and V can be very difficult to measure. For larger streams, over longer, more regular reaches, V can be determined from:

$$V = C_r\,(R\,S)^{1/2} \tag{2}$$

where C_r is channel resistance, R is the hydraulic radius, and S is the "energy gradient" or channel slope. The hydraulic radius $R = A / w_p$, where w_p is the wetted perimeter. For most larger channels, w_p is approximately equal to the channel width, and R then equals the mean channel depth.

From the equations above the empirical Manning formula [Streeter, 1966] is developed:

$$V = \frac{R^{2/3} S^{1/2}}{n} \quad (3)$$

where n is Manning's roughness coefficient. The use of this approach has a number of problems which are difficult to solve. We need good information on channel geometry because we must know the cross sectional area (A) to calculate the discharge (Q). We must estimate channel roughness (C_r) or Manning's roughness coefficient n with some accuracy. We must also know the channel slope (S) accurately. In small channels, along short reaches like those at Emerald Lake, these parameters are very difficult to measure accurately and difficult to estimate. If the channels of interest are strewn with boulders or cascading waterfalls, or choked with weeds and grasses, conventional measurement or calculation of discharge using the techniques described above is not possible.

5.3. Dilution Discharge Measurement

An alternative to the methods discussed above is the use of tracer dilution methods. A complete discussion of these methods is presented by Church and Kellerhals [1970] and Church [1975]. The method was presented originally by Stromeyer [1905]. Though the tracer can take a variety of forms, such as a radio-isotope or fluorescent dye, chemical tracers tend to be the most common because they cause negligible environmental effects and can be measured using standard instrumentation. Of the chemical tracers, salt is the most practical. It is inexpensive, easy to acquire, environmentally safe, and has an almost linear relationship between concentration and conductivity when mixed with water.

The dilution of the tracer in the stream is directly related to its discharge. The conductivity of the salt solution is linearly related to the concentration. Conductivity can be easily and accurately measured in the field, while concentration cannot.

There are two types of salt dilution methods. The first is the continuous injection method. This involves the continuous injection of a salt solution of known conductivity at a known rate into the stream. By measuring the conductivity of the stream before injection begins, and then again after an equilibrium conductivity has been reached, discharge can be calculated. The other technique is the slug injection method. This involves the sudden injection of a slug of known volume and conductivity into the stream. By measuring the background conductivity of the stream, and then the conductivity wave as it passes downstream, discharge can be calculated from

$$Q = C_s \frac{V_s}{\int_{t_i}^{t_f} (C_{ct} - Bk)\, dt} \quad (4)$$

where V_s is volume of the salt solution slug (m^3), C_{ct} is channel conductivity at time t ($\mu S\, cm^{-1}$), Bk is channel background conductivity ($\mu S\, cm^{-1}$), C_s is conductivity of the salt solution slug ($\mu S\, cm^{-1}$), t is time (s), t_i is initial time of conductivity wave passage, and t_f is final time of conductivity wave passage

This calculation is independent of the units of conductivity, which cancel, and gives discharge in $m^3\, s^{-1}$. The method, described in the above equation, assumes that the measurement site is sufficiently downstream from the slug injection site that complete mixing of the slug has occurred, and that the measurement time resolution is fine enough to account for variations in the conductivity wave as it passes. Bjerve and Groterud [1980] point out that the continuous injection method is inherently more accurate because it does not rely on these assumptions. While this observation is correct on face value, the logistical details are much more involved and far fewer measurements would be obtained. Also, the tank injection and water sampling scheme has the potential for calibration problems due to a difference in temperature between the stream and the calibration tank. In an alpine watershed like Emerald Lake, temperatures are often near freezing, where conductivity is sensitive to temperature. Solar insolation, therefore, could cause temperature variations during the procedure, both in the injection tank and in the water samples.

In the past, the problem with the slug injection method has been the lack of ability to accurately and efficiently measure conductivity in the field. Conductivity meters were bulky, laboratory instruments that were not well suited to field use (e.g. Wheatstone Bridge). The instruments were designed to measure conductivity of a sample, rather than for continuous measurement of a stream. They had a narrow dynamic range, so a probe or conductivity cell used to measure stream conductivities could not be used to measure the higher conductivities of the salt wave. This meant that the technique required extensive temperature calibration, because slug samples had to be collected and returned to a laboratory for dilution and measurement. If stream flow velocities were high, samples could not be collected quickly enough for good temporal resolution as the conductivity wave passed.

The problems discussed above have been largely corrected with the development of new lightweight, digital conductivity meters. These meters have a larger dynamic range, and have submersible probes which can be placed in the stream so that conductivity readings can be made almost continuously during the wave passage. Many are temperature compensated, but this is not critical because all conductivity measurements are made in the field, in the stream, and at a constant temperature. Our technique allows both wave and slug conductivities to be measured on the same meter scale, eliminating calibration for the effects of temperature or the holding tank.

5.4. Slug Injection Method For Remote Areas

The slug injection method of measuring stream discharge, when properly administered, should be as accurate and repeatable as the continuous injection method described by Bjerve and Groterud [1980]. The method is independent of channel geometry or discharge characteristics. The following equipment is required:

1) A lightweight digital conductivity meter with submersible probe.

2) A stopwatch.

3) Two plastic buckets, with a volume of 6 to 10 L each.

4) A 1000–mL and a 10–mL plastic graduated cylinders.

5) common table salt.

6) A field book and pencil.

For our work at Emerald Lake, several conductivity meters were used. At most flows the 0–200 $\mu S\,cm^{-1}$ meter scale was adequate. At moderate flows (0.05–0.1 $m^3\,s^{-1}$) 250 g of salt mixed with 8 L of stream water (slug conductivity ~40,000 $\mu S\,cm^{-1}$) produced an effective conductivity wave. This mixture was reduced or increased, depending on flow.

The procedure is as follows:

(1) Select a channel reach for measurement. The reach should be without branches, and should have an adequate slug injection site with a measurement site some distance downstream. The injection site should allow dumping of the slug into the main part of the channel flow, and the measurement site should allow placement of the submersible probe into the main channel flow. The channel should not be extensively braided at the measurement site.

(2) Measure and record the stream stage.

(3) Measure and record the background conductivity of the stream (Bk). Measure several liters of stream water into one of the plastic buckets. Record the volume and amount of salt added to the slug mixture. The investigator should mix the salt slug with the channel flow characteristics in mind. Small, low velocity flows require a lower concentration slug solution. Care should be taken to assure that the salt has completely dissolved in the slug solution before conductivity is measured. Remove 10 mL of concentrated slug and put it into the second bucket; add 1000 mL of stream water to the same bucket and mix, being careful not to contaminate the diluted mixture with salt from the slug. Measure and record the conductivity and dilution factor or the slug dilution. The conductivity of the salt slug (C_s) is computed by correcting the diluted slug conductivity ($dil.C_s$) for background conductivity (Bk) and multiplying by the dilution factor (x):

$$C_s = dil.C_s - Bk\,(x-1) \qquad (5)$$

(4) The probe and meter should be set up at the measurement site. The distance between the measurement and injection sites is a function of flow volume and velocity in the channel. If the distance is short, the slug induced conductivity wave will pass too rapidly, and if the distance is long the wave will pass slowly. In the first case, it may be difficult to adequately record the shape of the conductivity wave, while in the second the measurement can be very tedious. Experience at a particular site will aid in this decision. At least duplicate measurements should be made. At this time the stream background conductivity should be remeasured to assure that the probe has not been contaminated by immersion in the diluted slug.

(5) Inject the slug and record the wave passage as two vectors of time (seconds) and conductivity ($\mu S\,cm^{-1}$). The slug should be dumped into the middle of the channel and the stopwatch started. Conductivity at the measurement site should then be recorded at 5 or 10 second intervals, depending on the flow velocities. It is important to record the time and magnitude of the conductivity peak as the wave passes.

The procedure takes 10 to 15 minutes to perform once it is familiar. It is best performed by two investigators, but can be done alone. If the flow velocities are too fast, it can be difficult to race the conductivity wave from the injection site to the measurement site in order to record the data. The procedure should be repeated at least twice to insure good results.

The conductivity wave can be integrated using a variety of standard procedures on the time-conductivity vectors. Some calculators do simple integration, including removing the background conductivity for the measured values, and can be programmed to do the entire calculation in the field (e.g. HP-15C). Discharge can be calculated using the above equations from measured values of the slug conductivity (C_s), the slug dilution factor (x), the background conductivity (Bk), the slug volume (V_s), and the conductivity wave integral.

This method provides a reliable technique for discharge measurement in remote areas. It is inexpensive, independent of channel geometry, and simple to perform. The method has been tested in remote areas of the Amazon basin in Brazil, in alpine basins in the Sierra Nevada, and in a fresh-water estuary in coastal southern California. Measured discharges have ranged from 0.002 to 2.5 m^3s^{-1}, with flow velocities from 1.5 $cm\,s^{-1}$ to a cascading waterfall in which velocity could not be measured. In most cases, pairs or triplets of measurements have shown agreement within 5%. The method was also compared against a USGS calibrated concrete reach for a range of flows from 0.02–0.80 $m^3\,s^{-1}$ at the Sierra Nevada Aquatic Research Laboratory, near Mammoth Lakes, California. Salt dilution calculations were within 6.4% of the calibrated values across the full range of flows, but disagreed 10% or more at flows greater than 0.75 $m^3\,s^{-1}$. The mean difference at flows less than 0.1 $m^3\,s^{-1}$ was 2.3%. These results were not conclusive because the reach had not been calibrated for several years, and only 9 measurements were made. Tests are planned during the next year to compare the slug-dilution method against continuous-injection measurement of discharge, and against a calibrated V-notch weir.

5.5. Stage-Discharge Relationships, Lake Outflow and Inflows 1 & 2

The statistical analysis and methodology used to create empirical relationships for the Outlet and Inlets 1 and 2 in the Emerald Lake watershed are presented in this section. Discussions follow on the relationships between transducer and stream stage, and between stream stage and discharge for the three streams mentioned above.

Input Data

Voltage data from each stream were recorded by an Easylogger from a pressure transducer installed in the vicinity of a staff gage. Staff gages were of the Stevens type and were permanently attached to a metal structure. In the inlets, the structure consisted of metal rods driven in the stream bed against the bank and in the outlet a significant metal structure was bolted to the bedrock forming one bank. Some of the discharge meas-

urements at the inlets were obtained at low flows using a bucket method. The bucket method consists of directing all flow into a container. A measure of time and volume then gives an accurate value for discharge. Estimation of flow was made for the ungaged inlets at several different discharge levels using the Manning Equation [Chow, 1964; Linsley et al., 1982]. The remaining inlet and all the outlet measurements were carried out using the salt dilution technique discussed in another section of this report.

Data Quality

The transducer data seems to be of good quality. The problem with the transducer has been occasional failure of the entire unit, rather than variability in the recorded data.

Staff gages were read manually by field personnel to obtain the stage record which produced several sources of error. Individuals were never be able to read the stage exactly, and lighting, vantage point and a plethora of human variables precluded absolute precision or accuracy. This element was magnified by the fact that several field workers recorded these data throughout the season. Although we attempted to standardize measurement protocol, there was inevitable variation. Stage readings were also difficult to read at higher stages as the stream surface changes from approximately laminar flow to turbulent flow where the stage varies rapidly at the staff. The gages were graduated in hundredths of feet which was converted to meters for analysis. At high flows in Inlet 1 and 2 precision was probably ±1.5 cm. The other gages were located in better places and the precision is probably better.

Discharge measurements are the largest source of uncertainty and error in the analysis. Bucket measurement could be made with a high degree of accuracy and precision when flows were low enough that complete isolation of the stream was insured. There was some rounding error resulting in replicate discharges for varying stage in the analysis. This was not due to measurement flaws, but rather discharge was rounded to the nearest liter per second (0.001 $m^3 s^{-1}$) for analysis. If future work mandates more accurate and precise measurements of discharge in the inlets and outlet, installation of weirs or flumes is necessary. It is doubtful if we will ever be able to characterize accurately the discharge at the highest flows in the inlets because bankfull discharge is attained at some level substantially below peak flows observed in the spring of 1986. It would be difficult to place a structure that could capture the entire flow in these channels. Portable flumes at the inlets would still be a great asset for flow at bankfull discharge and below. The well-defined channel in the outlet would allow construction of a weir capable of measuring all flows.

5.6. Outlet Rating Curve

The Outlet has been the subject of considerable attention in this project. It represents one of the few checks on other monitoring efforts and estimations within the watershed (eg. snow accumulation and snowmelt). For this reason it was critical to obtain the best possible estimates of discharge at all time resolutions. This meant obtaining as many quality discharge measurements as possible to have a statistically significant sample to work with. From these measurements a stage-discharge relationship was constructed, also known as a rating curve [Chow, 1964; Dunne and Leopold, 1978; Linsely et al., 1982]. The previous rating curve for the outlet was based on only 29 data points (see interim report). It was difficult to fit empirically and the final solution was to divide it into three equations based on stage height. Little confidence could be placed in this set of equations and they exhibited little stability. The linear relationship for higher flows could be based on only two points. This is clearly absurd from both a physically based standpoint, as well as a statistical one. Approximately 55 new measurements were gathered during the 1987 field season, giving 82 usable data points and sufficient sample size was now available, such that one curve could be applied to the entire data set. There is still a paucity of measurements in the higher flow range and the rating curve is suspect at these flows. Nothing can be done about this problem until further measurements are obtained. Outliers were included in the statistical analysis leading to the rating curve as there was no evidence indicating faulty measurement or analysis in the derived discharges. The are also physical reasons for retaining outliers. The relationship between stage and discharge is often hysteretic and is further complicated by changes in channel geometry with changes in stage height. Hysterisis produces different curves on the rising and falling limbs of the hydrograph. This effect is due to the slope of the water surface in the channel. Hysteresis is probably not significant is this short reach and at these small discharges and would not account for the range of variability observed. However, changes in the channel geometry may be significant. Statistically, the obvious outliers seem to have little effect. Removal of the two obvious outliers at a stage height of approximately 0.36 m only improves the R^2 by 0.023.

Obtaining rating curve coefficients is usually carried out by graphical techniques using log-log plots and by reading the coefficients from the graphs after fitting the data by eye [Chow, 1964; Dunne and Leopold, 1978; Linsely et al., 1982]. This technique has been used for many years and works well in practice. The alternative is to fit an equation to the data using a statistical technique such as least squares. To satisfy the continuity equation from which discharge is derived, a log-log transform is usually used, where logarithims are calculated for both stage and discharge. This was not done in this study because least squares analysis produced the best fit with untransformed stage regressed against log transformation of discharge. A log-log analysis will be carried out in the future to determine if a significant difference in the stage discharge relationship exists.

The data were analyzed graphically to check for errors, determine distribution and select appropriate transforms. A normal probability plot of discharge indicated that a log transform was appropriate. No transform of stage data was necessary.

Coefficients for a rating curve were obtained from a regression of stage against logged discharge. These coefficients were then exponentiated to get discharge as

the following equation shows:

$$Q = \exp((\alpha S) - \beta), \quad (6)$$

where:

Q = calculated discharge,
α = slope coefficient from the regression,
β = intercept coefficient from the regression,
S = observed stage height.

The rating equation derived from the regression for the outlet follows:

$$Q_{Outlet} = \exp((9.685 S) - 5.634). \quad (7)$$

Some explanation is necessary. The R^2 values should be examined with some caution. The low linear R^2 value of 0.74 is an obvious result of the curvilinear relationship in the raw data. A better value of 0.86 is obtained by the logging the discharge prior to regression, but this value is artificially high because the relationship is subsequently retransformed by exponentiation. The actual amount of the variance explained by the rating equation lies somewhere in between the two values.

Perhaps a better evaluation of the relationship comes from the standard errors and the confidence intervals of the coefficients. Confidence intervals were calculated using the t statistic as described by Zar [1984; p. 272]. Overall the relationship appears to be quite good and relatively stable. The rating curve indicates that discharge may be overestimated in the higher region by the present rating equation. More measurements are needed in the higher flows to add confidence to this region.

5.7. Inlet 1 Rating Curve

A large number of discharge measurements were obtained at Inlet 1 during the 1987 field season. This increased the sample size from 18 to a good statistical sample of 76. Some of the measurements were obtained at low flows using the bucket method. The remaining measurements were carried out using the salt dilution technique.

Graphical analysis showed that a transform was necessary for the discharge data. A normal probability plot showed a log transform to be appropriate. Stage data were not transformed for further analysis.

A rating curve was produced using the coefficients resulting from a regression of stage versus logged discharge. A realistic R^2 value lies somewhere between the linear regression R^2 of 0.68 and the logged discharge regression R^2 of 0.94. The rating equation for Inlet 1 is:

$$Q_{Inlet1} = \exp((15.438 S) - 9.773). \quad (8)$$

The relationship appears quite good and seems to do a reasonable job at higher flows based on the scant available data. Confidence in the higher flows is suspect, however, until more measurements are obtained.

5.8. Inlet 2 Rating Curve

Fewer discharge measurements were obtained for Inlet 2, however, a good statistical sample still exists with a sample size of 56. Both the bucket method, and salt dilution technique were used in this inlet. In this case it was possible to make estimates over almost the entire range of discharges. The agreement between the techniques throughout the entire range is encouraging.

Again, graphical analysis showed that a log transform was necessary for the discharge data. The log transform alleviated some of the leverage in the tail outliers but it exacerbated fitting problems in the mid-range flows. It was not obvious that the transform was desirable from examination of the plots. Several rating curves from different transformations plotted against the raw data showed that the log transform produced the best fit to the raw data.

The rating equation is:

$$Q_{Inlet2} = \exp((14.131 S) - 9.384) \quad (9)$$

The actual R^2 lies somewhere between the linear regression R^2 of 0.74 and the logged discharge regression R^2 of 0.92.

The relationship is good in the lowest discharge area and in medium to higher flows. It seems to underpredict discharge in the 0.05 to 0.10 $m^3 s^{-1}$ range. With only one measurement at high flow, this portion of the curve is suspect.

Outlet - Transducer to Stream Stage

It was necessary to separate the data set of voltage and stream stage and develop two relationships. On October 31, 1985 an an instrumental change was made in the system which changed the voltage output from the pressure transducer at the outlet. A relationship was developed to convert transducer data to stream stage before and after that date. Both produce a very good linear fit between stream stage and voltage output from the pressure transducer. Data parameters were checked graphically in normal probability plots. There were not significant problems that warranted data manipulation. Examination of the stage data shows a remarkable similarity to the voltage plots, which indicates the two data sets represent very similar distributions. A linear regression was carried out. There are two equations for converting voltage to stream stage. For voltage data acquired before October 31, 1985 the equation is:

$$S = 0.124 V - 0.093. \quad (10)$$

After this date the following equation should be used:

$$S = 0.200 V - 0.141, \quad (11)$$

where:

S = stream stage in meters,
V = voltage output from pressure transducer.

The R^2 values of 0.96 and 0.996 clearly indicate a strong linear relationship. Theoretically, the relationship between stage and voltage should be perfectly linear. In surface hydrology, water can be treated as an incompressible fluid which means depth and pressure

are related in a linear fashion. Two sources of error caused the less than perfect fit. The first was the instrument; there may have been some nonlinearity in the voltage output from the pressure transducer. The second was operator interpretation. The stage values used in the regression are manually read values from a staff permanently fixed in close proximity to the transducer. There was also noise due to the fact that several different operators read the staffs and there would be some noise even if only one observer was involved. As discharge increased and the streams became more turbulent, it became increasingly difficult to read the rapidly fluctuating water level. An attempt was made to read the "mean" level which clearly introduced variability and error. This was not a severe problem in the outlet, due to the good location of the staff gage, but the problem was worse in the inlets.

Inlet 1 - Transducer to Stream Stage

Inlet 1 produced a very good linear relationship between stream stage and voltage output from the pressure transducer. Before regressions were carried out both data parameters were checked graphically in normal probability plots. The overall good fit and the light tails indicate that no transform was necessary or appropriate. A linear regression was carried out. The R^2 of 0.98 is not unrealistic. Conversion from voltage to stream stage should be done using the following relation:

$$S = 0.235\,V - 0.207. \tag{12}$$

Inlet 2 - Transducer to Stream Stage

Inlet 2 also produced a strong linear relationship between stream stage and voltage. Again, before regressions were carried out, both data parameters were checked graphically in normal probability plots. Light tails at the lower end of the distributions of both parameters behaved poorly if the slight convexities in these data were removed and therefore, no transformation was executed. This does not appear to be a problem in this regression. A linear regression was carried out. The R^2 of 0.99 is pleasing. The equation describing the relationship is:

$$S = 0.210\,V - 0.116. \tag{13}$$

The mild tendency towards heteroscedasticity can be explained by the above mentioned operator errors. As the stage rises, it became increasingly difficult to read the staff accurately. This explains the trend of increased variance with increased discharge. The placement of the staff in Inlet 1 is particularly prone to this problem. The staff is located such that higher flows pillow up against it, causing rapid changes of several centimeters. The trend is probably not sufficient to cause concern in this case.

Summary of Discharge Rating Functions

Relationships have been derived to convert transducer voltage to stream stage, and from stream stage to discharge for the outlet and both instrumented inlets (1 and 2). Results of the statistical analysis have been presented, as well as the techniques and assumptions employed, and graphical and numerical results have been reviewed.

The voltage to stage relationships all exhibited well fitting linear relationships. These relationships exhibit a high degree of stability. They should be periodically checked against new data to identify the possibility that the transducer has been moved in the stream.

The rating curves are not as well defined. They exhibit the errors associated with the different discharge measurement techniques, operator error in reading the staffs, and instrument errors in the transducers. Further error results from fitting a curve to the data. Both the data transforms and the regressive techniques are approximations or "best fits" interpreted mathematically or by the analyst. It was necessary to transform all discharge data because it was lognormally distributed. The low to medium flows are probably approximated quite well by the rating curves. Flow estimates in the high regions are suspect and likely excessive. There are several techniques for extending rating curves to flows higher than those observed [Linsley et al., 1982]. None of the methods are completely adequate. The assumptions they are based on, such as stable hydraulic geometry across the range of flows, certainly do not hold for the inlets and are dubious for the outlet. Only acquisition of more discharge measurements in the high flow regions will support these conjectures. In summary, we have equations for the two major inflows and the outlet that are satisfactory for the research purposes being carried out in the Emerald Lake watershed. Better quality and more extensive data for inferences leading to these results would be nice, but at this time they do not exist.

Future Discharge Measurement

More discharge measurements are needed in all channels, at all flow levels, particularly in the medium to high discharge range. The most reliable way to collect these data in the future would be after installing weirs or flumes in the channels. If this solution is not feasible, then as many more salt dilution measurements as possible should be taken. With new data, the rating curves may be re-evaluated and adjusted accordingly.

Currently used relationships should be checked using conventional graphical methods and least squares analysis using a log-log fit to the stage and discharge data to see if there is a difference between the results. This problem must be addressed during peak flow next spring.

5.9. Discharge Into and Out of Emerald Lake

The stage records and rating curves discussed above were used to predict hourly discharges from the outflow for the 1984, 1985, and 1986 water years. Table 5.1 gives our estimate of monthly flow volumes for those three years. Table 5.2 presents monthly flow volumes from inflows 1 and 2, which are gaged, and for the outflow for the 1986 water year. It is clear that these two inflows account for most of the outflow volume (80% during the 1986 water year), and that there is almost no lag-time for lake recharge or storage between inflow volumes and outflow volumes. Tables 5.3, 5.4, and 5.5

give daily outflow volumes for each year. The total outflow volume from 1985 is about half that of 1984, which is in turn about half that of 1986. The total water flux during June 1986 was more than the entire year's flux in 1985. The volume of Emerald Lake (179,600 m^3) was replaced 6.3 times in 1984, 3.7 times in 1985, and 14.3 times in 1986. This represents an average depth of 0.94 m of water over the basin in 1984, 0.56 m in 1985, and 2.14 m in 1986. These figures correspond closely with our estimates of the input volume when corrected for sublimation. 83% of the annual flux occurred during spring melt (April through August) in 1984, 87% in 1985, and 90% in 1986. It is clear that snow is the dominant hydrologic input to this watershed, and massive amounts of snowmelt cycle through this watershed each year.

The 1984 data are somewhat in question because the USGS gage was not working properly. It is probably reliable at the monthly or even the daily level. Figure 5.1 shows the annual and melt season hydrographs for the 1984 water year. Because the bubble gage failed in May 1984, we re-constructed that portion of the hydrograph. Figure 5.2 and Figure 5.3 show the annual and melt season hydrographs for the 1985 and 1986 water years.

It is worth noting the spikes in the winter portion of the hydrographs for both the 1985 and 1986 water year. We had suspected that these were due to mid-winter icing at the gaging site [Rosenberg and Pentland, 1966; Santeford and Alger, 1986]. However, in February 1986 we witnessed a major avalanche cycle that lasted for several days. These avalanches brought thousands of m^3 of debris and snow down onto the lake surface, breaking the ice and causing a major flood to scour the outflow channel. The raw data spike from this event saturated the recording device, which thus gave a low estimate of the magnitude of the flood. The spike shown in the hydrograph is instead based on our estimate of the mass of debris that hit the lake. Avalanches had been observed to hit the lake several times during the past three years, so it is safe to assume that the other spikes shown are real and did result in sudden losses of water from the lake. Tables 5.6 and 5.7 present daily discharge into the lake from inflows 1 and 2.

5.10. References

Bjerve, L. and O. Groterud, Discharge measurements by a new-formed relative salt-dilution method in small turbulent streams, *Nordic Hydrol.*, *11*, 121-132, 1980.

Brakensiek, D. L., H. B. Osborn, and W. J. Rawls, *Field Manual For Research in Agricultural Hydrology*, vol. Agriculture Handbook 224, 550 pp., U.S. Dept. Agric., 1979.

Buchanan, T. J. and W. P. Somers, *Stage measurement at gaging stations*, Tech. Water Resour. Invest. U.S. Geol. Survey., 3-A7, p. 28, 1968.

Buchanan, T. J. and W. P. Somers, *Discharge measurements at gaging stations*, Tech. Water Resour. Invest. U.S. Geol. Survey., 3-A8, p. 65, 1969.

Chow, V. T., *Handbook of Applied Hydrology*, McGraw-Hill, New York, 1964.

Church, M., Electrochemical and fluorometric tracer techniques for streamflow measurements, *Tech. Bulletin*, *12*, 72, British Geomorph. Res. Group, 1975.

Church, M. and R. Kellerhals, Stream gauging techniques for remote areas using portable equipment, *Tech. Bull.*, 89 pp., Dept. Energy, Mines, Resour., 1970.

Dozier, J., A clear-sky spectral solar radiation model for snow-covered mountainous terrain, *Water Resour. Res.*, *16*, 709-718, 1980.

Dozier, J. and S. I. Outcalt, An approach toward energy balance simulation over rugged terrain, *Geogr. Anal.*, *11*, 65-85, 1979.

Dunne, T. and L. B. Leopold, *Water in Environmental Planning*, 818 pp., W. H. Freeman, New York, 1978.

Eagleson, P. S., *Dynamic Hydrology*, 462 pp., McGraw-Hill, New York, 1970.

Fisher, T. R. and J. M. Melack, *Nutrient supply and primary productivity in Amazon floodplain lakes*, vol. UMCEES 81-HEPL, 115 pp., Natl. Sci. Found., 1981.

Frampton, M. J. and D. Marks, Mapping snow surface temperature from thermal satellite data in the southern Sierra Nevada, *Proc. Western Snow Conf.*, *48*, 88-96, 1980.

King, H. W. and E. F. Brater, *Handbook of Hydraulics*, vol. Fifth ed., 675 pp., McGraw-Hill, 1963.

Linsley, R. K., M. A. Kohler, and J. Paulhus, *Hydrology for Engineers*, 3rd ed., 508 pp., McGraw-Hill, New York, 1982.

Marks, D., R. Kattelmann, J. Dozier, and R. E. Davis, Monitoring snowcover properties and processes in a small alpine watershed, in *Proceedings of Sixth International Northern Research Basins Symposium/Workshop*, edited by H. S. Santeford, pp. 259-275, Mich. Technol. Univ., Houghton, MI, 1986.

Rosenberg, H. B. and R. L. Pentland, Accuracy of winter streamflow records, *Proc. Eastern Snow Conf.*, 51-72, 1966.

Santeford, H.S. and G.R. Alger, Stage, discharge, and ice, in *Sixth International Northern Research Basins Workshop/Symposium*, edited by H. S. Santeford, vol. II, pp. 247-272, Mich. Technol. Univ., Houghton, MI, 1986.

Streeter, V. L., *Fluid Mechanics*, vol. Fourth ed., 705 pp., McGraw-Hill, 1966.

Stromeyer, C. E., The gauging of streams by chemical means, *Proc. Inst. Civil Engrs.*, *160*, 349-363, 1905.

U.S. Geological Survey, California streamflow characteristics, *Water Resour. Div. Open-file Rep.*, 1971.

U.S. Geological Survey, National handbook of recommended methods for water-data acquisition, *Open-file Rep., Two Volumes*, U.S. Dept. Int., Washington, DC, 1977.

Zar, J. H., *Biostatistical Analysis*, 2nd ed., 718 pp., Prentice-Hall, Englewood Cliffs, NJ, 1984.

TABLE 5.1: Total Monthly Water Flux from Emerald Lake
(October 1983 - September 1986)

Month	Volume (m^3) WY 1984	WY 1985	WY 1986
Oct	14,100	7,600	20,800
Nov	5,190	28,900	22,600
Dec	8,100	12,920	18,100
Jan	21,700	7,330	34,300
Feb	50,600	3,190	86,000
Mar	77,100	427	46,300
Apr	35,500	18,100	135,000
May	479,000	202,000	534,000
Jun	215,000	289,000	825,000
Jul	149,000	68,380	612,000
Aug	53,300	9,940	204,000
Sep	17,800	20,500	36,400
Total:	1,127,000	668,000	2,573,000

TABLE 5.2: Measured Monthly Water Flux In- and Out- of Emerald Lake

Inflows #1 & #2, and Outflow
1986 Water Year (Oct 1985 - Sept 1986)

Month	Volume (m^3) Outflow	% annual	Inflow #1	% annual	Inflow #2	% annual
Oct	20,800	1	4,260	1	8,540	1
Nov	22,600	1	3,730	1	2,310	<1
Dec	18,100	1	5,220	1	2,390	<1
Jan	34,300	1	7,130	1	4,610	<1
Feb	86,000	3	4,770	1	2,200	<1
Mar	46,300	2	6,990	1	3,920	<1
Apr	135,000	5	31,500	6	58,200	5
May	534,000	21	110,100	21	230,000	19
Jun	825,000	32	195,800	37	451,000	37
Jul	612,000	24	129,600	24	331,000	27
Aug	204,000	8	26,400	5	99,200	8
Sep	36,400	1	6,340	1	14,240	1
Total	2,573,000	100	532,000	100	1,208,000	100

TABLE 5.3: Daily Discharge Volume (m^3)
Emerald Lake Outflow, 1984 Water Year

Day	Oct	Nov	Dec	Jan	Feb	Mar	Apr	May	Jun	Jul	Aug	Sep
1	1300	68	240	220	780	1100	120	3300	10000	4000	3200	840
2	1300	97	290	310	780	1200	91	3600	10000	3700	2900	840
3	830	140	4400	82	1300	1400	240	4000	9200	8400	2800	830
4	310	74	530	17	790	1500	340	4400	8800	6400	2400	830
5	2800	110	230	23	1700	1700	4300	4900	8400	6100	1900	830
6	1900	170	130	91	1200	1900	230	5500	7100	5600	1700	820
7	1200	100	100	760	730	2100	920	5800	5500	5400	1500	820
8	1000	86	110	1600	1500	2400	1300	6600	7100	4700	1300	820
9	730	90	140	2600	3400	2700	1700	6900	6400	4700	960	810
10	500	96	110	1700	9200	2900	3600	8100	5700	4300	1400	810
11	210	100	69	790	3700	3000	2000	10000	7500	3700	810	800
12	530	110	270	700	2700	3200	370	15000	4500	4100	2100	800
13	250	120	160	250	400	3400	3000	19000	8600	4600	3600	800
14	120	130	150	210	3300	3500	190	20000	6400	4000	4300	790
15	62	130	84	1100	1400	1600	150	21000	1700	3300	4300	790
16	130	140	180	400	3200	2800	180	22000	1200	4700	3600	780
17	51	150	89	830	3300	1500	230	23000	7300	5100	2300	760
18	120	160	77	630	1500	2500	290	24000	8400	14000	1000	500
19	130	180	51	430	1200	1500	350	24000	9700	5400	890	460
20	68	190	91	690	850	110	430	24000	8100	4000	880	400
21	53	200	42	980	1200	1900	530	23000	5800	2800	880	450
22	30	220	24	690	680	3000	650	22000	8400	4500	870	480
23	28	240	22	490	1200	3600	790	21000	6800	9100	870	320
24	84	260	40	690	440	1700	970	21000	7700	4200	870	250
25	89	290	46	770	680	3400	1200	21000	6300	3700	860	280
26	34	310	67	780	730	5100	1500	20000	7600	3300	860	230
27	46	350	76	780	810	7100	1800	20000	8900	3000	860	190
28	65	390	120	780	900	5400	2300	20000	7600	3400	850	160
29	30	410	69	780	1000	1900	2700	19000	7300	3000	850	160
30	76	80	53	780		1300	3000	19000	7000	2200	850	130
31	37		33	780		680		18000		3700	840	

TABLE 5.4: Daily Discharge Volume (m^3)
Emerald Lake Outflow, 1985 Water Year

Day	Oct	Nov	Dec	Jan	Feb	Mar	Apr	May	Jun	Jul	Aug	Sep
1	94	350	830	150	320	6	49	3300	4300	3500	650	180
2	130	340	780	140	320	6	72	3300	4300	3700	600	180
3	150	310	740	130	320	7	93	2900	3600	4200	560	200
4	150	320	700	120	320	7	59	3100	5400	4300	530	300
5	140	360	660	110	320	4	150	1700	9500	3900	530	320
6	120	350	630	100	320	5	310	1500	15000	3500	470	310
7	130	340	600	95	320	22	530	1100	19000	3600	450	300
8	130	1500	570	87	320	11	710	1900	16000	3500	430	270
9	140	850	540	80	330	8	890	3600	17000	3400	390	230
10	120	610	510	76	170	5	710	3700	15000	3100	350	220
11	240	470	490	130	36	6	440	3500	15000	3200	350	580
12	130	450	460	180	7	7	590	4400	15000	3200	320	860
13	130	2300	440	220	4	5	1000	6600	14000	2800	290	1700
14	110	2900	420	280	4	5	1600	8700	15000	2700	280	1900
15	60	2900	400	310	4	5	1800	9100	14000	2300	270	1500
16	190	3000	380	320	5	5	830	8100	13000	1700	270	1100
17	360	3000	360	320	5	5	450	8200	13000	1600	270	720
18	270	150	340	320	5	4	380	9800	14000	1500	240	1400
19	140	190	320	320	5	6	310	10000	12000	1000	220	1700
20	220	230	310	320	3	6	200	9200	8500	1000	220	1300
21	210	290	290	320	4	6	170	9000	7300	1000	220	950
22	220	370	280	320	5	8	230	11000	6600	1000	210	750
23	220	490	260	320	5	10	400	13000	5700	1000	200	630
24	260	660	250	320	5	14	520	13000	4600	1000	190	530
25	330	940	230	320	6	11	290	11000	3700	1000	190	470
26	350	1100	220	320	8	10	240	10000	3900	1000	180	410
27	710	1100	210	320	8	62	410	8100	4100	1000	140	360
28	850	1100	190	320	7	60	820	7300	3900	1000	110	390
29	580	1000	180	320		37	1600	5800	3500	1000	390	360
30	420	880	170	320		37	2200	5300	3400	1000	250	330
31	300		160	320		37		4800		680	170	

TABLE 5.5: Daily Discharge Volume (m^3)
Emerald Lake Outflow, 1986 Water Year

Day	Oct	Nov	Dec	Jan	Feb	Mar	Apr	May	Jun	Jul	Aug	Sep
1	280	550	670	490	1100	720	3000	14000	34000	28000	12000	2100
2	220	540	4000	440	950	780	2500	15000	32000	28000	12000	1900
3	220	490	1400	410	990	760	2400	15000	32000	32000	12000	1900
4	220	440	710	1500	940	740	2900	11000	32000	30000	11000	1900
5	220	400	680	7300	620	710	2900	7800	27000	25000	9800	1800
6	270	390	620	3200	520	690	2700	4300	26000	21000	10000	1800
7	560	350	510	2100	470	720	2200	3900	25000	20000	9400	1800
8	180	300	470	1500	430	3400	2000	3900	23000	19000	8500	1900
9	410	240	450	1100	400	2700	1700	3600	26000	21000	8200	1500
10	1200	980	470	750	370	2800	2200	4300	27000	22000	8700	1200
11	1200	2200	450	560	360	1700	2000	5600	28000	25000	8800	990
12	1100	980	400	490	4100	1500	1900	8100	28000	29000	9000	880
13	840	510	380	510	4100	1300	1700	11000	29000	28000	7900	800
14	670	360	360	570	2000	1200	1800	10000	29000	23000	7400	730
15	560	280	340	640	18000	1100	2100	11000	28000	21000	6700	650
16	470	260	330	670	18000	1100	2100	13000	28000	19000	6000	640
17	420	260	320	630	5800	940	1800	15000	27000	17000	5400	570
18	390	270	310	610	8400	820	1600	17000	26000	16000	4800	870
19	360	250	310	610	13000	750	1800	19000	25000	17000	3800	990
20	320	300	300	610	1100	760	3500	21000	24000	18000	4900	760
21	590	380	300	590	780	850	6800	22000	26000	18000	4600	610
22	700	330	310	570	590	1000	8600	24000	28000	20000	4600	520
23	810	360	310	560	510	1200	6700	25000	28000	16000	4100	530
24	1700	2000	310	530	460	1200	6600	27000	31000	14000	3600	1100
25	1700	2400	320	500	430	1300	8500	28000	30000	13000	3200	2100
26	1300	860	320	500	410	1600	8900	28000	29000	13000	3200	1200
27	1100	540	340	510	500	2100	9700	31000	28000	11000	3200	900
28	890	960	340	550	600	2800	11000	33000	23000	12000	3100	880
29	750	3000	580	740		3000	11000	32000	21000	12000	3000	1100
30	620	1400	840	3000		2800	12000	36000	25000	12000	2700	1800
31	550		610	1600		3300		34000		12000	2200	

TABLE 5.6: Daily Discharge Volume (m^3)
Emerald Lake Inflow #1, 1986 Water Year

Day	Oct	Nov	Dec	Jan	Feb	Mar	Apr	May	Jun	Jul	Aug	Sep
1	110	130	170	160	180	180	280	2600	7900	6800	2000	380
2	110	130	180	160	180	180	340	2800	8500	7100	1800	380
3	110	110	190	160	180	180	390	2600	8300	8600	1400	380
4	110	120	180	300	180	170	450	1400	7500	7900	1200	350
5	110	100	180	690	170	160	500	900	6200	6100	1400	340
6	110	100	180	410	170	160	550	580	6000	4800	1300	330
7	110	99	180	300	170	160	610	480	5700	4000	1000	340
8	110	81	180	270	170	340	660	500	5500	4200	860	320
9	120	65	180	250	160	510	710	460	6300	5100	890	250
10	130	67	180	240	160	360	760	470	6500	5600	1000	200
11	140	210	180	230	160	290	820	630	6600	7700	1200	210
12	130	100	170	230	170	250	870	1200	6600	7400	1200	200
13	110	120	170	220	190	240	920	2400	7100	6200	1100	200
14	110	120	170	220	170	220	970	2000	6800	4600	940	170
15	100	120	170	210	170	220	1000	2600	6400	4100	800	150
16	100	120	160	200	160	210	1100	3400	6600	3300	700	160
17	100	120	160	200	160	200	1100	4400	6100	3000	650	160
18	99	120	160	200	170	200	1200	4600	5900	2900	560	190
19	94	120	160	200	170	190	1200	4900	5600	3200	510	160
20	96	120	160	200	170	190	1300	5000	5500	3700	610	140
21	100	130	160	200	170	190	1300	4500	6200	3000	620	120
22	110	130	160	190	170	190	1300	3600	6600	4100	570	110
23	190	130	160	190	170	200	1400	3100	6500	2900	520	88
24	370	120	160	180	170	200	1400	3600	7800	2000	480	100
25	340	160	160	180	170	210	1500	5600	7200	1900	480	140
26	270	160	160	180	170	210	1500	6700	7200	1500	470	140
27	220	150	160	180	170	220	1600	7500	6600	1300	480	140
28	150	160	160	190	170	230	2000	8100	4800	1400	470	140
29	99	150	160	200		240	1700	7500	5100	1400	430	160
30	98	170	160	200		240	2100	8400	6200	1800	390	190
31	100		160	190		250		7600		2000	380	

TABLE 5.7: Daily Discharge Volume (m^3)
Emerald Lake Inflow #2, 1986 Water Year

Day	Oct	Nov	Dec	Jan	Feb	Mar	Apr	May	Jun	Jul	Aug	Sep
1	380	73	78	69	78	84	270	5200	18000	16000	6300	870
2	380	64	100	70	78	86	370	5600	20000	17000	5900	820
3	380	78	92	78	78	80	470	5400	19000	22000	5200	820
4	380	110	82	180	78	73	580	3500	17000	19000	4900	860
5	380	99	79	860	78	69	680	2000	12000	14000	5200	850
6	380	89	83	500	77	69	790	960	12000	10000	5200	860
7	380	82	78	270	78	69	900	920	11000	8700	4700	870
8	380	72	78	200	78	200	1000	710	11000	8900	4400	860
9	460	59	78	160	78	350	1100	610	13000	11000	4500	640
10	460	46	78	150	78	220	1200	650	14000	12000	4800	470
11	430	74	78	140	75	160	1400	1000	15000	17000	4600	380
12	330	86	78	130	75	130	1500	2500	15000	19000	4100	320
13	190	79	78	120	130	110	1600	4500	16000	18000	3800	280
14	130	72	78	110	78	110	1700	4000	16000	13000	3600	240
15	100	74	78	110	75	100	1800	5000	15000	11000	3200	210
16	87	77	78	100	69	100	1900	6000	16000	9200	2800	180
17	78	78	78	100	69	99	2000	8400	14000	8200	2400	150
18	70	78	78	100	71	95	2100	9200	14000	8000	2000	420
19	61	72	78	95	77	90	2300	10000	13000	8600	1800	340
20	52	70	77	95	78	86	2400	10000	12000	9800	2500	200
21	66	70	77	95	78	89	2500	9700	14000	8300	2400	140
22	88	69	78	88	78	95	2600	7800	16000	10000	2200	110
23	500	69	76	86	77	100	2700	6200	17000	7700	1800	120
24	790	74	69	86	78	110	2800	7400	22000	5800	1500	250
25	530	91	69	86	77	120	2900	12000	20000	5900	1400	710
26	320	75	69	86	78	130	3000	13000	20000	5300	1400	270
27	230	73	69	86	78	140	3200	16000	16000	4800	1500	290
28	170	78	69	86	76	160	4100	17000	9600	5200	1500	350
29	140	87	69	92		180	3800	16000	9800	5200	1400	480
30	120	88	69	95		200	4500	21000	14000	5800	1200	880
31	93		69	86		220		18000		6300	970	

Figure 5.1. Outflow Discharge, 1984 Water Year

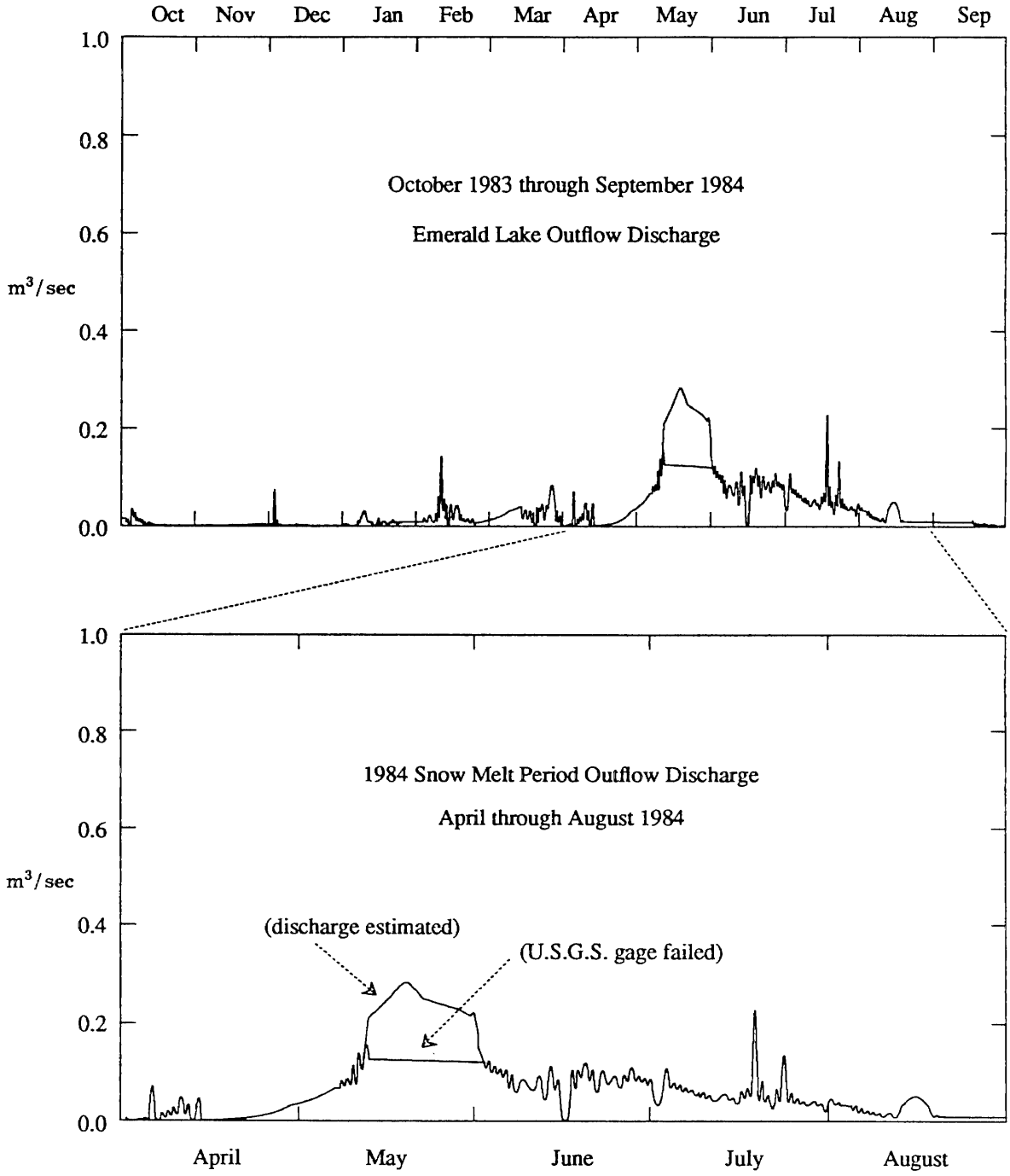

Figure 5.2. Outflow Discharge, 1985 Water Year

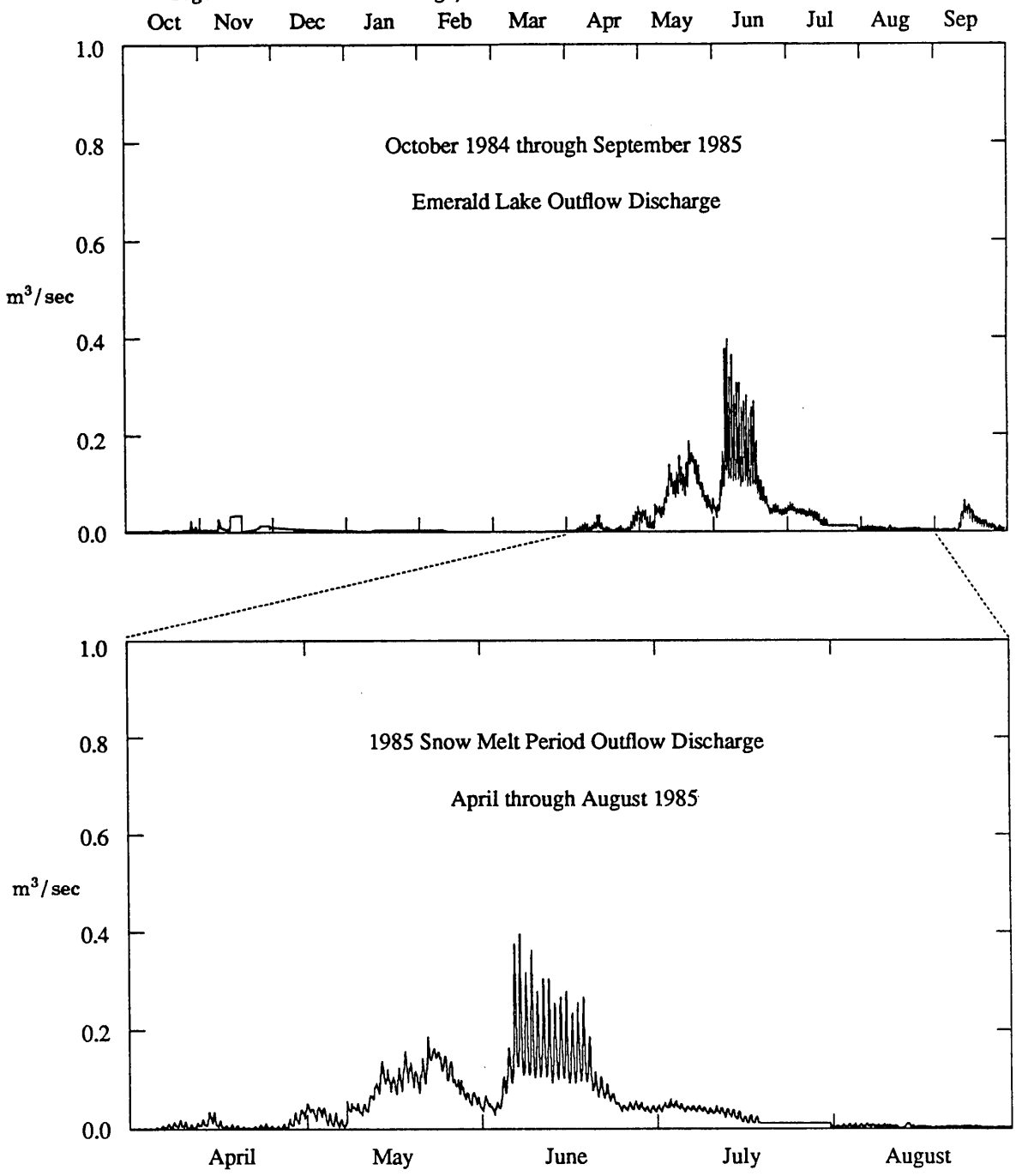
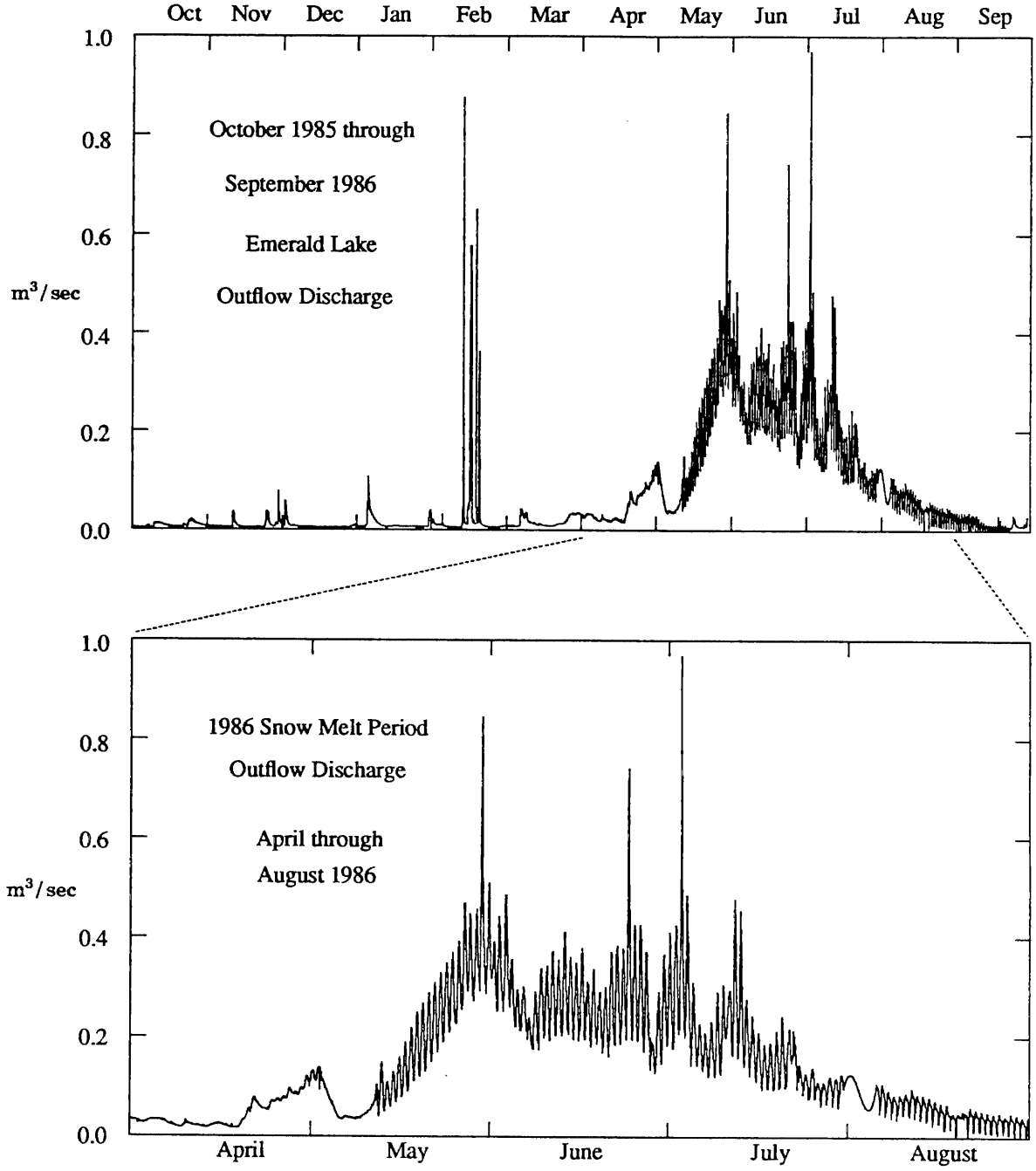
Figure 5.3. Outflow Discharge, 1986 Water Year